Title

Search for chargino-neutralino production with mass splittings near the electroweak scale in three-lepton final states in s =13 TeV pp collisions with the ATLAS detector

Journal

Physical Review D, 101(7)

ISSN

2470-0010

Authors

Aad, G
Abbott, B
Abbott, DC
et al.

Publication Date

2020-04-01

DOI

10.1103/PhysRevD.101.072001

Peer reviewed

Search for chargino-neutralino production with mass splittings near the electroweak scale in three-lepton final states in $\sqrt{s} = 13$ TeV pp collisions with the ATLAS detector

G. Aad *et al.*[*]
(ATLAS Collaboration)

(Received 18 December 2019; accepted 25 February 2020; published 7 April 2020)

A search for supersymmetry through the pair production of electroweakinos with mass splittings near the electroweak scale and decaying via on-shell W and Z bosons is presented for a three-lepton final state. The analyzed proton-proton collision data taken at a center-of-mass energy of $\sqrt{s} = 13$ TeV were collected between 2015 and 2018 by the ATLAS experiment at the Large Hadron Collider, corresponding to an integrated luminosity of 139 fb^{-1}. A search, emulating the recursive jigsaw reconstruction technique with easily reproducible laboratory-frame variables, is performed. The two excesses observed in the 2015–2016 data recursive jigsaw analysis in the low-mass three-lepton phase space are reproduced. Results with the full data set are in agreement with the Standard Model expectations. They are interpreted to set exclusion limits at the 95% confidence level on simplified models of chargino-neutralino pair production for masses up to 345 GeV.

DOI: 10.1103/PhysRevD.101.072001

I. INTRODUCTION

Supersymmetry (SUSY) [1–6] is a space-time symmetry that extends the Standard Model (SM), predicting the existence of new partners for each SM particle. The new particles have quantum numbers identical to those of their partners with the exception of spin, with SM fermions having bosonic partners and SM bosons having fermionic partners. This extension presents solutions to deficiencies in the SM, addressing the hierarchy problem [7–10] and providing a candidate for dark matter as the lightest supersymmetric particle (LSP), which will be stable if R parity [11] is conserved [12,13].

The electroweakinos consist of two generations of charginos ($\tilde{\chi}_i^{\pm}$, $i = 1, 2$) and four generations of neutralinos ($\tilde{\chi}_i^0$, $i = 1, 2, 3, 4$), where the indices are ordered by ascending mass, with the LSP assumed to be the lightest neutralino, $\tilde{\chi}_1^0$. The electroweakinos are formed from the mixing of the SUSY partners of the Higgs field (known as Higgsinos) with the SUSY partners of the electroweak gauge fields, the bino for the U(1) gauge field and winos for the W fields.

This paper presents a search for chargino-neutralino ($\tilde{\chi}_1^{\pm}\tilde{\chi}_2^0$) pair production with $\tilde{\chi}_1^{\pm} - \tilde{\chi}_1^0$ and $\tilde{\chi}_2^0 - \tilde{\chi}_1^0$ mass splittings near the electroweak scale. The targeted decay chain is shown in Fig. 1, with the chargino and neutralino decaying into the invisible LSP $\tilde{\chi}_1^0$ and either a W or Z gauge boson, respectively. Simplified models [14–16], where the masses of the SUSY particles are the only free parameters, are used for interpretation. The $\tilde{\chi}_1^{\pm}$ and $\tilde{\chi}_2^0$ are assumed to be purely wino and mass degenerate, and to decay with 100% branching ratio into W and Z bosons. The $\tilde{\chi}_1^0$ LSP is assumed to be pure bino. Both the W and Z bosons decay leptonically via SM branching ratios, leading to a final-state signature with three leptons and missing transverse momentum from two $\tilde{\chi}_1^0$ and a neutrino. The presence of initial-state radiation (ISR) may lead to jets in the final state and boost the $\tilde{\chi}_1^{\pm}\tilde{\chi}_2^0$ system, enhancing the signature of the missing transverse momentum. The search targets a range of $\tilde{\chi}_1^{\pm}/\tilde{\chi}_2^0$ masses between 100[1] and 450 GeV and mass splittings relative to the $\tilde{\chi}_1^0$ LSP, $\Delta m = m(\tilde{\chi}_1^{\pm}/\tilde{\chi}_2^0) - m(\tilde{\chi}_1^0)$, larger than the Z boson mass.

Previous searches for $\tilde{\chi}_1^{\pm}\tilde{\chi}_2^0$ production by the ATLAS [21–23] and CMS [24–27] collaborations using laboratory-frame, or conventional, observables in final states with two or three leptons, have found no significant excess of events in data over background expectations, yielding limits on the

[*]Full author list given at the end of the article.

[1]A model-independent lower limit of 103.5 GeV at the 95% confidence level on the mass of promptly decaying charginos was set at the Large Electron-Positron Collider experiment [17–20].

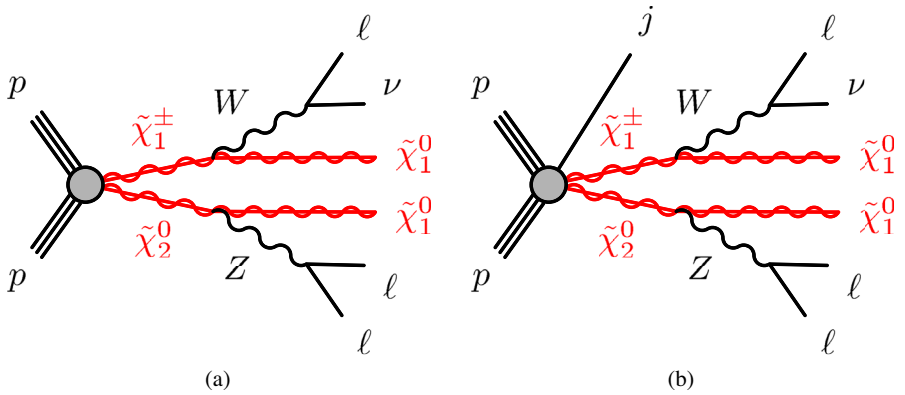

FIG. 1. Diagrams of $\tilde{\chi}_1^{\pm}\tilde{\chi}_2^0$ production with subsequent decays into two $\tilde{\chi}_1^0$ and, via leptonically decaying W and Z bosons, three leptons and a neutrino. Diagrams are shown both (a) without and (b) with a jet from initial-state radiation.

$\tilde{\chi}_1^{\pm}$ and $\tilde{\chi}_2^0$ masses up to 580 and 570 GeV, respectively. A search by the ATLAS Collaboration using the recursive jigsaw reconstruction (RJR) technique [28,29] in 36.1 fb^{-1} of data collected between 2015 and 2016 [30] found excesses of three-lepton events in two regions. The excesses corresponded to a local significance of 2.1σ in the signal region targeting low-mass $\tilde{\chi}_1^{\pm}\tilde{\chi}_2^0$ production, SR-low, and to a local significance of 3.0σ in the signal region targeting $\tilde{\chi}_1^{\pm}\tilde{\chi}_2^0$ produced in association with ISR, SR-ISR, with mass differences with respect to the LSP close to the Z boson mass. The signal regions of the RJR analysis targeting high-mass $\tilde{\chi}_1^{\pm}\tilde{\chi}_2^0$ production showed no substantial excess, with limits set on the $\tilde{\chi}_1^{\pm}$ and $\tilde{\chi}_2^0$ masses of up to 600 GeV for a massless $\tilde{\chi}_1^0$.

This new, independent analysis explores the intersection between the conventional and RJR approaches to better understand the tension between the exclusion limits produced by the two analyses. It emulates the variables used by the RJR technique with conventional laboratory-frame discriminating variables, providing a simple set of variables that are easily reproducible. The object and region definitions using these new emulated recursive jigsaw reconstruction (eRJR) variables are kept as close as possible to those in Ref. [30]. This technique reproduces the three-lepton excesses in the low-mass region and ISR regions in the laboratory frame using the same 36.1 fb^{-1} of pp collision data. Results of this conventional search are also presented using a larger data set, corresponding to 139 fb^{-1} of pp collision data collected between 2015 and 2018.

A brief overview of the ATLAS detector is presented in Sec. II, and a description of the data set and the simulation of the $\tilde{\chi}_1^{\pm}\tilde{\chi}_2^0$ signal process and SM background processes is given in Sec. III. The reconstruction of the event and of objects used in the search is described in Sec. IV. The eRJR kinematic discriminating variables are introduced in Sec. V. The search strategy is presented in Sec. VI, followed by the background estimation and validation in Sec. VII, and the systematic uncertainty derivation in Sec. VIII. The results of the search are presented in Sec. IX, followed by the conclusion in Sec. X.

II. ATLAS DETECTOR

The ATLAS detector [31] is a multipurpose particle detector with almost 4π coverage in solid angle.[2] It consists of an inner tracking system covering the pseudorapidity region $|\eta| < 2.5$, sampling electromagnetic and hadronic calorimeters covering $|\eta| < 4.9$, and a muon spectrometer covering $|\eta| < 2.7$. The inner detector (ID) reconstructs charged-particle tracks using silicon pixel and microstrip detectors and a straw-tube transition radiation tracker. An additional innermost layer of the silicon pixel tracker, the insertable B-layer [32,33], was installed before 2015 at an average radial distance of 3.3 cm from the beam line to improve track reconstruction and flavor identification of quark-initiated jets. The ID is surrounded by a thin, superconducting solenoid providing an axial magnetic field of 2 T, allowing the measurement of charged-particle momenta. Beyond the ID is a high-granularity lead/liquid-argon (LAr) electromagnetic sampling calorimeter covering $|\eta| < 3.2$ and a steel/scintillator-tile hadronic sampling calorimeter covering $|\eta| < 1.7$. The forward regions in $|\eta|$ are also covered by the copper/LAr hadronic end cap calorimeter ($1.7 < |\eta| < 3.2$) and by copper or tungsten/LAr forward calorimeters ($3.1 < |\eta| < 4.9$).

[2]ATLAS uses a right-handed coordinate system with its origin at the nominal interaction point (IP) in the center of the detector and the (z) axis along the beam pipe. The (x) axis points from the IP to the center of the LHC ring, and the (y) axis points upwards. Cylindrical coordinates (r, ϕ) are used in the transverse plane, with ϕ being the azimuthal angle around the (z) axis. The pseudorapidity η is defined in terms of the polar angle θ as $\eta = -\ln\tan(\theta/2)$ and the rapidity y is defined as $y = (1/2)\ln[(E + p_z)/(E - p_z)]$, where E is the energy and p_z is the longitudinal momentum of the physics object. Angular distance is measured in units of $\Delta R \equiv \sqrt{(\Delta\eta)^2 + (\Delta\phi)^2}$, defined using η unless otherwise specified.

The muon spectrometer (MS) surrounds the calorimeters and measures muon tracks within a system of three superconducting air-core toroidal magnets with eight coils each. The MS consists of three layers of precision tracking and triggering chambers.

The ATLAS trigger system consists of a hardware-based first-level (L1) trigger followed by a software-based high-level trigger (HLT) [34]. The L1 trigger is designed to use a subset of detector information to accept events at an average rate of 100 kHz, while the HLT is designed to reduce the rate to an average of 1 kHz. Candidate electrons are identified by the L1 trigger within the range $|\eta| < 2.5$ as compact electromagnetic energy deposits in the electromagnetic calorimeter, and by the HLT using additional fast track reconstruction [35]. Candidate muons are identified by the L1 trigger through a coincidence of MS trigger chamber layers and further selected by the HLT using fast reconstruction algorithms with input from the ID and MS.

III. DATA AND MONTE CARLO SIMULATION

The data used for this search were collected between 2015 and 2018 by the ATLAS experiment and correspond to an integrated luminosity of 139 fb^{-1}. The LHC collided protons at bunch-crossing intervals of 25 ns, with the average number of interactions per crossing measured in the data set to be $\langle\mu\rangle = 34$.

Monte Carlo (MC) simulation is used to model the expected contributions of various SM processes as well as possible SUSY signals. The MC simulation is also used to optimize the event selection criteria and estimate the systematic uncertainties of the event yield measurement. A full description of the MC simulation samples used is given below and summarized in Table I. For most SM backgrounds, the expected contributions are taken from MC simulation, either directly or after normalization to data in dedicated control regions. For Z + jets processes a data-driven method is used to predict the expected yield as described in Sec. VII, with MC simulation used in developing the method and estimating uncertainties.

Diboson, triboson, and Z + jets samples [36,37] were simulated with the SHERPA2.2 [38] generator. Diboson samples include fully leptonic and semileptonic decays as well as loop-induced and electroweak $VVjj$ production, where V refers to a Z or W vector boson and j indicates a jet. The WH and ZH processes, with the Higgs boson (H) decaying into two W or two Z bosons, are included in the diboson and triboson samples. The fully leptonic, the loop-induced, and the electroweak $VVjj$ diboson processes were simulated with SHERPA2.2.2, while the triboson, Z + jets, and semileptonically decaying diboson samples were simulated with SHERPA2.2.1.

In the SHERPA samples the additional hard parton emissions [39] were matched to parton showers based on Catani-Seymour dipole factorization [40]. The `NNPDF3.0nnlo` [41] set of parton distribution functions (PDFs) and a dedicated set of tuned parton-shower parameters (tune) developed by the SHERPA authors were used [40]. The matching of the matrix element to the parton shower [42–45] was employed for the various jet multiplicities, which were then merged into an inclusive sample using an improved CKKW matching procedure [44] that is extended to next-to-leading-order (NLO) accuracy using the MEPS@NLO prescription [43]. The virtual QCD correction for matrix elements at NLO accuracy was provided by the OpenLoops library [46,47]. The Z + jets (diboson) simulations were calculated for up to two (one) additional partons at NLO and up to four (three) additional partons at LO, while the triboson simulations were calculated for up to one additional parton at LO. The cross sections predicted by these event generators were used for all samples except for the Z + jets processes, which were normalized to a next-to-next-to-leading-order (NNLO) cross-section prediction [48].

The production of $t\bar{t}$ [49], $t\bar{t}H$ [50], and single-top tW [51], s-channel [52], and t-channel [53] events was modeled using the POWHEG-BOX [54–56] v2 generator at NLO with the `NNPDF3.0nnlo` PDF set. The events were interfaced with PYTHIA8.230 [57] using the A14 tune [58]

TABLE I. Monte Carlo simulation details by physics process. Listed are the generators used for matrix element calculation and for parton showering, the underlying-event parameter tunes, the PDF sets, and the order in α_S of cross-section calculations used for the yield normalization. "Other top" includes tZ, tWZ, $t\bar{t}WZ$, $t\bar{t}WW$, three-top, four-top, and rare top decay $t\bar{t}$ ($t \to Wb\ell\ell$) processes.

Process	Event generator	PS and hadronization	UE tune	Cross section
$\tilde{\chi}_1^{\pm}\tilde{\chi}_2^0$	MadGraph2.6	PYTHIA8	A14	NLO + NLL
Diboson	SHERPA2.2	SHERPA2.2	Default	NLO
Triboson	SHERPA2.2	SHERPA2.2	Default	LO
Z + jets	SHERPA2.2	SHERPA2.2	Default	NNLO
$t\bar{t}$	POWHEG-BOXv2	PYTHIA8	A14	NNLO + NNLL
Single top	POWHEG-BOX v2	PYTHIA8	A14	NLO + NNLL
$t\bar{t}H$	POWHEG-BOX v2	PYTHIA8	A14	NLO
$t\bar{t}V$	MadGraph5_aMC@NLO2	PYTHIA8	A14	NLO
Other top	MadGraph5_aMC@NLO2	PYTHIA8	A14	LO

and the NNPDF2.3lo PDF set [59]. The h_{damp} parameter[3] was set to 1.5 times the top-quark mass [60]. The $t\bar{t}$ inclusive production cross section was corrected to the theory prediction at NNLO in QCD including the resummation of next-to-next-to-leading-logarithmic (NNLL) soft-gluon terms calculated using TOP++2.0 [61]. The tW inclusive cross section was corrected to the theory prediction calculated at NLO in QCD with NNLL soft-gluon corrections [62,63]. Samples were generated in the five-flavor scheme, setting all quark masses to zero except for the top quark, and a diagram removal strategy [64] was employed in the tW sample to handle the interference with $t\bar{t}$ production [60].

The production of other top-quark processes was modeled using the MadGraph5_aMC@NLO v2 [65] generator with the NNPDF3.0nnlo PDF set for the calculation of the matrix elements, which were interfaced with PYTHIA8 using the A14 tune and the NNPDF2.3lo PDF set. Generator versions MadGraph5_aMC@NLO v2.2.2 and PYTHIA8.186 were used for $t\bar{t}WW$, three-top, and four-top processes, while MadGraph5_aMC@NLO v2.3.3 and PYTHIA8.212 were used for tZ, tWZ, $t\bar{t}V$, and $t\bar{t}WZ$ processes, as well as for $t\bar{t}$ events that include the rare top decay $t \to Wb\ell\ell$. All these top-quark processes were generated at LO except for $t\bar{t}V$, which was generated at NLO.

The SUSY $\tilde{\chi}_1^{\pm}\tilde{\chi}_2^0$ signal events were produced with up to two additional partons at LO using MadGraph5_AMC@NLO v2.6.1 with the NNPDF2.3lo PDF set, and were interfaced with PYTHIA8.230 using the A14 tune and NNPDF2.3lo PDF set. The scale parameter for jet-parton CKKW-L matching was set to a quarter of the $\tilde{\chi}_1^{\pm}/\tilde{\chi}_2^0$ mass. Signal cross sections were calculated at NLO in α_S, adding the resummation of soft-gluon emission at next-to-leading-logarithm accuracy (NLL) [66–70]. The nominal cross section and the uncertainty are taken from an envelope of cross section predictions using different PDF sets and factorization and renormalization scales [71]. The inclusive cross section for $\tilde{\chi}_1^{\pm}\tilde{\chi}_2^0$ production, when each has a mass of 200 GeV, is 1.8 ± 0.1 pb.

The decays of c and b hadrons in samples generated with MadGraph5_aMC@NLO or POWHEG-BOX were modeled with EvtGen1.2.0 [72]. Events from all generators were propagated through a full simulation of the ATLAS detector [73] using GEANT4 [74], which describes the interactions of particles with the detector. A parameterized simulation of the ATLAS calorimeter called Atlfast-II [73] was used for faster detector simulation of signal samples and is found to agree well with the full simulation. The effect of multiple interactions in the same and neighboring bunch crossings (pileup) was modeled by overlaying each hard-scattering event with simulated minimum-bias events generated with PYTHIA8.210 using the A3 tune [75] and NNPDF2.3lo PDF set.

[3]The h_{damp} parameter controls the transverse momentum p_T of the first additional emission beyond the leading-order Feynman diagram in the parton shower and therefore regulates the high-p_T emission against which the $t\bar{t}$ system recoils.

IV. EVENT RECONSTRUCTION

Analysis events were recorded during stable beam conditions and must pass detector and data quality requirements. Each event is required to have a primary vertex that is associated with a minimum of two tracks of transverse momentum $p_T > 500$ MeV, where the primary vertex is defined as the reconstructed vertex with the largest Σp_T^2 of associated tracks [76].

Two identification levels are defined for leptons and jets, referred to as "baseline" and "signal," with signal objects being a subset of baseline. The baseline leptons are required to satisfy looser identification and isolation criteria, providing a higher selection efficiency for leptons and jets for use in calculating missing transverse momentum ($\mathbf{p}_T^{\text{miss}}$), resolving ambiguities between overlapping physics objects, and calculating the data-driven estimate of the background arising from fake or nonprompt leptons.

Electron candidates are reconstructed using energy clusters in the electromagnetic calorimeter which are matched to an ID track, and they are calibrated *in situ* using $Z \to ee$ decays [77]. Baseline electrons must have $p_T > 10$ GeV and fall within the ID acceptance, $|\eta| < 2.47$. The electrons must also satisfy the "loose likelihood" quality criteria [77]. The trajectory of baseline electrons must be consistent with the primary vertex to suppress electrons originating from pileup. Therefore, the tracks associated with baseline electrons must have a longitudinal impact parameter relative to the primary vertex (z_0) such that $|z_0 \sin\theta| < 0.5$ mm. Signal electrons are required to satisfy the tighter "medium" identification criteria and must be well isolated from additional activity, passing a p_T -dependent "tight" isolation requirement that imposes fixed requirements on the values of the isolation variables. The isolation is measured within a cone of size $\Delta R = 0.2$ around the electron, and the amount of non-associated calorimeter transverse energy and scalar sum of track p_T must both be below 6% of the electron p_T. Tracks are only considered by the isolation criteria if they are consistent with the primary vertex. For track isolation, the cone size decreases linearly with p_T above 50 GeV as the electron's shower becomes more collimated. The track associated with each signal electron must also pass a requirement on the transverse-plane distance of closest approach to the beam line (d_0) such that $|d_0/\sigma_{d_0}| < 5$, where σ_{d_0} is the uncertainty in the value of d_0.

Muon candidates are reconstructed from either ID tracks matched to track segments in the MS or from tracks formed from a combined fit in the ID and MS [78], and they are calibrated *in situ* using $Z \to \mu\mu$ and $J/\psi \to \mu\mu$ decays [78]. Baseline muons must have $p_T > 10$ GeV, have $|\eta| < 2.4$

and pass an impact parameter cut of $|z_0 \sin\theta| < 0.5$ mm. Signal muons must meet the "medium" identification criteria [78] and the "tight" isolation criteria, defined similarly to those for electrons but rejecting candidates with nonassociated calorimeter energy above 15% and nonassociated track p_{T} above 4% of the muon p_{T}. The size of the track-isolation cone is $\Delta R = 0.3$ for muons with $p_{\mathrm{T}} \leq 33$ GeV and decreases linearly to $\Delta R = 0.2$ at $p_{\mathrm{T}} = 50$ GeV, improving the selection efficiency for higher-p_{T} muons. The track associated with each signal muon must pass an impact parameter requirement of $|d_0/\sigma_{d_0}| < 3$.

Jet candidates are reconstructed from three-dimensional topological energy clusters [79] using the anti-k_t algorithm [80,81] with radius parameter $R = 0.4$. The jet energy scale (JES) and resolution (JER) are first calibrated to particle level using MC simulation and then *in situ* through $Z +$ jet, $\gamma +$ jet, and multijet measurements [82]. Baseline jets are required to have $p_{\mathrm{T}} > 20$ GeV and fall within the full calorimeter acceptance of $|\eta| < 4.5$. To suppress jets originating from pileup, jets are required to pass the "medium" working point of the track-based jet vertex tagger [83,84] if the jet has $p_{\mathrm{T}} < 120$ GeV and falls within the ID acceptance of $|\eta| < 2.5$. Signal jets are required to have $|\eta| < 2.4$ to ensure full application of the pileup suppression, and events are rejected if they contain a jet that fails to meet the "loose" quality criteria [85], reducing contamination from noise bursts and noncollision backgrounds.

The identification of jets containing b hadrons, called b jets, is performed using a multivariate discriminant built with information from track impact parameters, the presence of displaced secondary vertices, and the reconstructed flight paths of b and c hadrons inside the jet [86]. The identification criteria are tuned to an average identification efficiency of 77% as obtained for b jets in simulated $t\bar{t}$ events, corresponding to rejection factors of 110, 4.9, and 15 for jets originating from light quarks and gluons, c quarks, and τ leptons, respectively.

To avoid reconstructing a single detector signature as multiple leptons or jets, an overlap removal procedure is applied to baseline leptons and jets. For overlap removal, ΔR is calculated using rapidity, rather than η, to ensure the distance measurement is Lorentz invariant for jets that may have non-negligible masses. First, any electron that shares a track with a muon in the ID is removed, as the track is seen to be consistent with track segments in the MS. Then, jets are removed if they are within $\Delta R = 0.2$ of a lepton, as they have likely formed from an electron shower or muon bremsstrahlung. For the overlap with associated muons, the nearby jet is discarded only if it is associated with less than three tracks of $p_{\mathrm{T}} \geq 500$ MeV. Finally, electrons and muons with $p_{\mathrm{T}} \leq 50$ GeV that are close to a remaining jet are discarded to reject nonprompt or fake leptons originating from hadron decays. Leptons with $p_{\mathrm{T}} \leq 25$ GeV are discarded if their distance from a jet is $\Delta R < 0.4$; for larger lepton p_{T} values up to 50 GeV the ΔR discard range decreases linearly to $\Delta R < 0.2$.

The missing transverse momentum $\mathbf{p}_{\mathrm{T}}^{\mathrm{miss}}$, with magnitude $E_{\mathrm{T}}^{\mathrm{miss}}$, is calculated as the negative vector sum of the transverse momenta of the baseline leptons, jets, and the soft term, the latter given by the sum of the transverse momenta of additional low-momentum objects in the event [87]. The soft term is reconstructed from particle tracks in the ID that are associated with the primary vertex but not with any reconstructed analysis objects.

Data events were collected with triggers requiring either two electrons, two muons or an electron plus a muon. The triggers have lepton p_{T} thresholds in the range 8–22 GeV, and higher p_{T} thresholds are applied offline to ensure that the trigger efficiencies are constant in the relevant phase space. All MC simulation samples emulate the triggers and have corrections applied to account for small differences with data in lepton identification, reconstruction, isolation and triggering efficiencies, as well as in jet pileup rejection and flavor identification efficiencies.

V. KINEMATIC DISCRIMINANTS

In most R-parity-conserving SUSY models, the LSP is an invisible particle that rarely, if ever, interacts with matter. It is therefore not directly observed by the ATLAS detector, but manifests itself as missing transverse momentum in an event whose particle transverse momenta would otherwise balance. The relative boost of quarks in the colliding protons makes it impossible to know the true vector of the missing momentum, allowing only the transverse component to be measured accurately. For SUSY particles with multiple decay steps the loss of this information can make it difficult to match the decay products and correctly reconstruct the originally produced particles, resulting in ambiguities in the reconstruction of the $\tilde{\chi}_1^{\pm}$ and the $\tilde{\chi}_2^0$.

The RJR technique [28,29] attempts to resolve these ambiguities by analyzing each event starting from the laboratory-frame particles and boosting back to the rest frames of the parent particles. Reconstructed jets, muons, and electrons are used as inputs for the RJR algorithm, which determines which leptons originate from the chargino or neutralino decays, assuming a specific decay chain. The ISR jets are selected by minimizing the invariant mass of the system formed by the potential ISR jets and the sparticle system (consisting of the leptons and the missing-momentum vector) in the center-of-mass frame. The only unknowns are the masses and longitudinal momenta of the invisible objects (two neutralinos and a neutrino), and how each individually contributes to the total missing energy. The RJR algorithm determines the smallest Lorentz-invariant function of the visible particles' four-momenta that results in non-negative mass parameters for the invisible particles [29].

This search targets $\tilde{\chi}_1^{\pm}\tilde{\chi}_2^0$ signals using an ISR region requiring the presence of one or more jets and a low-mass region with a jet veto. The eRJR technique emulates the RJR variables by using minimal assumptions about the mass of the invisible system and calculates all kinematic variables in the laboratory frame.

The eRJR variables, with original RJR variable names from Ref. [30], used to select the ISR regions are defined as follows:

(1) $E_{\mathrm{T}}^{\mathrm{miss}}$: $p_{\mathrm{T}}^{\mathrm{I}}$, the p_{T} of the invisible particles, is emulated as the magnitude of the missing transverse momentum.
(2) $p_{\mathrm{T}}^{\mathrm{jets}}$: $p_{\mathrm{T}}^{\mathrm{ISR}}$, the p_{T} in the vector sum of the ISR jets' momenta. In the eRJR technique, the ISR system includes all signal jets in the event.
(3) $|\Delta\phi(E_{\mathrm{T}}^{\mathrm{miss}},\mathrm{jets})|$: $\Delta\phi_{\mathrm{ISR},E_{\mathrm{T}}^{\mathrm{miss}}}$, the azimuthal angle between the ISR system and the invisible particles, is emulated using the missing transverse momentum, $\mathbf{p}_{\mathrm{T}}^{\mathrm{miss}}$, and the vector sum of the signal jets' momenta.
(4) $R(E_{\mathrm{T}}^{\mathrm{miss}},\mathrm{jets})$: R_{ISR}, the normalized projection of the invisible system onto the ISR system, representing a ratio of $\mathbf{p}_{\mathrm{T}}^{\mathrm{miss}}$ to total jet p_{T}, is emulated as $|\mathbf{p}_{\mathrm{T}}^{\mathrm{miss}}\cdot\hat{\mathbf{p}}_{\mathrm{T}}^{\mathrm{jets}}|/p_{\mathrm{T}}^{\mathrm{jets}}$, where $\hat{\mathbf{p}}_{\mathrm{T}}^{\mathrm{jets}}$ is the unit vector of the vector sum of the signal jets' transverse momenta.
(5) $p_{\mathrm{T}}^{\mathrm{soft}}$: $p_{\mathrm{T}}^{\mathrm{CM}}$, the transverse momentum in the center-of-mass frame, where the ISR system recoils against the system containing the leptons and the missing energy, is emulated as the p_{T} in the vector sum of the four-momenta of the signal jets, leptons, and $\mathbf{p}_{\mathrm{T}}^{\mathrm{miss}}$, and is highly correlated with the $E_{\mathrm{T}}^{\mathrm{miss}}$ soft term, defined in Sec. IV.

Similarly, the eRJR variables, with original RJR variable names from Ref. [30] in parentheses, used in the low-mass regions are defined as follows:

(1) $p_{\mathrm{T}}^{\mathrm{soft}}$: $p_{\mathrm{T}}^{\mathrm{PP}}$, the transverse momentum in the rest frame of the pair-produced sparticles (PP), is emulated as the p_{T} in the vector sum of the four-momenta of the signal leptons and $\mathbf{p}_{\mathrm{T}}^{\mathrm{miss}}$, and is identical to that of the ISR region except for the jet veto applied to the low-mass region.
(2) $m_{\mathrm{eff}}^{3\ell}$: $H_{\mathrm{T3,1}}^{\mathrm{PP}}$, the scalar sum of the p_{T} of the signal leptons and the invisible system (neutrino and LSPs) in the PP frame, is emulated as the scalar sum of the p_{T} of the signal leptons and $E_{\mathrm{T}}^{\mathrm{miss}}$.
(3) H^{boost}: $H_{3,1}^{\mathrm{PP}}$, the scalar sum of the magnitude of the momenta of the signal leptons and the invisible system (neutrino and LSPs) in the PP frame, is emulated as the scalar sum of the momentum of the signal leptons and the missing-momentum vector (which includes longitudinal and transverse components), $|\mathbf{p}^{\mathrm{miss}}|$, after applying a boost.

To calculate H^{boost}, the longitudinal component of the missing-momentum vector, $p_{\parallel}^{\mathrm{miss}}$, and the boost need to be determined. The $p_{\parallel}^{\mathrm{miss}}$ variable is calculated as [29]

$$p_{\parallel}^{\mathrm{miss}} = p_{V,\parallel}\frac{|\mathbf{p}_{\mathrm{T}}^{\mathrm{miss}}|}{\sqrt{(\mathbf{p}_{V,\mathrm{T}})^2+m_V^2}},$$

where $p_{V,\parallel}$ is the z component of the vector sum of the four-momenta of the three signal leptons, $p_{V,\mathrm{T}}$ is the magnitude of the transverse momentum in the vector sum of the four-momenta of the three leptons, and m_V is the mass of the three-lepton system. The invariant mass of the system of invisible particles is assumed to be zero and does not appear in the equation. The boost of the system can then be calculated as

$$\boldsymbol{\beta} = \frac{\mathbf{p}}{E} = \frac{\mathbf{p}^V + \mathbf{p}^{\mathrm{miss}}}{E^V + |\mathbf{p}^{\mathrm{miss}}|},$$

where $\mathbf{p}^V$ is the vector sum of the three-momenta of the three leptons, calculated in the laboratory frame. This boost is applied to the three leptons and the $\mathbf{p}^{\mathrm{miss}}$. These new objects are used in the calculation of H^{boost}.

The eRJR technique was validated against the published RJR result [30] and was able to reproduce an excess similar to that seen in the RJR analysis with the data set collected in 2015 and 2016. In SR-low, exactly the same data events were selected using the emulated variables as when using the RJR variables with similar background expectation. In SR-ISR, because all signal jets are considered part of the ISR system in the eRJR method, additional data events were selected alongside a proportional increase in the expected number of background events, with the significance of the excess in agreement with the RJR search. The signal significance in both the low-mass and ISR regions is comparable for both techniques. A strong correlation is found between eRJR and RJR variables in loosened signal regions, with only a slight decorrelation seen in $p_{\mathrm{T}}^{\mathrm{soft}}$ due to the differing jet selection, leading to the additional SR-ISR events. The eRJR technique provides a simple set of conventional variables in the laboratory frame that can easily be reproduced.

VI. SEARCH STRATEGY

This search is performed in signal regions (SRs) designed to select the targeted $\tilde{\chi}_1^{\pm}\tilde{\chi}_2^0$ signal events while accepting only a small but well-measured number of SM background events. The SM background yields in the SRs are estimated using dedicated control regions (CRs) and confirmed in validation regions (VRs), as described in Sec. VII. The full set of event selections is summarized in Table II and described below. To target leptonically decaying W and Z bosons from the electroweakinos, events must have exactly three leptons which pass the baseline and signal requirements defined in Sec. IV. The leptons must have at least one same-flavor opposite-charge (SFOS) pair (e^+e^- or $\mu^+\mu^-$) with an invariant mass $m_{\ell\ell}$ of the pair

TABLE II. Selection criteria for the low-mass and ISR regions. The variables are defined in the text. In addition, events are required to have three signal leptons, and a b-jet veto is applied. The invariant mass of the two leptons identified as coming from the Z boson decay is between 75 and 105 GeV, and the invariant mass of the three leptons is greater than 105 GeV.

	Selection criteria									
Low-mass region	$p_{\mathrm{T}}^{\ell_1}$ [GeV]	$p_{\mathrm{T}}^{\ell_2}$ [GeV]	$p_{\mathrm{T}}^{\ell_3}$ [GeV]	N_{jet}	m_{T} [GeV]	$E_{\mathrm{T}}^{\mathrm{miss}}$ [GeV]	H^{boost} [GeV]	$\frac{m_{\mathrm{eff}}^{3\ell}}{H^{\mathrm{boost}}}$	$\frac{p_{\mathrm{T}}^{\mathrm{soft}}}{p_{\mathrm{T}}^{\mathrm{soft}}+m_{\mathrm{eff}}^{3\ell}}$	
CR-low	>60	>40	>30	$=0$	$\in(0,70)$	>40	>250	>0.75	<0.2	
VR-low	>60	>40	>30	$=0$	$\in(70,100)$	-	>250	>0.75	<0.2	
SR-low	>60	>40	>30	$=0$	>100	-	>250	>0.9	<0.05	
ISR region	$p_{\mathrm{T}}^{\ell_1}$ [GeV]	$p_{\mathrm{T}}^{\ell_2}$ [GeV]	$p_{\mathrm{T}}^{\ell_3}$ [GeV]	N_{jet}	m_{T} [GeV]	$E_{\mathrm{T}}^{\mathrm{miss}}$ [GeV]	$\lvert\Delta\phi(E_{\mathrm{T}}^{\mathrm{miss}},\mathrm{jets})\rvert$	$R(E_{\mathrm{T}}^{\mathrm{miss}},\mathrm{jets})$	$p_{\mathrm{T}}^{\mathrm{jets}}$ [GeV]	$p_{\mathrm{T}}^{\mathrm{soft}}$ [GeV]
CR-ISR	>25	>25	>20	≥ 1	<100	>60	>2.0	$\in(0.55,1.0)$	>80	<25
VR-ISR	>25	>25	>20	≥ 1	>60	>60	>2.0	$\in(0.55,1.0)$	>80	>25
VR-ISR-small $p_{\mathrm{T}}^{\mathrm{soft}}$	>25	>25	>20	≥ 1	>60	>60	>2.0	$\in(0.55,1.0)$	<80	<25
VR-ISR-small $R(E_{\mathrm{T}}^{\mathrm{miss}},\mathrm{jets})$	>25	>25	>20	≥ 1	>60	>60	>2.0	$\in(0.30,0.55)$	>80	<25
SR-ISR	>25	>25	>20	$\in[1,3]$	>100	>80	>2.0	$\in(0.55,1.0)$	>100	<25

between 75 and 105 GeV, consistent with the Z boson mass. If there is more than one SFOS pair, the pair chosen is the one that has an invariant mass closest to the Z boson mass.

The leading source of SM background is WZ production, which for fully leptonic decays has three leptons and $E_{\mathrm{T}}^{\mathrm{miss}}$ from a neutrino in the final state. To reduce the WZ contribution, the transverse mass is calculated from the unpaired third lepton and the $E_{\mathrm{T}}^{\mathrm{miss}}$. It is defined as $m_{\mathrm{T}}=\sqrt{2p_{\mathrm{T}}E_{\mathrm{T}}^{\mathrm{miss}}(1-\cos(\Delta\phi))}$, where $\Delta\phi$ is the azimuthal separation between the lepton and $\mathbf{p}_{\mathrm{T}}^{\mathrm{miss}}$, and it will typically be at or below the W boson mass in SM events where the $E_{\mathrm{T}}^{\mathrm{miss}}$ is predominantly from the neutrino of the W decay. The m_{T} calculated in $\tilde{\chi}_1^{\pm}\tilde{\chi}_2^0$ events does not have such a constraint, and the SRs therefore require $m_{\mathrm{T}}\geq 100$ GeV to reduce the SM WZ background. Additionally, signal events usually have larger values of $E_{\mathrm{T}}^{\mathrm{miss}}$ due to the undetected LSPs. The backgrounds in which one or more leptons are fake or nonprompt are reduced by targeting the source of the additional leptons. Events containing b-tagged jets are rejected to minimize contributions from the top backgrounds $t\bar{t}$ and Wt. In the $Z+$ jets background, a third signal lepton can arise from photon conversion, where the photon originates from the bremsstrahlung of a lepton off the Z boson. In this situation, all three signal leptons originate from the Z boson, and this background can be reduced by requiring that the invariant mass $m_{\ell\ell\ell}$ of the three-lepton system be larger than 105 GeV.

The signal regions are split into two different topologies: SR-low, the low-mass region that requires a signal jet veto, and SR-ISR, the ISR region that requires at least one central signal jet. Both SRs are optimized for signals with small mass splittings, which can lead to events with lower-p_{T} leptons or smaller $E_{\mathrm{T}}^{\mathrm{miss}}$ in the final state. The inclusion of recoiling ISR boosts the invisible decay products in the same direction, enhancing the measured $E_{\mathrm{T}}^{\mathrm{miss}}$ and improving the discrimination between signal and the lower-$E_{\mathrm{T}}^{\mathrm{miss}}$ WZ background.

The low-mass signal region requires the p_{T} of the first, second, and third leptons (ordered in decreasing p_{T}) to be greater than 60, 40, and 30 GeV, respectively, to minimize contributions from backgrounds with fake or nonprompt leptons. Tight selection thresholds for H^{boost}, $p_{\mathrm{T}}^{\mathrm{soft}}/(p_{\mathrm{T}}^{\mathrm{soft}}+m_{\mathrm{eff}}^{3\ell})$, and $m_{\mathrm{eff}}^{3\ell}/H^{\mathrm{boost}}$ further reduce the WZ contribution in the signal region. The ISR region has a requirement of $E_{\mathrm{T}}^{\mathrm{miss}}\geq 80$ GeV to reduce the $Z+$ jets background, which does not have a source of real $E_{\mathrm{T}}^{\mathrm{miss}}$. The p_{T} requirements on the three leptons can then be relaxed to be greater than 25, 25, and 20 GeV, respectively, while ensuring that the dilepton triggers remain fully efficient. To select the ISR topology in which the system of leptons and $E_{\mathrm{T}}^{\mathrm{miss}}$ is recoiling against the ISR jets, the azimuthal separation between the signal jets and $\mathbf{p}_{\mathrm{T}}^{\mathrm{miss}}$, $\Delta\phi(E_{\mathrm{T}}^{\mathrm{miss}},\mathrm{jets})$, is required to be greater than 2.0. The ratio of the $\mathbf{p}_{\mathrm{T}}^{\mathrm{miss}}$ to the total transverse momenta of the jets is required to be $0.55\leq R(E_{\mathrm{T}}^{\mathrm{miss}},\mathrm{jets})\leq 1.0$ to ensure that most of the transverse momentum along the jet axis is carried by the invisible particles and not by the high-p_{T} leptons from the WZ background. Requirements of $p_{\mathrm{T}}^{\mathrm{soft}}$ less than 25 GeV and jet multiplicity N_{jet} less than four further reduce background contamination from WZ events.

VII. BACKGROUND ESTIMATION AND VALIDATION

The backgrounds in this analysis can be classified into two groups: irreducible backgrounds with at least three prompt leptons in the final state, and reducible backgrounds

containing at least one fake or nonprompt lepton. The dominant irreducible background is WZ production, which is estimated by normalizing the yields in MC simulation to data in CRs using a log-likelihood fit described in Sec. IX. Additional irreducible backgrounds include ZZ and triboson production and processes that include a Higgs boson, three or more tops, and tops produced in association with a W or Z boson. These backgrounds are estimated directly from MC simulation because of their small contribution. The reducible backgrounds can be categorized into the top-quark-like $t\bar{t}$, Wt, and WW processes, which are kinematically similar and mostly consist of nonprompt leptons from heavy-flavor hadron decays, and the $Z+\text{jets}$ process, which also accounts for the $Z+\gamma$ process, with fake or nonprompt leptons originating primarily from misidentified jets or photon conversions. The majority of the fake leptons from $Z+\text{jets}$ are electrons from light flavor hadron decays, while few events are from photon conversions. The reducible backgrounds are estimated separately in regions enriched in fake and nonprompt leptons, one region targeting top-quark-like processes and another targeting other fake/nonprompt sources, usually $Z+\text{jets}$ processes, as described below.

The CRs for the WZ background are designed to be kinematically similar but orthogonal to SR-low and SR-ISR. They are enriched in WZ events and the potential signal contamination is kept small (less than 10% for all signal models). To achieve this, an upper bound is placed on the m_{T} of the CRs, targeting events that are likely to have a leptonically decaying W boson and no other sources of real $E_{\mathrm{T}}^{\mathrm{miss}}$. The low-mass CR (CR-low) therefore requires $m_{\mathrm{T}} < 70$ GeV while the ISR CR (CR-ISR) has a slightly looser requirement of $m_{\mathrm{T}} < 100$ GeV, benefiting from the boost of the $E_{\mathrm{T}}^{\mathrm{miss}}$ system by the ISR. The other kinematic selections are similar to those for the corresponding SRs but are also loosened to accept more WZ events and reduce contamination from signal, as shown in Table II. Figure 2 shows the background composition in the CR-low and CR-ISR regions, with good agreement seen between data and the background prediction after the fit.

The data-driven fake-factor method [88,89] is used to estimate the fake/nonprompt-lepton background associated with the $Z+\text{jets}$ process. The fake-factor method uses two levels of lepton identification criteria. The regular identification ("reg-ID") criteria correspond to the signal lepton criteria used in the analysis. The reversed identification ("anti-ID") criteria have one or more of the identification, isolation, or impact parameter criteria inverted relative to those of the signal leptons to obtain a selection enriched in fake leptons. A fake factor is then defined as the ratio of the yield of reg-ID leptons to the yield of anti-ID leptons in a given region of phase space. The fake factors are measured in a region dominated by $Z+\text{jets}$ events, requiring $E_{\mathrm{T}}^{\mathrm{miss}} < 40$ GeV, $m_{\mathrm{T}} < 30$ GeV, $|m_{\ell\ell} - m_Z| < 15$ GeV, and a b-jet veto. The two leptons identified as the Z boson decay products must pass the signal lepton requirements, while the unpaired lepton must satisfy either the reg-ID or anti-ID criteria. Electron and muon fake factors are then

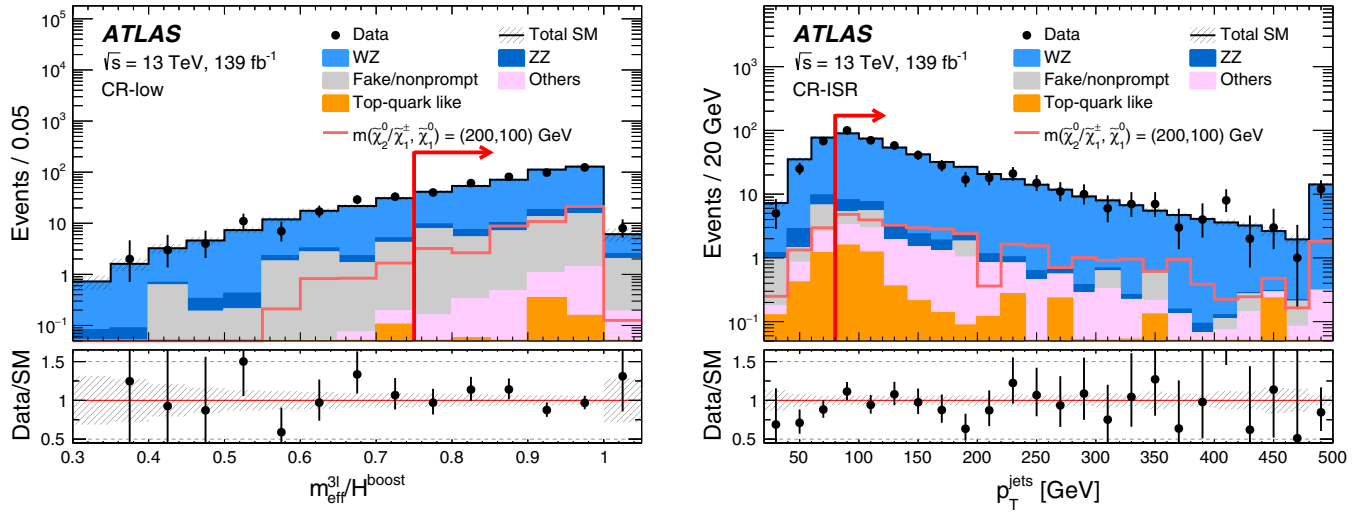

FIG. 2. Examples of kinematic distributions after the background-only fit, showing the data and the post-fit background in (a) CR-low for $m_{\mathrm{eff}}^{3\ell}/H^{\mathrm{boost}}$ and (b) CR-ISR for $p_{\mathrm{T}}^{\mathrm{jets}}$. The corresponding CR event selections are applied for each distribution except for the variable shown, where the selection is indicated by a red arrow. The first (last) bin includes underflow (overflow). The "Top-quark like" category contains the $t\bar{t}$, Wt, and WW processes while the "Others" category contains backgrounds from triboson production and processes that include a Higgs boson, three or more tops, and tops produced in association with W or Z bosons. The bottom panel shows the ratio of the data to the post-fit background prediction. The hatched bands indicate the combined theoretical, experimental, and MC statistical uncertainties.

TABLE III. The observed and expected yields after the background-only fit in the low-mass CR and VR. The normalization factors of the WZ sample for the low-mass and ISR regions are different and are treated separately in the combined fit. The "Top-quark like" category contains the $t\bar{t}$, Wt, and WW processes while the "Others" category contains backgrounds from triboson production and processes that include a Higgs boson, three or more tops, and tops produced in association with W or Z bosons. Combined statistical and systematic uncertainties are presented. The individual uncertainties can be correlated and do not necessarily add in quadrature to equal the total background uncertainty.

	CR-low	VR-low
Observed events	412	338
Fitted SM events	412 ± 20	291 ± 20
WZ	343 ± 27	262 ± 22
ZZ	19.2 ± 1.6	18.2 ± 1.7
Others	3.0 ± 1.5	1.6 ± 0.8
Top-quark like	0.5 ± 0.4	$0.02^{+0.25}_{-0.02}$
Fake/nonprompt leptons	46 ± 17	10 ± 5

measured separately and as a function of lepton p_{T}. They are validated in a statistically independent region with a similar selection but requiring $E_{\mathrm{T}}^{\mathrm{miss}} < 40$ GeV and $30 < m_{\mathrm{T}} < 50$ GeV, so as to be closer to the signal region. The derived fake factors are applied to events satisfying the same criteria as for the CRs, VRs, and SRs (defined in Table II), while additionally requiring that at least one of the signal leptons is replaced by an anti-ID lepton. In both the derivation and application of the fake factors, the prompt lepton and top-quark-like backgrounds that have one or more anti-ID leptons are subtracted to avoid double counting.

The top-quark-like background contribution is estimated using MC simulation normalized to data in a top-quark-dominated CR. The region is constructed using different-flavor, opposite-charge ($e^{\pm}e^{\pm}\mu^{\mp}$ or $\mu^{\pm}\mu^{\pm}e^{\mp}$) trilepton events with lepton p_{T} thresholds of 25, 25, and 20 GeV as well as a b-jet veto. The normalization factors are applied to the same-flavor opposite-charge events in the top-quark-like MC simulation.

Four validation regions are designed in order to check that the background estimate agrees with data in regions kinematically closer to the SRs, typically targeting the extrapolation from CR to SR in a specific variable. The full VR definitions are summarized in Table II. The VR definitions are also chosen to keep the contamination from signal below 10%. A low-mass validation region, VR-low, is designed to test the extrapolation in m_{T} between CR-low and SR-low, requiring $70 < m_{\mathrm{T}} < 100$ GeV. Three ISR validation regions, VR-ISR, VR-ISR-small $p_{\mathrm{T}}^{\mathrm{soft}}$, and VR-ISR-small $R(E_{\mathrm{T}}^{\mathrm{miss}}, \mathrm{jets})$, invert different selections to validate the modeling in a varied phase space. The total yields in the CRs and VRs are shown in Table III for the low-mass regions and in Table IV for the ISR regions. Figure 3 shows distributions in VR-low, VR-ISR, VR-ISR-small $p_{\mathrm{T}}^{\mathrm{soft}}$, and VR-ISR-small $R(E_{\mathrm{T}}^{\mathrm{miss}}, \mathrm{jets})$ for the full background prediction. The background predictions and the observed data are generally in good agreement after the fit. The data and background predictions in VR-low and VR-ISR-small $p_{\mathrm{T}}^{\mathrm{soft}}$ agree within 2σ, and good agreement is seen in the shapes of relevant kinematic distributions.

VIII. SYSTEMATIC UNCERTAINTIES

Systematic uncertainties are derived for the signal and background predictions and include experimental uncertainties in detector measurements as well as theoretical uncertainties in the expected yields and MC simulation modeling.

Experimental uncertainties reflect the accuracy of the experimental measurements of jets, electrons, muons, and $E_{\mathrm{T}}^{\mathrm{miss}}$. The JES and JER uncertainties [82,90] are derived as a function of jet p_{T} and η and account for dependencies on

TABLE IV. The observed and expected yields after the background-only fit in the ISR CR and VRs. The normalization factors of the WZ sample for the low-mass and ISR regions are different and are treated separately in the combined fit. The "Top-quark like" category contains the $t\bar{t}$, Wt, and WW processes while the "Others" category contains backgrounds from triboson production and processes that include a Higgs boson, three or more tops, and tops produced in association with W or Z bosons. Combined statistical and systematic uncertainties are presented. The individual uncertainties can be correlated and do not necessarily add in quadrature to equal the total background uncertainty.

	CR-ISR	VR-ISR	VR-ISR-small $p_{\mathrm{T}}^{\mathrm{soft}}$	VR-ISR-small $R(E_{\mathrm{T}}^{\mathrm{miss}}, \mathrm{jets})$
Observed events	442	101	72	253
Fitted SM events	442 ± 21	111 ± 19	96 ± 7	256 ± 13
WZ	415 ± 22	98 ± 17	89 ± 7	245 ± 13
ZZ	9.1 ± 0.8	2.1 ± 0.5	2.6 ± 0.4	2.7 ± 0.4
Others	12 ± 6	6.9 ± 3.5	1.7 ± 0.9	6.2 ± 3.2
Top-quark like	4.7 ± 1.6	2.7 ± 1.1	1.5 ± 1.2	2.0 ± 1.0
Fake/nonprompt leptons	$1.5^{+2.3}_{-1.5}$	$0.9^{+1.6}_{-0.9}$	$1.3^{+1.6}_{-1.3}$	$0.01^{+0.05}_{-0.01}$

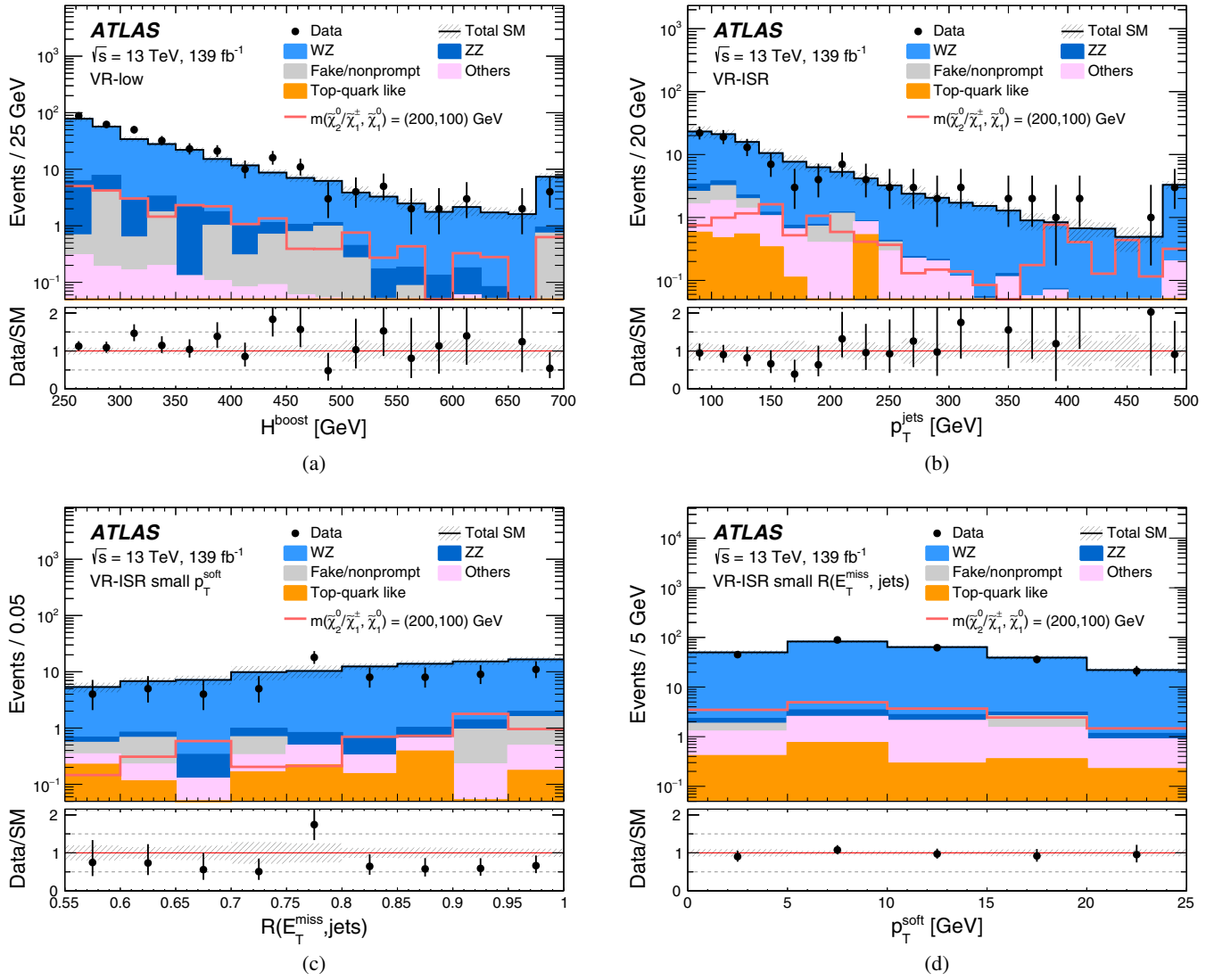

FIG. 3. Kinematic distributions showing the data and post-fit background in (a) VR-low for H^{boost}, (b) VR-ISR for $p_{\text{T}}^{\text{jets}}$, (c) VR-ISR-small $p_{\text{T}}^{\text{soft}}$ for $R(E_{\text{T}}^{\text{miss}},\text{jets})$, and (d) VR-ISR-small $R(E_{\text{T}}^{\text{miss}},\text{jets})$ for $p_{\text{T}}^{\text{soft}}$. The first (last) bin includes underflow (overflow). The "Top-quark like" category contains the $t\bar{t}$, Wt, and WW processes while the "Others" category contains backgrounds from triboson production and processes that include a Higgs boson, three or more tops, and tops produced in association with W or Z bosons. The bottom panel shows the ratio of the data to the post-fit background prediction. The hatched bands indicate the combined theoretical, experimental, and MC statistical uncertainties.

the pileup conditions and on the flavor composition of jets. The JES reflects the uncertainty in the average jet p_{T} measurement, varying from about 4% for 20 GeV jets to 1% above 300 GeV, while the JER reflects the uncertainty in the precision of the jet p_{T} measurement, varying from about 2% to 0.4% across the same p_{T} range. Varying the JES and JER can alter the jet multiplicity of an event, affecting its inclusion in the SR-low or SR-ISR regions, as well as affecting the eRJR variables that depend on jet and $E_{\text{T}}^{\text{miss}}$ kinematics. Similar types of uncertainties account for the energy scales and resolutions for electrons [77] and muons [78]. Variations reflecting the per-object uncertainties are propagated through the $E_{\text{T}}^{\text{miss}}$ calculation, with additional uncertainties for the scale and resolution of the soft term [87].

Additional experimental uncertainties account for differences between the data and MC simulation in the efficiency of the identification, reconstruction, isolation, and triggering of electrons [77] and muons [78], in the identification of pileup jets by the jet vertex tagger [83], and in the identification of b jets by the flavor-tagging algorithm [86]. An uncertainty on the pileup modeling is also considered and found to be small. The uncertainty in the combined 2015–2018 integrated luminosity is 1.7% [91], obtained using the LUCID-2 detector [92] for the primary luminosity measurements.

TABLE V. Summary of the dominant experimental and theoretical uncertainties in the SM background prediction in the low-mass and ISR signal regions. The individual uncertainties can be correlated and do not necessarily add in quadrature to equal the total post-fit background uncertainty.

Uncertainty in signal regions	SR-low	SR-ISR
Jet energy scale and resolution	7.1%	6.1%
WZ normalization procedure	6.6%	4.5%
$E_{\mathrm{T}}^{\mathrm{miss}}$	3.3%	2.1%
MC statistics	2.9%	3.9%
Anti-ID CR statistics	2.7%	0.21%
WZ theory	1.9%	1.3%
30% uncertainty in minor backgrounds ("Others")	1.7%	3.1%
Fake-factor estimation	1.2%	<0.01%
Muon momentum scale and resolution	0.30%	0.04%
Electron energy scale and resolution	0.22%	0.34%
Pileup	0.20%	0.94%
Top-quark-like background estimation	<0.01%	1.4%
Flavor tagging	<0.01%	0.47%

TABLE VI. The observed and expected yields after the background-only fit in the SRs. The normalization factors of the WZ sample for the low-mass and ISR regions are different and are treated separately in the combined fit. The "Top-quark like" category contains the $t\bar{t}$, Wt, and WW processes while the "Others" category contains backgrounds from triboson production and processes that include a Higgs boson, three or more tops, and tops produced in association with W or Z bosons. Combined statistical and systematic uncertainties are presented. The individual uncertainties can be correlated and do not necessarily add in quadrature to equal the total background uncertainty.

	SR-low	SR-ISR
Observed events	51	30
Fitted SM events	46 ± 5	23.4 ± 2.1
WZ	38 ± 5	19.7 ± 2.0
ZZ	4.9 ± 0.6	0.38 ± 0.08
Others	1.6 ± 0.8	1.5 ± 0.8
Top-quark like	$0.03^{+0.18}_{-0.03}$	1.9 ± 0.8
Fake/non-prompt leptons	1.6 ± 1.3	$0.01^{+0.05}_{-0.01}$

The theoretical uncertainties account for mismodeling in the MC simulation, particularly for the WZ process. They include QCD scale uncertainties affecting the WZ cross section, PDF uncertainties, and the uncertainty in α_{S}. The effects of QCD scale uncertainties are evaluated using seven-point variations of the factorization and renormalization scales in the matrix elements. The scales are varied upwards and downwards by a factor of 2, allowing for both independent and correlated variations of the two scales but prohibiting the anticorrelated variations. The PDF uncertainties are evaluated by taking the envelope of the 100 variation replicas of the nominal PDF set and the central values of the `CT14nnlo` [93] and `MMHT2014 NNLO` [94] PDF sets. The impact of ± 0.001 shifts of α_{S} on the acceptance is also considered. The QCD scale uncertainty is dominant and affects the prediction of the amount of additional radiation, and therefore the jet multiplicity, within an event. The effect of the QCD scale uncertainty grows with the number of jets in an event, but the total uncertainty in the CR-to-SR transfer factor is reduced by similarities between the jet multiplicity distributions in the control and signal

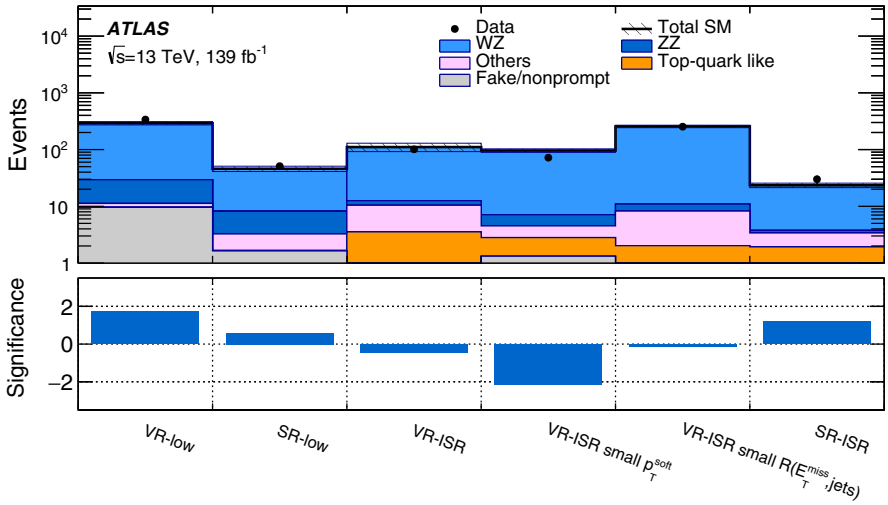

FIG. 4. The observed data and expected SM background yields in the VRs and SRs. The SM background prediction is derived with the background-only fit configuration, and the hatched band includes the experimental, theoretical, and statistical uncertainties. The "Top-quark like" category contains the $t\bar{t}$, Wt, and WW processes while the "Others" category contains backgrounds from triboson production and processes that include a Higgs boson, three or more tops, and tops produced in association with W or Z bosons. The bottom panel shows the significance [98] of the differences between the observed and expected yields.

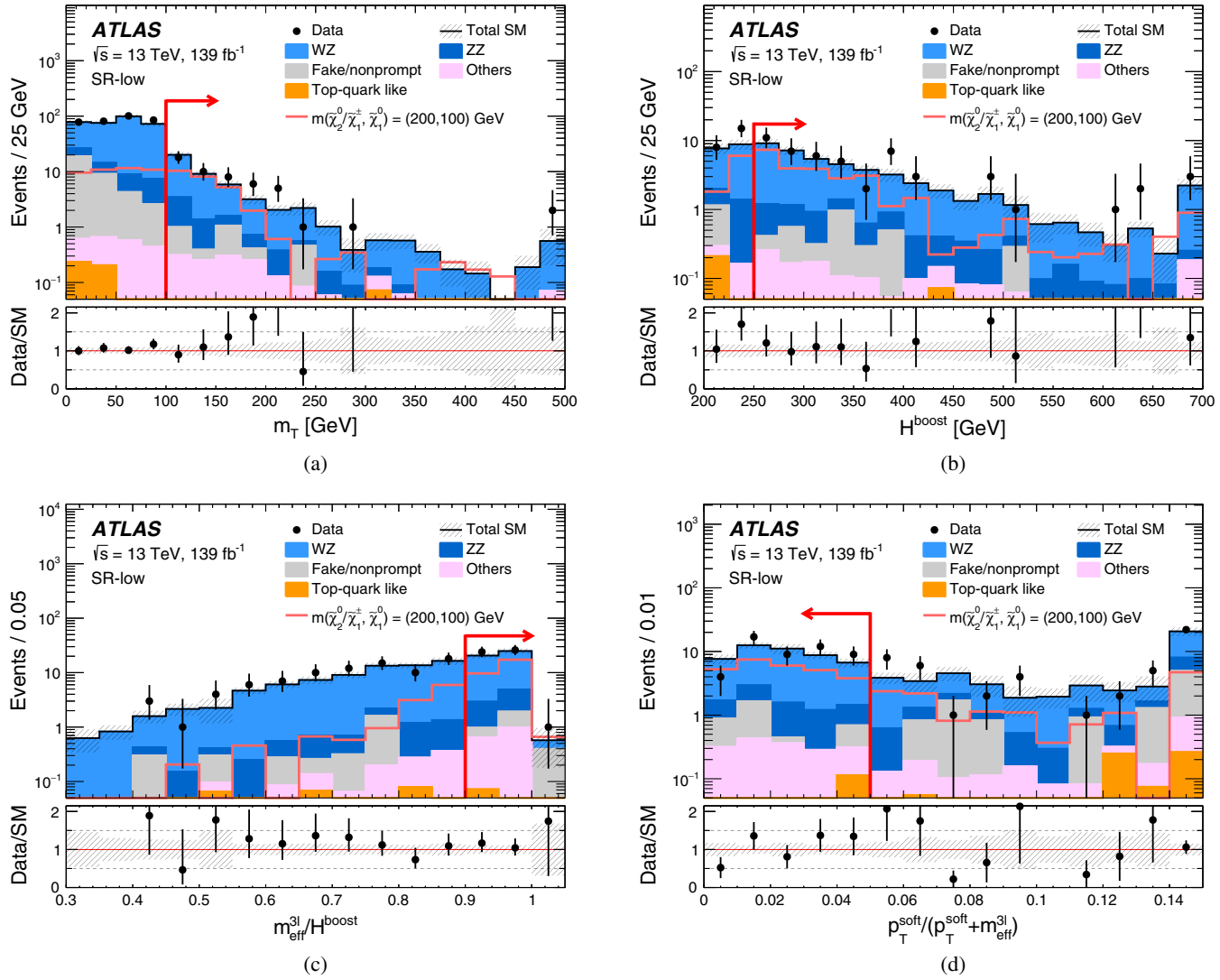

FIG. 5. Distributions in SR-low of the data and post-fit background prediction for (a) m_{T}, (b) H^{boost}, (c) $m_{\mathrm{eff}}^{3\ell}/H^{\mathrm{boost}}$, and (d) $p_{\mathrm{T}}^{\mathrm{soft}}/(p_{\mathrm{T}}^{\mathrm{soft}}+m_{\mathrm{eff}}^{3\ell})$. The SR-low event selections are applied for each distribution except for the variable shown, where the selection is indicated by a red arrow. The normalization factor for the WZ background is derived from the background-only estimation described in Sec. VII. The expected distribution for a benchmark signal model is included for comparison. The first (last) bin includes underflow (overflow). The "Top-quark like" category contains the $t\bar{t}$, Wt, and WW processes while the "Others" category contains backgrounds from triboson production and processes that include a Higgs boson, three or more tops, and tops produced in association with W or Z bosons. The bottom panel shows the ratio of the data to the post-fit background prediction. The hatched bands indicate the combined theoretical, experimental, and MC statistical uncertainties.

regions. An additional uncertainty on the WZ normalization procedure arises from the use of CRs to normalize the WZ contributions in the SRs.

Uncertainties in the cross section are included for the signals and minor backgrounds whose yields are taken directly from MC simulation, with signal uncertainties varying with $\tilde{\chi}_1^{\pm}/\tilde{\chi}_2^0$ mass from 4.3% at 100 GeV to 11.5% at 750 GeV. Uncertainties in the amount of initial- and final-state radiation are derived for each signal sample in the two signal regions by considering the ten eigenvariations of the A14 [58] tune summed in quadrature, giving uncertainties of 15%.

The systematic uncertainty of the data-driven fake/nonprompt (FNP) lepton estimate accounts for statistical uncertainties of the measured fake factors, assumptions made in the fake-factor method, and the closure of the method using MC simulation. The number of MC simulation events with prompt leptons, primarily from WZ events, that is subtracted in the fake-factor estimation is varied upwards and downwards by the WZ cross-section uncertainty of 5% [95], leading to an uncertainty in the FNP lepton estimate of 6.7% for electrons and 15.3% for muons. The nominal FNP lepton estimate is derived as a function of lepton p_{T}, and good agreement is generally seen for other

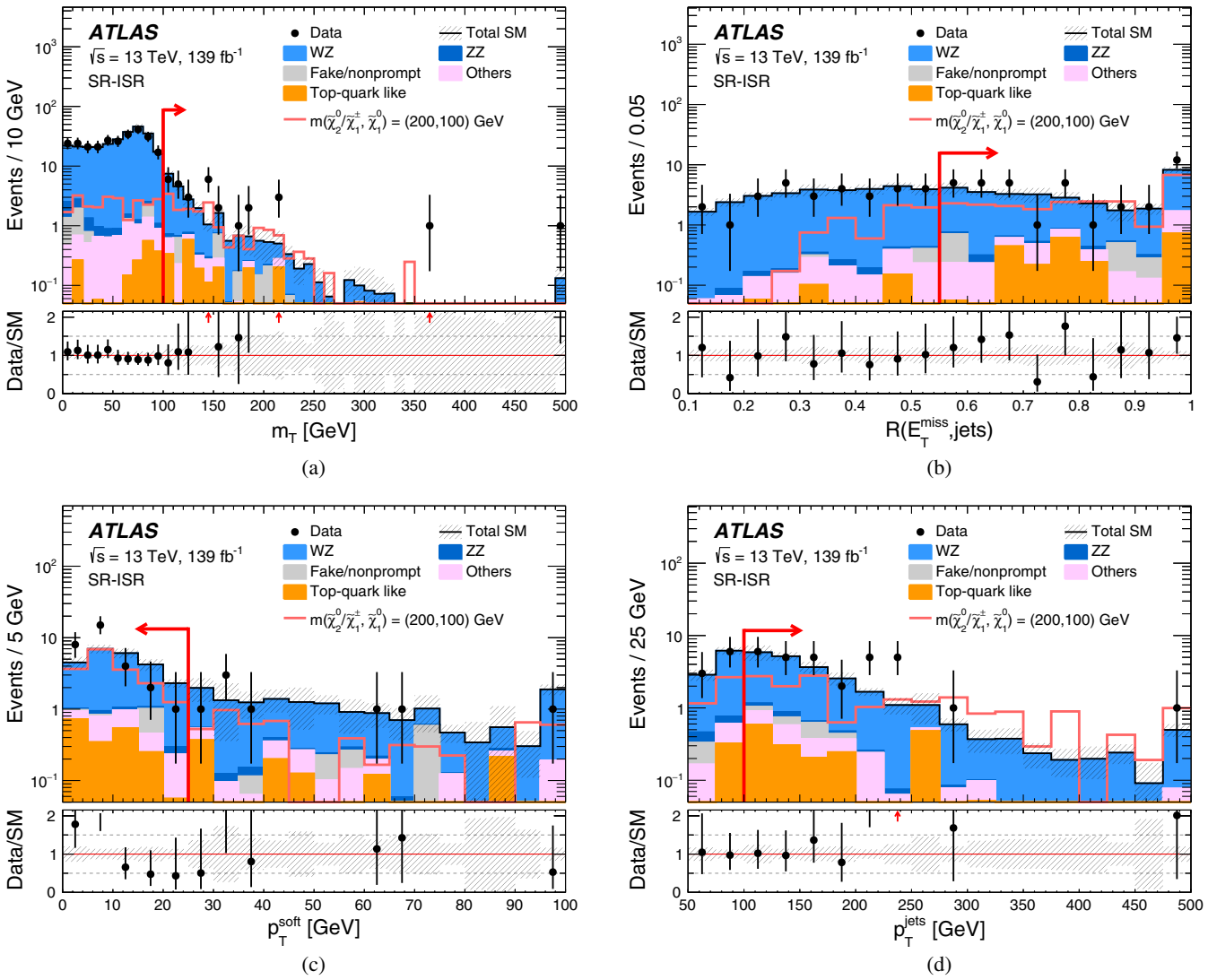

FIG. 6. Distributions in SR-ISR of the data and post-fit background prediction for (a) m_{T}, (b) $R(E_{\mathrm{T}}^{\mathrm{miss}}, \mathrm{jets})$, (c) $p_{\mathrm{T}}^{\mathrm{soft}}$, and (d) $p_{\mathrm{T}}^{\mathrm{jets}}$. The SR-ISR event selections are applied for each distribution except for the variable shown, where the selection is indicated by a red arrow. The normalization factor for the WZ background is derived from the background-only estimation described in Sec. VII. The expected distribution for a benchmark signal model is included for comparison. The first (last) bin includes underflow (overflow). The "Top-quark like" category contains the $t\bar{t}$, Wt, and WW processes while the "Others" category contains backgrounds from triboson production and processes that include a Higgs boson, three or more tops, and tops produced in association with W or Z bosons. The bottom panel shows the ratio of the data to the post-fit background prediction. The hatched bands indicate the combined theoretical, experimental, and MC statistical uncertainties.

kinematic variables in the FNP lepton control and validation regions. A slight dependence on $|\eta|$ is seen, with typical deviations of 25% for electrons and 21% for muons taken as additional uncertainties. The method closure uncertainty instead uses the $Z+$jets MC simulation to derive the FNP lepton estimate and compares the predictions in a loosened signal region with the known FNP lepton yield from MC simulation, accounting for potential differences in the FNP lepton composition between regions. Uncertainties of 12% and 18% are derived for electrons and muons, respectively. The total impact of the fake-factor uncertainties is relatively small in both signal regions given the small contribution from backgrounds with FNP leptons.

The dominant uncertainties are summarized in Table V for both the SR-low and SR-ISR regions. The largest experimental uncertainties reflect the unknowns of the energy and p_{T} calibration of jets and the measurement of the soft term of the $E_{\mathrm{T}}^{\mathrm{miss}}$. The largest theoretical source is the uncertainty in the QCD factorization and renormalization scales for the WZ cross section. The analysis also accounts for the statistical uncertainty of the MC simulation samples.

TABLE VII. Summary of the expected background and data yields in SR-low and SR-ISR. The second and third columns show the data and total expected background with systematic uncertainties. The fourth column gives the model-independent upper limits at 95% C.L. on the visible cross section (σ_{vis}). The fifth and sixth columns give the visible number of observed (S^{95}_{obs}) and expected (S^{95}_{exp}) events of a generic beyond-the-SM process, where uncertainties in S^{95}_{exp} reflect the $\pm 1\sigma$ uncertainties of the background estimates. The last column shows the discovery p-value and Gaussian significance Z assuming no signal.

Signal channel	N_{obs}	N_{exp}	σ_{vis}[fb]	S^{95}_{obs}	S^{95}_{exp}	$p(s=0)$ (Z)
SR-low	51	46 ± 5	0.16	22.1	$19.9^{+7.8}_{-3.6}$	0.27 (0.61)
SR-ISR	30	23.4 ± 2.1	0.13	17.8	$12.0^{+5.3}_{-1.8}$	0.11 (1.21)

IX. RESULTS

The HistFitter package [96] is used to compute the statistical interpretation based on a log-likelihood method [97]. All the systematic uncertainties are treated as Gaussian nuisance parameters in the likelihood.

To determine the background prediction, the control regions are used to constrain the WZ normalization assuming no signal events in the CR, referred to as a background-only fit. Normalization factors for the WZ MC simulation are derived from a simultaneous background-only fit of the two orthogonal CRs with all other background processes held constant. The normalization factors are found to be 0.84 ± 0.07 for CR-low and 0.95 ± 0.05 for CR-ISR. The two normalization factors are compatible within their uncertainties (described in Sec. VIII), with small differences due to the modeling of higher-order radiation in the electroweak WZ process.

The observed event yields in the low-mass and ISR regions are compared with the fitted background estimates derived from the log-likelihood fits in Table VI and visualized alongside the validation regions in Fig. 4. The data agree well with the background estimates in both signal regions. Kinematic distributions for these SRs are shown in Figs. 5 and 6, demonstrating good agreement between the data and the background estimates in the SRs and across the boundaries of the SR selections.

As no significant excess is observed, model-independent limits are derived at the 95% confidence level (C.L.) using the CL_s prescription [99]. An upper limit on the visible cross section of beyond-the-SM (BSM) processes is derived for each SR. A log-likelihood fit is applied to the number of observed events in the target SR and the associated CR, and a generic BSM process is assumed to contribute to the SR only. No uncertainties are considered for the signal model except the luminosity uncertainty. The observed (S^{95}_{obs}) and expected (S^{95}_{exp}) limits on the number of BSM events are shown in Table VII. Also shown are the observed limits on the visible cross section σ_{vis}, defined as S^{95}_{obs} normalized to the integrated luminosity, which represents the product of the production cross section, acceptance, and selection efficiency of a generic BSM signal. Limits on σ_{vis} are set at 0.16 fb in SR-low and 0.13 fb in SR-ISR. The p-value, representing the probability of the SM background alone fluctuating to at least the observed number of events, and the associated significance Z are also shown.

Exclusion limits are derived at 95% C.L. for models in which pair-produced $\tilde{\chi}_1^{\pm}\tilde{\chi}_2^0$ decay exclusively into two $\tilde{\chi}_1^0$ LSPs, a W boson and a Z boson. Limits are obtained through a profile log-likelihood ratio test using the CL_s prescription, following the simultaneous fit to the low-mass and ISR CRs and SRs [96]. The signal models are accounted for in this likelihood in both the CRs and SRs. The low-mass and ISR regions do not affect the nominal fit in the other region due to their orthogonality, but uncertainties that are correlated across regions may be constrained. Experimental uncertainties are treated as correlated between signal and background events and across low-mass and ISR regions. The theoretical uncertainty of the signal cross section is accounted for by repeating the limit-setting procedure with the varied signal cross sections and reporting the effect on the observed limit.

The expected and observed exclusion contours as a function of the signal $\tilde{\chi}_1^{\pm}/\tilde{\chi}_2^0$ and LSP $\tilde{\chi}_1^0$ masses are shown in Fig. 7. Masses can be excluded when the Z/W bosons of the decay are on the mass shell, such that the mass splittings Δm are close to or larger than the Z boson mass. Signal

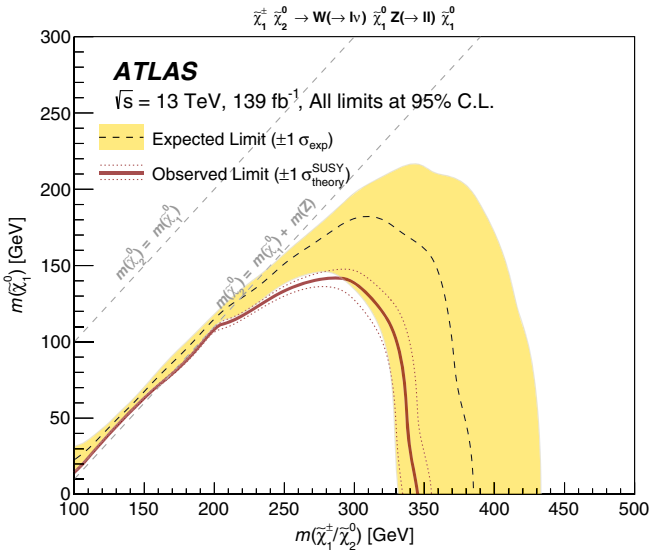

FIG. 7. Expected (dashed black) and observed (solid red) exclusion contours for $\tilde{\chi}_1^{\pm}\tilde{\chi}_2^0$ production assuming on-shell W/Z decays as a function of the $\tilde{\chi}_1^{\pm}/\tilde{\chi}_2^0$ and $\tilde{\chi}_1^0$ masses, and derived from the combined fit of low-mass and ISR regions. The yellow band reflects the $\pm 1\sigma$ uncertainty of the expected limits due to uncertainties in the background prediction and experimental uncertainties affecting the signal. The dotted red lines correspond to the $\pm 1\sigma$ cross-section uncertainty of the observed limit derived by varying the signal cross section within its uncertainty.

$\tilde{\chi}_1^{\pm}/\tilde{\chi}_2^0$ events are excluded for masses up to 345 GeV for small $\tilde{\chi}_1^0$ masses, for which Δm is large.

These results extend the exclusion limits in the low-mass and ISR regions beyond those of the RJR analysis from Ref. [30]. The excesses from the RJR analysis were validated in the 36 fb^{-1} of data from the 2015 and 2016 data sets and found to be reduced with the inclusion of 103 fb^{-1} of data from the 2017 and 2018 data sets, corresponding to local significances of 0.6σ in SR-low and 1.2σ in SR-ISR.

X. CONCLUSION

This paper presented a search for pair-produced $\tilde{\chi}_1^{\pm}\tilde{\chi}_2^0$ decaying via W and Z bosons into final states with three leptons and missing transverse momentum. The search targeted electroweakino production for which current limits derived from the recursive jigsaw reconstruction technique and from conventional techniques in the laboratory frame are in tension. This new search used 139 fb^{-1} of proton-proton collisions collected at $\sqrt{s} = 13$ TeV by the ATLAS detector at the LHC between 2015 and 2018. The data were analyzed with a new emulated recursive jigsaw reconstruction method that uses conventional variables in the laboratory frame to target low-mass electroweakinos and those produced in the presence of initial-state radiation. A subset of the data collected between 2015 and 2016 was analyzed and excesses were seen for two signal regions of similar construction to those of the recursive jigsaw reconstruction search [30]. In the full data set the observed event yields were found to be in agreement with Standard Model expectations, with no significant excess seen in either signal region. The results were interpreted with simplified models of electroweakino pair production, excluding neutralinos and charginos with masses up to 345 GeV at the 95% confidence level when the W and Z bosons are on the mass shell.

ACKNOWLEDGMENTS

We thank CERN for the very successful operation of the LHC, as well as the support staff from our institutions without whom ATLAS could not be operated efficiently. We acknowledge the support of ANPCyT, Argentina; YerPhI, Armenia; ARC, Australia; BMWFW and FWF, Austria; ANAS, Azerbaijan; SSTC, Belarus; CNPq and FAPESP, Brazil; NSERC, NRC and CFI, Canada; CERN; CONICYT, Chile; CAS, MOST and NSFC, China; COLCIENCIAS, Colombia; MSMT CR, MPO CR and VSC CR, Czech Republic; DNRF and DNSRC, Denmark; IN2P3-CNRS and CEA-DRF/IRFU, France; SRNSFG, Georgia; BMBF, HGF and MPG, Germany; GSRT, Greece; RGC and Hong Kong SAR, China; ISF and Benoziyo Center, Israel; INFN, Italy; MEXT and JSPS, Japan; CNRST, Morocco; NWO, Netherlands; RCN, Norway; MNiSW and NCN, Poland; FCT, Portugal; MNE/IFA, Romania; MES of Russia and NRC KI, Russia Federation; JINR; MESTD, Serbia; MSSR, Slovakia; ARRS and MIZŠ, Slovenia; DST/NRF, South Africa; MINECO, Spain; SRC and Wallenberg Foundation, Sweden; SERI, SNSF and Cantons of Bern and Geneva, Switzerland; MOST, Taiwan; TAEK, Turkey; STFC, United Kingdom; DOE and NSF, United States of America. In addition, individual groups and members have received support from BCKDF, CANARIE, Compute Canada and CRC, Canada; ERC, ERDF, Horizon 2020, Marie Skłodowska-Curie Actions and COST, European Union; Investissements d'Avenir Labex, Investissements d'Avenir Idex and ANR, France; DFG and AvH Foundation, Germany; Herakleitos, Thales and Aristeia programmes co-financed by EU-ESF and the Greek NSRF, Greece; BSF-NSF and GIF, Israel; CERCA Programme Generalitat de Catalunya and PROMETEO Programme Generalitat Valenciana, Spain; Göran Gustafssons Stiftelse, Sweden; The Royal Society and Leverhulme Trust, United Kingdom. The crucial computing support from all WLCG partners is acknowledged gratefully, in particular from CERN, the ATLAS Tier-1 facilities at TRIUMF (Canada), NDGF (Denmark, Norway, Sweden), CC-IN2P3 (France), KIT/GridKA (Germany), INFN-CNAF (Italy), NL-T1 (Netherlands), PIC (Spain), ASGC (Taiwan), RAL (UK) and BNL (USA), the Tier-2 facilities worldwide and large non-WLCG resource providers. Major contributors of computing resources are listed in Ref. [100].

[1] Yu. A. Golfand and E. P. Likhtman, Extension of the algebra of Poincare group generators and violation of p invariance, Pis'ma Zh. Eksp. Teor. Fiz. **13**, 452 (1971) [JETP Lett. **13**, 323 (1971)].
[2] D. V. Volkov and V. P. Akulov, Is the neutrino a goldstone particle?, Phys. Lett. **46B**, 109 (1973).
[3] J. Wess and B. Zumino, Supergauge transformations in four dimensions, Nucl. Phys. **B70**, 39 (1974).
[4] J. Wess and B. Zumino, Supergauge invariant extension of quantum electrodynamics, Nucl. Phys. **B78**, 1 (1974).
[5] S. Ferrara and B. Zumino, Supergauge invariant Yang-Mills theories, Nucl. Phys. **B79**, 413 (1974).
[6] A. Salam and J. A. Strathdee, Super-symmetry and non-Abelian gauges, Phys. Lett. B **51**, 353 (1974).
[7] N. Sakai, Naturalness in supersymmetric GUTS, Z. Phys. C **11**, 153 (1981).

[8] S. Dimopoulos, S. Raby, and F. Wilczek, Supersymmetry and the scale of unification, Phys. Rev. D **24**, 1681 (1981).

[9] L. E. Ibanez and G. G. Ross, Low-energy predictions in supersymmetric grand unified theories, Phys. Lett. B **105**, 439 (1981).

[10] S. Dimopoulos and H. Georgi, Softly broken supersymmetry and SU(5), Nucl. Phys. **B193**, 150 (1981).

[11] G. R. Farrar and P. Fayet, Phenomenology of the production, decay, and detection of new hadronic states associated with supersymmetry, Phys. Lett. B **76**, 575 (1978).

[12] H. Goldberg, Constraint on the Photino Mass from Cosmology, Phys. Rev. Lett. **50**, 1419 (1983); Erratum, Phys. Rev. Lett. **103**, 099905 (2009).

[13] J. R. Ellis, J. S. Hagelin, D. V. Nanopoulos, K. A. Olive, and M. Srednicki, Supersymmetric relics from the big bang, Nucl. Phys. **B238**, 453 (1984).

[14] J. Alwall, M.-P. Le, M. Lisanti, and J. G. Wacker, Searching for directly decaying gluinos at the Tevatron, Phys. Lett. B **666**, 34 (2008).

[15] J. Alwall, P. Schuster, and N. Toro, Simplified models for a first characterization of new physics at the LHC, Phys. Rev. D **79**, 075020 (2009).

[16] D. Alves *et al.*, Simplified models for LHC new physics searches, J. Phys. G **39**, 105005 (2012).

[17] ALEPH, DELPHI, L3, OPAL Experiments, Combined LEP Chargino results, up to 208 GeV for low DM, LEPSUSYWG/02-04.1, 2002, http://lepsusy.web.cern.ch/lepsusy/www/inoslowdmsummer02/charginolowdm_pub.html.

[18] ALEPH Collaboration, Absolute mass lower limit for the lightest neutralino of the MSSM from e^+e^- data at $\sqrt{s}$ up to 209 GeV, Phys. Lett. B **583**, 247 (2004).

[19] DELPHI Collaboration, Searches for supersymmetric particles in e^+e^- collisions up to 208 GeV and interpretation of the results within the MSSM, Eur. Phys. J. C **31**, 421 (2003).

[20] OPAL Collaboration, Search for anomalous production of dilepton events with missing transverse momentum in e^+e^- collisions at $\sqrt{s} = 183$ GeV to 209 GeV, Eur. Phys. J. C **32**, 453 (2004).

[21] ATLAS Collaboration, Search for electroweak production of supersymmetric particles in final states with two or three leptons at $\sqrt{s} = 13$ TeV with the ATLAS detector, Eur. Phys. J. C **78**, 995 (2018).

[22] ATLAS Collaboration, Search for the electroweak production of supersymmetric particles in $\sqrt{s} = 8$ TeV pp collisions with the ATLAS detector, Phys. Rev. D **93**, 052002 (2016).

[23] ATLAS Collaboration, Search for direct production of charginos and neutralinos in events with three leptons and missing transverse momentum in $\sqrt{s} = 8$ TeV pp collisions with the ATLAS detector, J. High Energy Phys. 04 (2014) 169.

[24] CMS Collaboration, Search for electroweak production of charginos and neutralinos in multilepton final states in proton-proton collisions at $\sqrt{s} = 13$ TeV, J. High Energy Phys. 03 (2018) 166.

[25] CMS Collaboration, Combined search for electroweak production of charginos and neutralinos in proton-proton collisions at $\sqrt{s} = 13$ TeV, J. High Energy Phys. 03 (2018) 160.

[26] CMS Collaboration, Searches for electroweak production of charginos, neutralinos, and sleptons decaying to leptons and W, Z, and Higgs bosons in pp collisions at 8 TeV, Eur. Phys. J. C **74**, 3036 (2014).

[27] CMS Collaboration, Search for electroweak production of charginos and neutralinos using leptonic final states in pp collisions at $\sqrt{s} = 7$ TeV, J. High Energy Phys. 11 (2012) 147.

[28] P. Jackson, C. Rogan, and M. Santoni, Sparticles in motion: Analyzing compressed SUSY scenarios with a new method of event reconstruction, Phys. Rev. D **95**, 035031 (2017).

[29] P. Jackson and C. Rogan, Recursive Jigsaw reconstruction: HEP event analysis in the presence of kinematic and combinatoric ambiguities, Phys. Rev. D **96**, 112007 (2017).

[30] ATLAS Collaboration, Search for chargino-neutralino production using recursive jigsaw reconstruction in final states with two or three charged leptons in proton-proton collisions at $\sqrt{s} = 13$ TeV with the ATLAS detector, Phys. Rev. D **98**, 092012 (2018).

[31] ATLAS Collaboration, The ATLAS experiment at the CERN large Hadron collider, J. Instrum. **3**, S08003 (2008).

[32] ATLAS Collaboration, ATLAS insertable B-layer technical design report, CERN Report No. ATLAS-TDR-19, 2010, https://cds.cern.ch/record/1291633; Addendum, CERN Report No. ATLAS-TDR-19-ADD-1, 2012, https://cds.cern.ch/record/1451888.

[33] B. Abbott *et al.*, Production and integration of the ATLAS Insertable B-Layer, J. Instrum. **13**, T05008 (2018).

[34] ATLAS Collaboration, Performance of the ATLAS trigger system in 2015, Eur. Phys. J. C **77**, 317 (2017).

[35] ATLAS Collaboration, Performance of electron and photon triggers in ATLAS during LHC Run 2, Eur. Phys. J. C **80**, 47 (2020).

[36] ATLAS Collaboration, Multi-Boson simulation for 13 TeV ATLAS analyses, CERN Report No. ATL-PHYS-PUB-2017-005, 2017, https://cds.cern.ch/record/2261933.

[37] ATLAS Collaboration, ATLAS simulation of boson plus jets processes in Run 2, CERN Report No. ATL-PHYS-PUB-2017-006, 2017, https://cds.cern.ch/record/2261937.

[38] E. Bothmann *et al.*, Event generation with SHERPA2.2, SciPost Phys. **7**, 034 (2019).

[39] T. Gleisberg and S. Höche, Comix, A new matrix element generator, J. High Energy Phys. 12 (2008) 039.

[40] S. Schumann and F. Krauss, A parton shower algorithm based on Catani-Seymour dipole factorisation, J. High Energy Phys. 03 (2008) 038.

[41] R. D. Ball *et al.*, Parton distributions for the LHC Run II, J. High Energy Phys. 04 (2015) 040.

[42] S. Höche, F. Krauss, M. Schonherr, and F. Siegert, A critical appraisal of NLO + PS matching methods, J. High Energy Phys. 09 (2012) 049.

[43] S. Höche, F. Krauss, M. Schönherr, and F. Siegert, QCD matrix elements + parton showers: The NLO case, J. High Energy Phys. 04 (2013) 027.

[44] S. Catani, F. Krauss, R. Kuhn, and B. R. Webber, QCD matrix elements + parton showers, J. High Energy Phys. 11 (2001) 063.

[45] S. Höche, F. Krauss, S. Schumann, and F. Siegert, QCD matrix elements and truncated showers, J. High Energy Phys. 05 (2009) 053.
[46] F. Cascioli, P. Maierhofer, and S. Pozzorini, Scattering Amplitudes with Open Loops, Phys. Rev. Lett. **108**, 111601 (2012).
[47] A. Denner, S. Dittmaier, and L. Hofer, Collier: A fortran-based complex one-loop library in extended regularizations, Comput. Phys. Commun. **212**, 220 (2017).
[48] C. Anastasiou, L. J. Dixon, K. Melnikov, and F. Petriello, High-precision QCD at hadron colliders: Electroweak gauge boson rapidity distributions at next-to-next-to leading order, Phys. Rev. D **69**, 094008 (2004).
[49] S. Frixione, P. Nason, and G. Ridolfi, A positive-weight next-to-leading-order Monte Carlo for heavy flavour hadroproduction, J. High Energy Phys. 09 (2007) 126.
[50] H. B. Hartanto, B. Jager, L. Reina, and D. Wackeroth, Higgs boson production in association with top quarks in the POWHEG BOX, Phys. Rev. D **91**, 094003 (2015).
[51] E. Re, Single-top Wt-channel production matched with parton showers using the POWHEG method, Eur. Phys. J. C **71**, 1547 (2011).
[52] S. Alioli, P. Nason, C. Oleari, and E. Re, NLO single-top production matched with shower in POWHEG: s- and t-channel contributions, J. High Energy Phys. 09 (2009) 111; Erratum, J. High Energy Phys. 02 (2010) 11.
[53] R. Frederix, E. Re, and P. Torrielli, Single-top t-channel hadroproduction in the four-flavour scheme with POWHEG and aMC@NLO, J. High Energy Phys. 09 (2012) 130.
[54] P. Nason, A new method for combining NLO QCD with shower Monte Carlo algorithms, J. High Energy Phys. 11 (2004) 040.
[55] S. Frixione, P. Nason, and C. Oleari, Matching NLO QCD computations with parton shower simulations: The POWHEG method, J. High Energy Phys. 11 (2007) 070.
[56] S. Alioli, P. Nason, C. Oleari, and E. Re, A general framework for implementing NLO calculations in shower Monte Carlo programs: The POWHEG BOX, J. High Energy Phys. 06 (2010) 043.
[57] T. Sjöstrand, S. Ask, J. R. Christiansen, R. Corke, N. Desai, P. Ilten, S. Mrenna, S. Prestel, C. O. Rasmussen, and P. Z. Skands, An introduction to PYTHIA8.2, Comput. Phys. Commun. **191**, 159 (2015).
[58] ATLAS Collaboration, ATLAS Pythia 8 tunes to 7 TeV data, CERN Report No. ATL-PHYS-PUB-2014-021, 2014, https://cds.cern.ch/record/1966419.
[59] R. D. Ball *et al.*, Parton distributions with LHC data, Nucl. Phys. **B867**, 244 (2013).
[60] ATLAS Collaboration, Studies on top-quark Monte Carlo modelling for Top2016, CERN Report No. ATL-PHYS-PUB-2016-020, 2016, https://cds.cern.ch/record/2216168.
[61] M. Czakon and A. Mitov, Top++: A program for the calculation of the top-pair cross-section at hadron colliders, Comput. Phys. Commun. **185**, 2930 (2014).
[62] M. Aliev, H. Lacker, U. Langenfeld, S. Moch, P. Uwer, and M. Wiedermann, HATHOR: HAdronic Top and Heavy quarks crOss section calculatoR, Comput. Phys. Commun. **182**, 1034 (2011).
[63] P. Kant, O. M. Kind, T. Kintscher, T. Lohse, T. Martini, S. Mölbitz, P. Rieck, and P. Uwer, HatHor for single top-quark production: Updated predictions and uncertainty estimates for single top-quark production in hadronic collisions, Comput. Phys. Commun. **191**, 74 (2015).
[64] S. Frixione, E. Laenen, P. Motylinski, B. R. Webber, and C. D. White, Single-top hadroproduction in association with a W boson, J. High Energy Phys. 07 (2008) 029.
[65] J. Alwall, R. Frederix, S. Frixione, V. Hirschi, F. Maltoni, O. Mattelaer, H.-S. Shao, T. Stelzer, P. Torrielli, and M. Zaro, The automated computation of tree-level and next-to-leading order differential cross sections, and their matching to parton shower simulations, J. High Energy Phys. 07 (2014) 079.
[66] W. Beenakker, M. Klasen, M. Krämer, T. Plehn, M. Spira, and P. M. Zerwas, Production of Charginos, Neutralinos, and Sleptons at Hadron Colliders, Phys. Rev. Lett. **83**, 3780 (1999).
[67] J. Debove, B. Fuks, and M. Klasen, Threshold resummation for gaugino pair production at hadron colliders, Nucl. Phys. **B842**, 51 (2011).
[68] B. Fuks, M. Klasen, D. R. Lamprea, and M. Rothering, Gaugino production in proton-proton collisions at a center-of-mass energy of 8 TeV, J. High Energy Phys. 10 (2012) 081.
[69] B. Fuks, M. Klasen, D. R. Lamprea, and M. Rothering, Precision predictions for electroweak superpartner production at hadron colliders with Resummino, Eur. Phys. J. C **73**, 2480 (2013).
[70] J. Fiaschi and M. Klasen, Neutralino-chargino pair production at NLO + NLL with resummation-improved parton density functions for LHC Run II, Phys. Rev. D **98**, 055014 (2018).
[71] C. Borschensky, M. Krämer, A. Kulesza, M. Mangano, S. Padhi, T. Plehn, and X. Portell, Squark and gluino production cross sections in pp collisions at $\sqrt{s} = 13$, 14, 33 and 100 TeV, Eur. Phys. J. C **74**, 3174 (2014).
[72] D. J. Lange, The EvtGen particle decay simulation package, Nucl. Instrum. Methods Phys. Res., Sect. A **462**, 152 (2001).
[73] ATLAS Collaboration, The ATLAS simulation infrastructure, Eur. Phys. J. C **70**, 823 (2010).
[74] S. Agostinelli *et al.*, GEANT4—A simulation toolkit, Nucl. Instrum. Methods Phys. Res., Sect. A **506**, 250 (2003).
[75] ATLAS Collaboration, The Pythia 8 A3 tune description of ATLAS minimum bias and inelastic measurements incorporating the Donnachie-Landshoff diffractive model, CERN Report No. ATL-PHYS-PUB-2016-017, 2016, https://cds.cern.ch/record/2206965.
[76] ATLAS Collaboration, Vertex reconstruction performance of the ATLAS detector at $\sqrt{s} = 13$ TeV, CERN Report No. ATL-PHYS-PUB-2015-026, 2015, https://cds.cern.ch/record/2037717.
[77] ATLAS Collaboration, Electron and photon performance measurements with the ATLAS detector using the 2015-2017 LHC proton-proton collision data, J. Instrum. **14**, P12006 (2019).
[78] ATLAS Collaboration, Muon reconstruction performance of the ATLAS detector in proton-proton collision data at $\sqrt{s} = 13$ TeV, Eur. Phys. J. C **76**, 292 (2016).

[79] ATLAS Collaboration, Topological cell clustering in the ATLAS calorimeters and its performance in LHC Run 1, Eur. Phys. J. C **77**, 490 (2017).
[80] M. Cacciari, G. P. Salam, and G. Soyez, FastJet user manual, Eur. Phys. J. C **72**, 1896 (2012).
[81] M. Cacciari, G. P. Salam, and G. Soyez, The anti-k_t jet clustering algorithm, J. High Energy Phys. 04 (2008) 063.
[82] ATLAS Collaboration, Jet energy scale measurements and their systematic uncertainties in proton-proton collisions at $\sqrt{s} = 13$ TeV with the ATLAS detector, Phys. Rev. D **96**, 072002 (2017).
[83] ATLAS Collaboration, Performance of pile-up mitigation techniques for jets in pp collisions at $\sqrt{s} = 8$ TeV using the ATLAS detector, Eur. Phys. J. C **76**, 581 (2016).
[84] ATLAS Collaboration, Tagging and suppression of pileup jets with the ATLAS detector, CERN Report No. ATLASCONF-2014-018, 2014, https://cds.cern.ch/record/1700870.
[85] ATLAS Collaboration, Selection of jets produced in 13 TeV proton-proton collisions with the ATLAS detector, CERN Report No. ATLAS-CONF-2015-029, 2015, https://cds.cern.ch/record/2037702.
[86] ATLAS Collaboration, ATLAS b-jet identification performance and efficiency measurement with $t\bar{t}$ events in pp collisions at $\sqrt{s} = 13$ TeV, Eur. Phys. J. C **79**, 970 (2019).
[87] ATLAS Collaboration, Performance of missing transverse momentum reconstruction with the ATLAS detector using proton-proton collisions at $\sqrt{s} = 13$ TeV, Eur. Phys. J. C **78**, 903 (2018).
[88] ATLAS Collaboration, Measurement of the WW cross section in $\sqrt{s} = 7$ TeV pp collisions with the ATLAS detector and limits on anomalous gauge couplings, Phys. Lett. B **712**, 289 (2012).
[89] ATLAS Collaboration, Prospects for Higgs boson searches using the $H \to WW^{(*)} \to \ell\nu\ell\nu$ decay mode with the ATLAS detector at 10 TeV, CERN Report No. ATL-PHYS-PUB-2010-005, 2010, https://cds.cern.ch/record/1270568.
[90] ATLAS Collaboration, Jet energy resolution in proton-proton collisions at $\sqrt{s} = 7$ TeV recorded in 2010 with the ATLAS detector, Eur. Phys. J. C **73**, 2306 (2013).
[91] ATLAS Collaboration, Luminosity determination in pp collisions at $\sqrt{s} = 13$ TeV using the ATLAS detector at the LHC, CERN Report No. ATLAS-CONF-2019-021, 2019, https://cds.cern.ch/record/2677054.
[92] G. Avoni *et al.*, The new LUCID-2 detector for luminosity measurement and monitoring in ATLAS, J. Instrum. **13**, P07017 (2018).
[93] S. Dulat, T.-J. Hou, J. Gao, M. Guzzi, J. Huston, P. Nadolsky, J. Pumplin, C. Schmidt, D. Stump, and C.-P. Yuan, New parton distribution functions from a global analysis of quantum chromodynamics, Phys. Rev. D **93**, 033006 (2016).
[94] L. Harland-Lang, A. Martin, P. Motylinski, and R. Thorne, Parton distributions in the LHC era: MMHT 2014 PDFs, Eur. Phys. J. C **75**, 204 (2015).
[95] ATLAS Collaboration, Measurement of $W^{\pm}Z$ production cross sections and gauge boson polarisation in pp collisions at $\sqrt{s} = 13$ TeV with the ATLAS detector, Eur. Phys. J. C **79**, 535 (2019).
[96] M. Baak, G. J. Besjes, D. Côté, A. Koutsman, J. Lorenz, and D. Short, HistFitter software framework for statistical data analysis, Eur. Phys. J. C **75**, 153 (2015).
[97] G. Cowan, K. Cranmer, E. Gross, and O. Vitells, Asymptotic formulae for likelihood-based tests of new physics, Eur. Phys. J. C **71**, 1554 (2011); Erratum, Eur. Phys. J. C **73**, 2501 (2013).
[98] R. D. Cousins, J. T. Linnemann, and J. Tucker, Evaluation of three methods for calculating statistical significance when incorporating a systematic uncertainty into a test of the background-only hypothesis for a Poisson process, Nucl. Instrum. Methods Phys. Res., Sect. A **595**, 480 (2008).
[99] A. L. Read, Presentation of search results: The CLS technique, J. Phys. G **28**, 2693 (2002).
[100] ATLAS Collaboration, ATLAS computing acknowledgements, CERN Report No. ATL-GEN-PUB-2016-002, https://cds.cern.ch/record/2202407.

G. Aad,[102] B. Abbott,[129] D. C. Abbott,[103] A. Abed Abud,[71a,71b] K. Abeling,[53] D. K. Abhayasinghe,[94] S. H. Abidi,[167] O. S. AbouZeid,[40] N. L. Abraham,[156] H. Abramowicz,[161] H. Abreu,[160] Y. Abulaiti,[6] B. S. Acharya,[67a,67b,b] B. Achkar,[53] S. Adachi,[163] L. Adam,[100] C. Adam Bourdarios,[5] L. Adamczyk,[84a] L. Adamek,[167] J. Adelman,[121] M. Adersberger,[114] A. Adiguzel,[12c,c] S. Adorni,[54] T. Adye,[144] A. A. Affolder,[146] Y. Afik,[160] C. Agapopoulou,[65] M. N. Agaras,[38] A. Aggarwal,[119] C. Agheorghiesei,[27c] J. A. Aguilar-Saavedra,[140f,140a,d] F. Ahmadov,[80] W. S. Ahmed,[104] X. Ai,[18] G. Aielli,[74a,74b] S. Akatsuka,[86] T. P. A. Åkesson,[97] E. Akilli,[54] A. V. Akimov,[111] K. Al Khoury,[65] G. L. Alberghi,[23b,23a] J. Albert,[176] M. J. Alconada Verzini,[161] S. Alderweireldt,[36] M. Aleksa,[36] I. N. Aleksandrov,[80] C. Alexa,[27b] D. Alexandre,[19] T. Alexopoulos,[10] A. Alfonsi,[120] F. Alfonsi,[23b,23a] M. Alhroob,[129] B. Ali,[142] G. Alimonti,[69a] J. Alison,[37] S. P. Alkire,[148] C. Allaire,[65] B. M. M. Allbrooke,[156] B. W. Allen,[132] P. P. Allport,[21] A. Aloisio,[70a,70b] A. Alonso,[40] F. Alonso,[89] C. Alpigiani,[148] A. A. Alshehri,[57] M. Alvarez Estevez,[99] D. Álvarez Piqueras,[174] M. G. Alviggi,[70a,70b] Y. Amaral Coutinho,[81b] A. Ambler,[104] L. Ambroz,[135] C. Amelung,[26] D. Amidei,[106] S. P. Amor Dos Santos,[140a] S. Amoroso,[46] C. S. Amrouche,[54] F. An,[79] C. Anastopoulos,[149] N. Andari,[145] T. Andeen,[11] C. F. Anders,[61b] J. K. Anders,[20] A. Andreazza,[69a,69b] V. Andrei,[61a] C. R. Anelli,[176] S. Angelidakis,[38] A. Angerami,[39] A. V. Anisenkov,[122b,122a] A. Annovi,[72a]

C. Antel,[61a] M. T. Anthony,[149] M. Antonelli,[51] D. J. A. Antrim,[171] F. Anulli,[73a] M. Aoki,[82] J. A. Aparisi Pozo,[174] L. Aperio Bella,[15a] G. Arabidze,[107] J. P. Araque,[140a] V. Araujo Ferraz,[81b] R. Araujo Pereira,[81b] C. Arcangeletti,[51] A. T. H. Arce,[49] F. A. Arduh,[89] J-F. Arguin,[110] S. Argyropoulos,[78] J.-H. Arling,[46] A. J. Armbruster,[36] A. Armstrong,[171] O. Arnaez,[167] H. Arnold,[120] A. Artamonov,[124,a] G. Artoni,[135] S. Artz,[100] S. Asai,[163] N. Asbah,[59] E. M. Asimakopoulou,[172] L. Asquith,[156] J. Assahsah,[35d] K. Assamagan,[29] R. Astalos,[28a] R. J. Atkin,[33a] M. Atkinson,[173] N. B. Atlay,[19] H. Atmani,[65] K. Augsten,[142] G. Avolio,[36] R. Avramidou,[60a] M. K. Ayoub,[15a] A. M. Azoulay,[168b] G. Azuelos,[110,e] H. Bachacou,[145] K. Bachas,[68a,68b] M. Backes,[135] F. Backman,[45a,45b] P. Bagnaia,[73a,73b] M. Bahmani,[85] H. Bahrasemani,[152] A. J. Bailey,[174] V. R. Bailey,[173] J. T. Baines,[144] M. Bajic,[40] C. Bakalis,[10] O. K. Baker,[183] P. J. Bakker,[120] D. Bakshi Gupta,[8] S. Balaji,[157] E. M. Baldin,[122b,122a] P. Balek,[180] F. Balli,[145] W. K. Balunas,[135] J. Balz,[100] E. Banas,[85] A. Bandyopadhyay,[24] Sw. Banerjee,[181,f] A. A. E. Bannoura,[182] L. Barak,[161] W. M. Barbe,[38] E. L. Barberio,[105] D. Barberis,[55b,55a] M. Barbero,[102] G. Barbour,[95] T. Barillari,[115] M-S. Barisits,[36] J. Barkeloo,[132] T. Barklow,[153] R. Barnea,[160] S. L. Barnes,[60c] B. M. Barnett,[144] R. M. Barnett,[18] Z. Barnovska-Blenessy,[60a] A. Baroncelli,[60a] G. Barone,[29] A. J. Barr,[135] L. Barranco Navarro,[45a,45b] F. Barreiro,[99] J. Barreiro Guimarães da Costa,[15a] S. Barsov,[138] R. Bartoldus,[153] G. Bartolini,[102] A. E. Barton,[90] P. Bartos,[28a] A. Basalaev,[46] A. Bassalat,[65,g] M. J. Basso,[167] R. L. Bates,[57] S. Batlamous,[35e] J. R. Batley,[32] B. Batool,[151] M. Battaglia,[146] M. Bauce,[73a,73b] F. Bauer,[145] K. T. Bauer,[171] H. S. Bawa,[31,h] J. B. Beacham,[49] T. Beau,[136] P. H. Beauchemin,[170] F. Becherer,[52] P. Bechtle,[24] H. C. Beck,[53] H. P. Beck,[20,i] K. Becker,[52] M. Becker,[100] C. Becot,[46] A. Beddall,[12d] A. J. Beddall,[12a] V. A. Bednyakov,[80] M. Bedognetti,[120] C. P. Bee,[155] T. A. Beermann,[77] M. Begalli,[81b] M. Begel,[29] A. Behera,[155] J. K. Behr,[46] F. Beisiegel,[24] A. S. Bell,[95] G. Bella,[161] L. Bellagamba,[23b] A. Bellerive,[34] P. Bellos,[9] K. Beloborodov,[122b,122a] K. Belotskiy,[112] N. L. Belyaev,[112] D. Benchekroun,[35a] N. Benekos,[10] Y. Benhammou,[161] D. P. Benjamin,[6] M. Benoit,[54] J. R. Bensinger,[26] S. Bentvelsen,[120] L. Beresford,[135] M. Beretta,[51] D. Berge,[46] E. Bergeaas Kuutmann,[172] N. Berger,[5] B. Bergmann,[142] L. J. Bergsten,[26] J. Beringer,[18] S. Berlendis,[7] N. R. Bernard,[103] G. Bernardi,[136] C. Bernius,[153] F. U. Bernlochner,[24] T. Berry,[94] P. Berta,[100] C. Bertella,[15a] I. A. Bertram,[90] O. Bessidskaia Bylund,[182] N. Besson,[145] A. Bethani,[101] S. Bethke,[115] A. Betti,[24] A. J. Bevan,[93] J. Beyer,[115] D. S. Bhattacharya,[177] R. Bi,[139] R. M. Bianchi,[139] O. Biebel,[114] D. Biedermann,[19] R. Bielski,[36] K. Bierwagen,[100] N. V. Biesuz,[72a,72b] M. Biglietti,[75a] T. R. V. Billoud,[110] M. Bindi,[53] A. Bingul,[12d] C. Bini,[73a,73b] S. Biondi,[23b,23a] M. Birman,[180] T. Bisanz,[53] J. P. Biswal,[161] D. Biswas,[181,f] A. Bitadze,[101] C. Bittrich,[48] K. Bjørke,[134] K. M. Black,[25] T. Blazek,[28a] I. Bloch,[46] C. Blocker,[26] A. Blue,[57] U. Blumenschein,[93] G. J. Bobbink,[120] V. S. Bobrovnikov,[122b,122a] S. S. Bocchetta,[97] A. Bocci,[49] D. Boerner,[46] D. Bogavac,[14] A. G. Bogdanchikov,[122b,122a] C. Bohm,[45a] V. Boisvert,[94] P. Bokan,[53,172] T. Bold,[84a] A. S. Boldyrev,[113] A. E. Bolz,[61b] M. Bomben,[136] M. Bona,[93] J. S. Bonilla,[132] M. Boonekamp,[145] H. M. Borecka-Bielska,[91] A. Borisov,[123] G. Borissov,[90] J. Bortfeldt,[36] D. Bortoletto,[135] D. Boscherini,[23b] M. Bosman,[14] J. D. Bossio Sola,[104] K. Bouaouda,[35a] J. Boudreau,[139] E. V. Bouhova-Thacker,[90] D. Boumediene,[38] S. K. Boutle,[57] A. Boveia,[127] J. Boyd,[36] D. Boye,[33c,j] I. R. Boyko,[80] A. J. Bozson,[94] J. Bracinik,[21] N. Brahimi,[102] G. Brandt,[182] O. Brandt,[32] F. Braren,[46] B. Brau,[103] J. E. Brau,[132] W. D. Breaden Madden,[57] K. Brendlinger,[46] L. Brenner,[46] R. Brenner,[172] S. Bressler,[180] B. Brickwedde,[100] D. L. Briglin,[21] D. Britton,[57] D. Britzger,[115] I. Brock,[24] R. Brock,[107] G. Brooijmans,[39] W. K. Brooks,[147c] E. Brost,[121] J. H Broughton,[21] P. A. Bruckman de Renstrom,[85] D. Bruncko,[28b] A. Bruni,[23b] G. Bruni,[23b] L. S. Bruni,[120] S. Bruno,[74a,74b] B. H. Brunt,[32] M. Bruschi,[23b] N. Bruscino,[139] P. Bryant,[37] L. Bryngemark,[97] T. Buanes,[17] Q. Buat,[36] P. Buchholz,[151] A. G. Buckley,[57] I. A. Budagov,[80] M. K. Bugge,[134] F. Bührer,[52] O. Bulekov,[112] T. J. Burch,[121] S. Burdin,[91] C. D. Burgard,[120] A. M. Burger,[130] B. Burghgrave,[8] J. T. P. Burr,[46] C. D. Burton,[11] J. C. Burzynski,[103] V. Büscher,[100] E. Buschmann,[53] P. J. Bussey,[57] J. M. Butler,[25] C. M. Buttar,[57] J. M. Butterworth,[95] P. Butti,[36] W. Buttinger,[36] A. Buzatu,[158] A. R. Buzykaev,[122b,122a] G. Cabras,[23b,23a] S. Cabrera Urbán,[174] D. Caforio,[56] H. Cai,[173] V. M. M. Cairo,[153] O. Cakir,[4a] N. Calace,[36] P. Calafiura,[18] A. Calandri,[102] G. Calderini,[136] P. Calfayan,[66] G. Callea,[57] L. P. Caloba,[81b] S. Calvente Lopez,[99] D. Calvet,[38] S. Calvet,[38] T. P. Calvet,[155] M. Calvetti,[72a,72b] R. Camacho Toro,[136] S. Camarda,[36] D. Camarero Munoz,[99] P. Camarri,[74a,74b] D. Cameron,[134] R. Caminal Armadans,[103] C. Camincher,[36] S. Campana,[36] M. Campanelli,[95] A. Camplani,[40] A. Campoverde,[151] V. Canale,[70a,70b] A. Canesse,[104] M. Cano Bret,[60c] J. Cantero,[130] T. Cao,[161] Y. Cao,[173] M. D. M. Capeans Garrido,[36] M. Capua,[41b,41a] R. Cardarelli,[74a] F. Cardillo,[149] G. Carducci,[41b,41a] I. Carli,[143] T. Carli,[36] G. Carlino,[70a] B. T. Carlson,[139] L. Carminati,[69a,69b] R. M. D. Carney,[45a,45b] S. Caron,[119] E. Carquin,[147c] S. Carrá,[46] J. W. S. Carter,[167] M. P. Casado,[14,k] A. F. Casha,[167] D. W. Casper,[171] R. Castelijn,[120] F. L. Castillo,[174] V. Castillo Gimenez,[174] N. F. Castro,[140a,140e] A. Catinaccio,[36] J. R. Catmore,[134] A. Cattai,[36] J. Caudron,[24] V. Cavaliere,[29] E. Cavallaro,[14] M. Cavalli-Sforza,[14] V. Cavasinni,[72a,72b] E. Celebi,[12b] F. Ceradini,[75a,75b] L. Cerda Alberich,[174] K. Cerny,[131]

A. S. Cerqueira,[81a] A. Cerri,[156] L. Cerrito,[74a,74b] F. Cerutti,[18] A. Cervelli,[23b,23a] S. A. Cetin,[12b] Z. Chadi,[35a] D. Chakraborty,[121] S. K. Chan,[59] W. S. Chan,[120] W. Y. Chan,[91] J. D. Chapman,[32] B. Chargeishvili,[159b] D. G. Charlton,[21] T. P. Charman,[93] C. C. Chau,[34] S. Che,[127] S. Chekanov,[6] S. V. Chekulaev,[168a] G. A. Chelkov,[80,l] M. A. Chelstowska,[36] B. Chen,[79] C. Chen,[60a] C. H. Chen,[79] H. Chen,[29] J. Chen,[60a] J. Chen,[39] S. Chen,[137] S. J. Chen,[15c] X. Chen,[15b,m] Y. Chen,[83] Y-H. Chen,[46] H. C. Cheng,[63a] H. J. Cheng,[15a] A. Cheplakov,[80] E. Cheremushkina,[123] R. Cherkaoui El Moursli,[35e] E. Cheu,[7] K. Cheung,[64] T. J. A. Chevalérias,[145] L. Chevalier,[145] V. Chiarella,[51] G. Chiarelli,[72a] G. Chiodini,[68a] A. S. Chisholm,[21] A. Chitan,[27b] I. Chiu,[163] Y. H. Chiu,[176] M. V. Chizhov,[80] K. Choi,[66] A. R. Chomont,[73a,73b] S. Chouridou,[162] Y. S. Chow,[120] M. C. Chu,[63a] X. Chu,[15a,15d] J. Chudoba,[141] A. J. Chuinard,[104] J. J. Chwastowski,[85] L. Chytka,[131] D. Cieri,[115] K. M. Ciesla,[85] D. Cinca,[47] V. Cindro,[92] I. A. Cioară,[27b] A. Ciocio,[18] F. Cirotto,[70a,70b] Z. H. Citron,[180,n] M. Citterio,[69a] D. A. Ciubotaru,[27b] B. M. Ciungu,[167] A. Clark,[54] M. R. Clark,[39] P. J. Clark,[50] C. Clement,[45a,45b] Y. Coadou,[102] M. Cobal,[67a,67c] A. Coccaro,[55b] J. Cochran,[79] H. Cohen,[161] A. E. C. Coimbra,[36] L. Colasurdo,[119] B. Cole,[39] A. P. Colijn,[120] J. Collot,[58] P. Conde Muiño,[140a,o] E. Coniavitis,[52] S. H. Connell,[33c] I. A. Connelly,[57] S. Constantinescu,[27b] F. Conventi,[70a,p] A. M. Cooper-Sarkar,[135] F. Cormier,[175] K. J. R. Cormier,[167] L. D. Corpe,[95] M. Corradi,[73a,73b] E. E. Corrigan,[97] F. Corriveau,[104,q] A. Cortes-Gonzalez,[36] M. J. Costa,[174] F. Costanza,[5] D. Costanzo,[149] G. Cowan,[94] J. W. Cowley,[32] J. Crane,[101] K. Cranmer,[125] S. J. Crawley,[57] R. A. Creager,[137] S. Crépé-Renaudin,[58] F. Crescioli,[136] M. Cristinziani,[24] V. Croft,[120] G. Crosetti,[41b,41a] A. Cueto,[5] T. Cuhadar Donszelmann,[149] A. R. Cukierman,[153] S. Czekierda,[85] P. Czodrowski,[36] M. J. Da Cunha Sargedas De Sousa,[60b] J. V. Da Fonseca Pinto,[81b] C. Da Via,[101] W. Dabrowski,[84a] T. Dado,[28a] S. Dahbi,[35e] T. Dai,[106] C. Dallapiccola,[103] M. Dam,[40] G. D'amen,[29] V. D'Amico,[75a,75b] J. Damp,[100] J. R. Dandoy,[137] M. F. Daneri,[30] N. P. Dang,[181,f] N. S. Dann,[101] M. Danninger,[175] V. Dao,[36] G. Darbo,[55b] O. Dartsi,[5] A. Dattagupta,[132] T. Daubney,[46] S. D'Auria,[69a,69b] W. Davey,[24] C. David,[46] T. Davidek,[143] D. R. Davis,[49] I. Dawson,[149] K. De,[8] R. De Asmundis,[70a] M. De Beurs,[120] S. De Castro,[23b,23a] S. De Cecco,[73a,73b] N. De Groot,[119] P. de Jong,[120] H. De la Torre,[107] A. De Maria,[15c] D. De Pedis,[73a] A. De Salvo,[73a] U. De Sanctis,[74a,74b] M. De Santis,[74a,74b] A. De Santo,[156] K. De Vasconcelos Corga,[102] J. B. De Vivie De Regie,[65] C. Debenedetti,[146] D. V. Dedovich,[80] A. M. Deiana,[42] M. Del Gaudio,[41b,41a] J. Del Peso,[99] Y. Delabat Diaz,[46] D. Delgove,[65] F. Deliot,[145,r] C. M. Delitzsch,[7] M. Della Pietra,[70a,70b] D. Della Volpe,[54] A. Dell'Acqua,[36] L. Dell'Asta,[74a,74b] M. Delmastro,[5] C. Delporte,[65] P. A. Delsart,[58] D. A. DeMarco,[167] S. Demers,[183] M. Demichev,[80] G. Demontigny,[110] S. P. Denisov,[123] D. Denysiuk,[120] L. D'Eramo,[136] D. Derendarz,[85] J. E. Derkaoui,[35d] F. Derue,[136] P. Dervan,[91] K. Desch,[24] C. Deterre,[46] K. Dette,[167] C. Deutsch,[24] M. R. Devesa,[30] P. O. Deviveiros,[36] A. Dewhurst,[144] F. A. Di Bello,[54] A. Di Ciaccio,[74a,74b] L. Di Ciaccio,[5] W. K. Di Clemente,[137] C. Di Donato,[70a,70b] A. Di Girolamo,[36] G. Di Gregorio,[72a,72b] B. Di Micco,[75a,75b] R. Di Nardo,[103] K. F. Di Petrillo,[59] R. Di Sipio,[167] D. Di Valentino,[34] C. Diaconu,[102] F. A. Dias,[40] T. Dias Do Vale,[140a] M. A. Diaz,[147a] J. Dickinson,[18] E. B. Diehl,[106] J. Dietrich,[19] S. Díez Cornell,[46] A. Dimitrievska,[18] W. Ding,[15b] J. Dingfelder,[24] F. Dittus,[36] F. Djama,[102] T. Djobava,[159b] J. I. Djuvsland,[17] M. A. B. Do Vale,[81c] M. Dobre,[27b] D. Dodsworth,[26] C. Doglioni,[97] J. Dolejsi,[143] Z. Dolezal,[143] M. Donadelli,[81d] B. Dong,[60c] J. Donini,[38] A. D'onofrio,[93] M. D'Onofrio,[91] J. Dopke,[144] A. Doria,[70a] M. T. Dova,[89] A. T. Doyle,[57] E. Drechsler,[152] E. Dreyer,[152] T. Dreyer,[53] A. S. Drobac,[170] Y. Duan,[60b] F. Dubinin,[111] M. Dubovsky,[28a] A. Dubreuil,[54] E. Duchovni,[180] G. Duckeck,[114] A. Ducourthial,[136] O. A. Ducu,[110] D. Duda,[115] A. Dudarev,[36] A. C. Dudder,[100] E. M. Duffield,[18] L. Duflot,[65] M. Dührssen,[36] C. Dülsen,[182] M. Dumancic,[180] A. E. Dumitriu,[27b] A. K. Duncan,[57] M. Dunford,[61a] A. Duperrin,[102] H. Duran Yildiz,[4a] M. Düren,[56] A. Durglishvili,[159b] D. Duschinger,[48] B. Dutta,[46] D. Duvnjak,[1] G. I. Dyckes,[137] M. Dyndal,[36] S. Dysch,[101] B. S. Dziedzic,[85] K. M. Ecker,[115] R. C. Edgar,[106] M. G. Eggleston,[49] T. Eifert,[36] G. Eigen,[17] K. Einsweiler,[18] T. Ekelof,[172] H. El Jarrari,[35e] M. El Kacimi,[35c] R. El Kosseifi,[102] V. Ellajosyula,[172] M. Ellert,[172] F. Ellinghaus,[182] A. A. Elliot,[93] N. Ellis,[36] J. Elmsheuser,[29] M. Elsing,[36] D. Emeliyanov,[144] A. Emerman,[39] Y. Enari,[163] M. B. Epland,[49] J. Erdmann,[47] A. Ereditato,[20] M. Errenst,[36] M. Escalier,[65] C. Escobar,[174] O. Estrada Pastor,[174] E. Etzion,[161] H. Evans,[66] A. Ezhilov,[138] F. Fabbri,[57] L. Fabbri,[23b,23a] V. Fabiani,[119] G. Facini,[95] R. M. Faisca Rodrigues Pereira,[140a] R. M. Fakhrutdinov,[123] S. Falciano,[73a] P. J. Falke,[5] S. Falke,[5] J. Faltova,[143] Y. Fang,[15a] Y. Fang,[15a] G. Fanourakis,[44] M. Fanti,[69a,69b] M. Faraj,[67a,67c,s] A. Farbin,[8] A. Farilla,[75a] E. M. Farina,[71a,71b] T. Farooque,[107] S. Farrell,[18] S. M. Farrington,[50] P. Farthouat,[36] F. Fassi,[35e] P. Fassnacht,[36] D. Fassouliotis,[9] M. Faucci Giannelli,[50] W. J. Fawcett,[32] L. Fayard,[65] O. L. Fedin,[138,t] W. Fedorko,[175] M. Feickert,[42] L. Feligioni,[102] A. Fell,[149] C. Feng,[60b] E. J. Feng,[36] M. Feng,[49] M. J. Fenton,[57] A. B. Fenyuk,[123] J. Ferrando,[46] A. Ferrante,[173] A. Ferrari,[172] P. Ferrari,[120] R. Ferrari,[71a] D. E. Ferreira de Lima,[61b] A. Ferrer,[174] D. Ferrere,[54] C. Ferretti,[106] F. Fiedler,[100] A. Filipčič,[92] F. Filthaut,[119] K. D. Finelli,[25] M. C. N. Fiolhais,[140a,140c,u] L. Fiorini,[174] F. Fischer,[114] W. C. Fisher,[107] I. Fleck,[151] P. Fleischmann,[106] R. R. M. Fletcher,[137] T. Flick,[182] B. M. Flierl,[114]

L. Flores,[137] L. R. Flores Castillo,[63a] F. M. Follega,[76a,76b] N. Fomin,[17] J. H. Foo,[167] G. T. Forcolin,[76a,76b] A. Formica,[145] F. A. Förster,[14] A. C. Forti,[101] A. G. Foster,[21] M. G. Foti,[135] D. Fournier,[65] H. Fox,[90] P. Francavilla,[72a,72b] S. Francescato,[73a,73b] M. Franchini,[23b,23a] S. Franchino,[61a] D. Francis,[36] L. Franconi,[20] M. Franklin,[59] A. N. Fray,[93] P. M. Freeman,[21] B. Freund,[110] W. S. Freund,[81b] E. M. Freundlich,[47] D. C. Frizzell,[129] D. Froidevaux,[36] J. A. Frost,[135] C. Fukunaga,[164] E. Fullana Torregrosa,[174] E. Fumagalli,[55b,55a] T. Fusayasu,[116] J. Fuster,[174] A. Gabrielli,[23b,23a] A. Gabrielli,[18] G. P. Gach,[84a] S. Gadatsch,[54] P. Gadow,[115] G. Gagliardi,[55b,55a] L. G. Gagnon,[110] C. Galea,[27b] B. Galhardo,[140a] G. E. Gallardo,[135] E. J. Gallas,[135] B. J. Gallop,[144] G. Galster,[40] R. Gamboa Goni,[93] K. K. Gan,[127] S. Ganguly,[180] J. Gao,[60a] Y. Gao,[50] Y. S. Gao,[31,h] C. García,[174] J. E. García Navarro,[174] J. A. García Pascual,[15a] C. Garcia-Argos,[52] M. Garcia-Sciveres,[18] R. W. Gardner,[37] N. Garelli,[153] S. Gargiulo,[52] V. Garonne,[134] A. Gaudiello,[55b,55a] G. Gaudio,[71a] I. L. Gavrilenko,[111] A. Gavrilyuk,[124] C. Gay,[175] G. Gaycken,[46] E. N. Gazis,[10] A. A. Geanta,[27b] C. M. Gee,[146] C. N. P. Gee,[144] J. Geisen,[53] M. Geisen,[100] M. P. Geisler,[61a] C. Gemme,[55b] M. H. Genest,[58] C. Geng,[106] S. Gentile,[73a,73b] S. George,[94] T. Geralis,[44] L. O. Gerlach,[53] P. Gessinger-Befurt,[100] G. Gessner,[47] S. Ghasemi,[151] M. Ghasemi Bostanabad,[176] A. Ghosh,[65] A. Ghosh,[78] B. Giacobbe,[23b] S. Giagu,[73a,73b] N. Giangiacomi,[23b,23a] P. Giannetti,[72a] A. Giannini,[70a,70b] G. Giannini,[14] S. M. Gibson,[94] M. Gignac,[146] D. Gillberg,[34] G. Gilles,[182] D. M. Gingrich,[3,e] M. P. Giordani,[67a,67c] F. M. Giorgi,[23b] P. F. Giraud,[145] G. Giugliarelli,[67a,67c] D. Giugni,[69a] F. Giuli,[74a,74b] S. Gkaitatzis,[162] I. Gkialas,[9,v] E. L. Gkougkousis,[14] P. Gkountoumis,[10] L. K. Gladilin,[113] C. Glasman,[99] J. Glatzer,[14] P. C. F. Glaysher,[46] A. Glazov,[46] G. R. Gledhill,[132] M. Goblirsch-Kolb,[26] D. Godin,[110] S. Goldfarb,[105] T. Golling,[54] D. Golubkov,[123] A. Gomes,[140a,140b] R. Goncalves Gama,[53] R. Gonçalo,[140a] G. Gonella,[52] L. Gonella,[21] A. Gongadze,[80] F. Gonnella,[21] J. L. Gonski,[59] S. González de la Hoz,[174] S. Gonzalez-Sevilla,[54] G. R. Gonzalvo Rodriguez,[174] L. Goossens,[36] P. A. Gorbounov,[124] H. A. Gordon,[29] B. Gorini,[36] E. Gorini,[68a,68b] A. Gorišek,[92] A. T. Goshaw,[49] M. I. Gostkin,[80] C. A. Gottardo,[119] M. Gouighri,[35b] D. Goujdami,[35c] A. G. Goussiou,[148] N. Govender,[33c] C. Goy,[5] E. Gozani,[160] I. Grabowska-Bold,[84a] E. C. Graham,[91] J. Gramling,[171] E. Gramstad,[134] S. Grancagnolo,[19] M. Grandi,[156] V. Gratchev,[138] P. M. Gravila,[27f] F. G. Gravili,[68a,68b] C. Gray,[57] H. M. Gray,[18] C. Grefe,[24] K. Gregersen,[97] I. M. Gregor,[46] P. Grenier,[153] K. Grevtsov,[46] C. Grieco,[14] N. A. Grieser,[129] J. Griffiths,[8] A. A. Grillo,[146] K. Grimm,[31,w] S. Grinstein,[14,x] J.-F. Grivaz,[65] S. Groh,[100] E. Gross,[180] J. Grosse-Knetter,[53] Z. J. Grout,[95] C. Grud,[106] A. Grummer,[118] L. Guan,[106] W. Guan,[181] J. Guenther,[36] A. Guerguichon,[65] J. G. R. Guerrero Rojas,[174] F. Guescini,[115] D. Guest,[171] R. Gugel,[52] T. Guillemin,[5] S. Guindon,[36] U. Gul,[57] J. Guo,[60c] W. Guo,[106] Y. Guo,[60a,y] Z. Guo,[102] R. Gupta,[46] S. Gurbuz,[12c] G. Gustavino,[129] M. Guth,[52] P. Gutierrez,[129] C. Gutschow,[95] C. Guyot,[145] C. Gwenlan,[135] C. B. Gwilliam,[91] A. Haas,[125] C. Haber,[18] H. K. Hadavand,[8] N. Haddad,[35e] A. Hadef,[60a] S. Hageböck,[36] M. Haleem,[177] J. Haley,[130] G. Halladjian,[107] G. D. Hallewell,[102] K. Hamacher,[182] P. Hamal,[131] K. Hamano,[176] H. Hamdaoui,[35e] G. N. Hamity,[149] K. Han,[60a,z] L. Han,[60a] S. Han,[15a] Y. F. Han,[167] K. Hanagaki,[82,aa] M. Hance,[146] D. M. Handl,[114] B. Haney,[137] R. Hankache,[136] E. Hansen,[97] J. B. Hansen,[40] J. D. Hansen,[40] M. C. Hansen,[24] P. H. Hansen,[40] E. C. Hanson,[101] K. Hara,[169] T. Harenberg,[182] S. Harkusha,[108] P. F. Harrison,[178] N. M. Hartmann,[114] Y. Hasegawa,[150] A. Hasib,[50] S. Hassani,[145] S. Haug,[20] R. Hauser,[107] L. B. Havener,[39] M. Havranek,[142] C. M. Hawkes,[21] R. J. Hawkings,[36] D. Hayden,[107] C. Hayes,[155] R. L. Hayes,[175] C. P. Hays,[135] J. M. Hays,[93] H. S. Hayward,[91] S. J. Haywood,[144] F. He,[60a] M. P. Heath,[50] V. Hedberg,[97] L. Heelan,[8] S. Heer,[24] K. K. Heidegger,[52] W. D. Heidorn,[79] J. Heilman,[34] S. Heim,[46] T. Heim,[18] B. Heinemann,[46,bb] J. J. Heinrich,[132] L. Heinrich,[36] C. Heinz,[56] J. Hejbal,[141] L. Helary,[61b] A. Held,[175] S. Hellesund,[134] C. M. Helling,[146] S. Hellman,[45a,45b] C. Helsens,[36] R. C. W. Henderson,[90] Y. Heng,[181] S. Henkelmann,[175] A. M. Henriques Correia,[36] G. H. Herbert,[19] H. Herde,[26] V. Herget,[177] Y. Hernández Jiménez,[33e] H. Herr,[100] M. G. Herrmann,[114] T. Herrmann,[48] G. Herten,[52] R. Hertenberger,[114] L. Hervas,[36] T. C. Herwig,[137] G. G. Hesketh,[95] N. P. Hessey,[168a] A. Higashida,[163] S. Higashino,[82] E. Higón-Rodriguez,[174] K. Hildebrand,[37] E. Hill,[176] J. C. Hill,[32] K. K. Hill,[29] K. H. Hiller,[46] S. J. Hillier,[21] M. Hils,[48] I. Hinchliffe,[18] F. Hinterkeuser,[24] M. Hirose,[133] S. Hirose,[52] D. Hirschbuehl,[182] B. Hiti,[92] O. Hladik,[141] D. R. Hlaluku,[33e] X. Hoad,[50] J. Hobbs,[155] N. Hod,[180] M. C. Hodgkinson,[149] A. Hoecker,[36] F. Hoenig,[114] D. Hohn,[52] D. Hohov,[65] T. R. Holmes,[37] M. Holzbock,[114] L. B. A. H. Hommels,[32] S. Honda,[169] T. M. Hong,[139] A. Hönle,[115] B. H. Hooberman,[173] W. H. Hopkins,[6] Y. Horii,[117] P. Horn,[48] L. A. Horyn,[37] S. Hou,[158] A. Hoummada,[35a] J. Howarth,[101] J. Hoya,[89] M. Hrabovsky,[131] J. Hrdinka,[77] I. Hristova,[19] J. Hrivnac,[65] A. Hrynevich,[109] T. Hryn'ova,[5] P. J. Hsu,[64] S.-C. Hsu,[148] Q. Hu,[29] S. Hu,[60c] D. P. Huang,[95] Y. Huang,[60a] Y. Huang,[15a] Z. Hubacek,[142] F. Hubaut,[102] M. Huebner,[24] F. Huegging,[24] T. B. Huffman,[135] M. Huhtinen,[36] R. F. H. Hunter,[34] P. Huo,[155] A. M. Hupe,[34] N. Huseynov,[80,cc] J. Huston,[107] J. Huth,[59] R. Hyneman,[106] S. Hyrych,[28a] G. Iacobucci,[54] G. Iakovidis,[29] I. Ibragimov,[151] L. Iconomidou-Fayard,[65] Z. Idrissi,[35e] P. Iengo,[36] R. Ignazzi,[40] O. Igonkina,[120,a,dd] R. Iguchi,[163] T. Iizawa,[54] Y. Ikegami,[82]

M. Ikeno,[82] D. Iliadis,[162] N. Ilic,[119,167,q] F. Iltzsche,[48] G. Introzzi,[71a,71b] M. Iodice,[75a] K. Iordanidou,[168a] V. Ippolito,[73a,73b] M. F. Isacson,[172] M. Ishino,[163] W. Islam,[130] C. Issever,[135] S. Istin,[160] F. Ito,[169] J. M. Iturbe Ponce,[63a] R. Iuppa,[76a,76b] A. Ivina,[180] H. Iwasaki,[82] J. M. Izen,[43] V. Izzo,[70a] P. Jacka,[141] P. Jackson,[1] R. M. Jacobs,[24] B. P. Jaeger,[152] V. Jain,[2] G. Jäkel,[182] K. B. Jakobi,[100] K. Jakobs,[52] S. Jakobsen,[77] T. Jakoubek,[141] J. Jamieson,[57] K. W. Janas,[84a] R. Jansky,[54] J. Janssen,[24] M. Janus,[53] P. A. Janus,[84a] G. Jarlskog,[97] N. Javadov,[80,cc] T. Javůrek,[36] M. Javurkova,[52] F. Jeanneau,[145] L. Jeanty,[132] J. Jejelava,[159a,ee] A. Jelinskas,[178] P. Jenni,[52,ff] J. Jeong,[46] N. Jeong,[46] S. Jézéquel,[5] H. Ji,[181] J. Jia,[155] H. Jiang,[79] Y. Jiang,[60a] Z. Jiang,[153,gg] S. Jiggins,[52] F. A. Jimenez Morales,[38] J. Jimenez Pena,[115] S. Jin,[15c] A. Jinaru,[27b] O. Jinnouchi,[165] H. Jivan,[33e] P. Johansson,[149] K. A. Johns,[7] C. A. Johnson,[66] K. Jon-And,[45a,45b] R. W. L. Jones,[90] S. D. Jones,[156] S. Jones,[7] T. J. Jones,[91] J. Jongmanns,[61a] P. M. Jorge,[140a] J. Jovicevic,[36] X. Ju,[18] J. J. Junggeburth,[115] A. Juste Rozas,[14,x] A. Kaczmarska,[85] M. Kado,[73a,73b] H. Kagan,[127] M. Kagan,[153] C. Kahra,[100] T. Kaji,[179] E. Kajomovitz,[160] C. W. Kalderon,[97] A. Kaluza,[100] A. Kamenshchikov,[123] M. Kaneda,[163] L. Kanjir,[92] Y. Kano,[163] V. A. Kantserov,[112] J. Kanzaki,[82] L. S. Kaplan,[181] D. Kar,[33e] K. Karava,[135] M. J. Kareem,[168b] S. N. Karpov,[80] Z. M. Karpova,[80] V. Kartvelishvili,[90] A. N. Karyukhin,[123] L. Kashif,[181] R. D. Kass,[127] A. Kastanas,[45a,45b] C. Kato,[60d,60c] J. Katzy,[46] K. Kawade,[150] K. Kawagoe,[88] T. Kawaguchi,[117] T. Kawamoto,[163] G. Kawamura,[53] E. F. Kay,[176] V. F. Kazanin,[122b,122a] R. Keeler,[176] R. Kehoe,[42] J. S. Keller,[34] E. Kellermann,[97] D. Kelsey,[156] J. J. Kempster,[21] J. Kendrick,[21] O. Kepka,[141] S. Kersten,[182] B. P. Kerševan,[92] S. Ketabchi Haghighat,[167] M. Khader,[173] F. Khalil-Zada,[13] M. Khandoga,[145] A. Khanov,[130] A. G. Kharlamov,[122b,122a] T. Kharlamova,[122b,122a] E. E. Khoda,[175] A. Khodinov,[166] T. J. Khoo,[54] E. Khramov,[80] J. Khubua,[159b] S. Kido,[83] M. Kiehn,[54] C. R. Kilby,[94] Y. K. Kim,[37] N. Kimura,[95] O. M. Kind,[19] B. T. King,[91,a] D. Kirchmeier,[48] J. Kirk,[144] A. E. Kiryunin,[115] T. Kishimoto,[163] D. P. Kisliuk,[167] V. Kitali,[46] O. Kivernyk,[5] T. Klapdor-Kleingrothaus,[52] M. Klassen,[61a] M. H. Klein,[106] M. Klein,[91] U. Klein,[91] K. Kleinknecht,[100] P. Klimek,[121] A. Klimentov,[29] T. Klingl,[24] T. Klioutchnikova,[36] F. F. Klitzner,[114] P. Kluit,[120] S. Kluth,[115] E. Kneringer,[77] E. B. F. G. Knoops,[102] A. Knue,[52] D. Kobayashi,[88] T. Kobayashi,[163] M. Kobel,[48] M. Kocian,[153] P. Kodys,[143] P. T. Koenig,[24] T. Koffas,[34] N. M. Köhler,[36] T. Koi,[153] M. Kolb,[61b] I. Koletsou,[5] T. Komarek,[131] T. Kondo,[82] N. Kondrashova,[60c] K. Köneke,[52] A. C. König,[119] T. Kono,[126] R. Konoplich,[125,hh] V. Konstantinides,[95] N. Konstantinidis,[95] B. Konya,[97] R. Kopeliansky,[66] S. Koperny,[84a] K. Korcyl,[85] K. Kordas,[162] G. Koren,[161] A. Korn,[95] I. Korolkov,[14] E. V. Korolkova,[149] N. Korotkova,[113] O. Kortner,[115] S. Kortner,[115] T. Kosek,[143] V. V. Kostyukhin,[166] A. Kotwal,[49] A. Koulouris,[10] A. Kourkoumeli-Charalampidi,[71a,71b] C. Kourkoumelis,[9] E. Kourlitis,[149] V. Kouskoura,[29] A. B. Kowalewska,[85] R. Kowalewski,[176] C. Kozakai,[163] W. Kozanecki,[145] A. S. Kozhin,[123] V. A. Kramarenko,[113] G. Kramberger,[92] D. Krasnopevtsev,[60a] M. W. Krasny,[136] A. Krasznahorkay,[36] D. Krauss,[115] J. A. Kremer,[84a] J. Kretzschmar,[91] P. Krieger,[167] F. Krieter,[114] A. Krishnan,[61b] K. Krizka,[18] K. Kroeninger,[47] H. Kroha,[115] J. Kroll,[141] J. Kroll,[137] J. Krstic,[16] U. Kruchonak,[80] H. Krüger,[24] N. Krumnack,[79] M. C. Kruse,[49] J. A. Krzysiak,[85] T. Kubota,[105] O. Kuchinskaia,[166] S. Kuday,[4b] J. T. Kuechler,[46] S. Kuehn,[36] A. Kugel,[61a] T. Kuhl,[46] V. Kukhtin,[80] R. Kukla,[102] Y. Kulchitsky,[108,ii] S. Kuleshov,[147c] Y. P. Kulinich,[173] M. Kuna,[58] T. Kunigo,[86] A. Kupco,[141] T. Kupfer,[47] O. Kuprash,[52] H. Kurashige,[83] L. L. Kurchaninov,[168a] Y. A. Kurochkin,[108] A. Kurova,[112] M. G. Kurth,[15a,15d] E. S. Kuwertz,[36] M. Kuze,[165] A. K. Kvam,[148] J. Kvita,[131] T. Kwan,[104] A. La Rosa,[115] L. La Rotonda,[41b,41a] F. La Ruffa,[41b,41a] C. Lacasta,[174] F. Lacava,[73a,73b] D. P. J. Lack,[101] H. Lacker,[19] D. Lacour,[136] E. Ladygin,[80] R. Lafaye,[5] B. Laforge,[136] T. Lagouri,[33e] S. Lai,[53] S. Lammers,[66] W. Lampl,[7] C. Lampoudis,[162] E. Lançon,[29] U. Landgraf,[52] M. P. J. Landon,[93] M. C. Lanfermann,[54] V. S. Lang,[46] J. C. Lange,[53] R. J. Langenberg,[36] A. J. Lankford,[171] F. Lanni,[29] K. Lantzsch,[24] A. Lanza,[71a] A. Lapertosa,[55b,55a] S. Laplace,[136] J. F. Laporte,[145] T. Lari,[69a] F. Lasagni Manghi,[23b,23a] M. Lassnig,[36] T. S. Lau,[63a] A. Laudrain,[65] A. Laurier,[34] M. Lavorgna,[70a,70b] S. D. Lawlor,[94] M. Lazzaroni,[69a,69b] B. Le,[105] E. Le Guirriec,[102] M. LeBlanc,[7] T. LeCompte,[6] F. Ledroit-Guillon,[58] A. C. A. Lee,[95] C. A. Lee,[29] G. R. Lee,[17] L. Lee,[59] S. C. Lee,[158] S. J. Lee,[34] B. Lefebvre,[168a] M. Lefebvre,[176] F. Legger,[114] C. Leggett,[18] K. Lehmann,[152] N. Lehmann,[182] G. Lehmann Miotto,[36] W. A. Leight,[46] A. Leisos,[162,jj] M. A. L. Leite,[81d] C. E. Leitgeb,[114] R. Leitner,[143] D. Lellouch,[180,a] K. J. C. Leney,[42] T. Lenz,[24] B. Lenzi,[36] R. Leone,[7] S. Leone,[72a] C. Leonidopoulos,[50] A. Leopold,[136] G. Lerner,[156] C. Leroy,[110] R. Les,[167] C. G. Lester,[32] M. Levchenko,[138] J. Levêque,[5] D. Levin,[106] L. J. Levinson,[180] D. J. Lewis,[21] B. Li,[15b] B. Li,[106] C-Q. Li,[60a] F. Li,[60c] H. Li,[60a] H. Li,[60b] J. Li,[60c] K. Li,[153] L. Li,[60c] M. Li,[15a,15d] Q. Li,[15a,15d] Q. Y. Li,[60a] S. Li,[60d,60c] X. Li,[46] Y. Li,[46] Z. Li,[60b] Z. Liang,[15a] B. Liberti,[74a] A. Liblong,[167] K. Lie,[63c] C. Y. Lin,[32] K. Lin,[107] T. H. Lin,[100] R. A. Linck,[66] J. H. Lindon,[21] A. L. Lionti,[54] E. Lipeles,[137] A. Lipniacka,[17] M. Lisovyi,[61b] T. M. Liss,[173,kk] A. Lister,[175] A. M. Litke,[146] J. D. Little,[8] B. Liu,[79] B. L. Liu,[6] H. B. Liu,[29] H. Liu,[106] J. B. Liu,[60a] J. K. K. Liu,[135] K. Liu,[136] M. Liu,[60a] P. Liu,[18] Y. Liu,[15a,15d] Y. L. Liu,[106] Y. W. Liu,[60a] M. Livan,[71a,71b] A. Lleres,[58] J. Llorente Merino,[152] S. L. Lloyd,[93] C. Y. Lo,[63b] F. Lo Sterzo,[42] E. M. Lobodzinska,[46] P. Loch,[7]

S. Loffredo,[74a,74b] T. Lohse,[19] K. Lohwasser,[149] M. Lokajicek,[141] J. D. Long,[173] R. E. Long,[90] L. Longo,[36] K. A. Looper,[127] J. A. Lopez,[147c] I. Lopez Paz,[101] A. Lopez Solis,[149] J. Lorenz,[114] N. Lorenzo Martinez,[5] M. Losada,[22] P. J. Lösel,[114] A. Lösle,[52] X. Lou,[46] X. Lou,[15a] A. Lounis,[65] J. Love,[6] P. A. Love,[90] J. J. Lozano Bahilo,[174] M. Lu,[60a] Y. J. Lu,[64] H. J. Lubatti,[148] C. Luci,[73a,73b] A. Lucotte,[58] C. Luedtke,[52] F. Luehring,[66] I. Luise,[136] L. Luminari,[73a] B. Lund-Jensen,[154] M. S. Lutz,[103] D. Lynn,[29] R. Lysak,[141] E. Lytken,[97] F. Lyu,[15a] V. Lyubushkin,[80] T. Lyubushkina,[80] H. Ma,[29] L. L. Ma,[60b] Y. Ma,[60b] G. Maccarrone,[51] A. Macchiolo,[115] C. M. Macdonald,[149] J. Machado Miguens,[137] D. Madaffari,[174] R. Madar,[38] W. F. Mader,[48] N. Madysa,[48] J. Maeda,[83] S. Maeland,[17] T. Maeno,[29] M. Maerker,[48] A. S. Maevskiy,[113] V. Magerl,[52] N. Magini,[79] D. J. Mahon,[39] C. Maidantchik,[81b] T. Maier,[114] A. Maio,[140a,140b,140d] K. Maj,[84a] O. Majersky,[28a] S. Majewski,[132] Y. Makida,[82] N. Makovec,[65] B. Malaescu,[136] Pa. Malecki,[85] V. P. Maleev,[138] F. Malek,[58] U. Mallik,[78] D. Malon,[6] C. Malone,[32] S. Maltezos,[10] S. Malyukov,[80] J. Mamuzic,[174] G. Mancini,[51] I. Mandić,[92] L. Manhaes de Andrade Filho,[81a] I. M. Maniatis,[162] J. Manjarres Ramos,[48] K. H. Mankinen,[97] A. Mann,[114] A. Manousos,[77] B. Mansoulie,[145] I. Manthos,[162] S. Manzoni,[120] A. Marantis,[162] G. Marceca,[30] L. Marchese,[135] G. Marchiori,[136] M. Marcisovsky,[141] C. Marcon,[97] C. A. Marin Tobon,[36] M. Marjanovic,[129] Z. Marshall,[18] M. U. F. Martensson,[172] S. Marti-Garcia,[174] C. B. Martin,[127] T. A. Martin,[178] V. J. Martin,[50] B. Martin dit Latour,[17] L. Martinelli,[75a,75b] M. Martinez,[14,x] V. I. Martinez Outschoorn,[103] S. Martin-Haugh,[144] V. S. Martoiu,[27b] A. C. Martyniuk,[95] A. Marzin,[36] S. R. Maschek,[115] L. Masetti,[100] T. Mashimo,[163] R. Mashinistov,[111] J. Masik,[101] A. L. Maslennikov,[122b,122a] L. Massa,[74a,74b] P. Massarotti,[70a,70b] P. Mastrandrea,[72a,72b] A. Mastroberardino,[41b,41a] T. Masubuchi,[163] D. Matakias,[10] A. Matic,[114] P. Mättig,[24] J. Maurer,[27b] B. Maček,[92] D. A. Maximov,[122b,122a] R. Mazini,[158] I. Maznas,[162] S. M. Mazza,[146] S. P. Mc Kee,[106] T. G. McCarthy,[115] W. P. McCormack,[18] E. F. McDonald,[105] J. A. Mcfayden,[36] G. Mchedlidze,[159b] M. A. McKay,[42] K. D. McLean,[176] S. J. McMahon,[144] P. C. McNamara,[105] C. J. McNicol,[178] R. A. McPherson,[176,q] J. E. Mdhluli,[33e] Z. A. Meadows,[103] S. Meehan,[36] T. Megy,[52] S. Mehlhase,[114] A. Mehta,[91] T. Meideck,[58] B. Meirose,[43] D. Melini,[174] B. R. Mellado Garcia,[33e] J. D. Mellenthin,[53] M. Melo,[28a] F. Meloni,[46] A. Melzer,[24] S. B. Menary,[101] E. D. Mendes Gouveia,[140a,140e] L. Meng,[36] X. T. Meng,[106] S. Menke,[115] E. Meoni,[41b,41a] S. Mergelmeyer,[19] S. A. M. Merkt,[139] C. Merlassino,[20] P. Mermod,[54] L. Merola,[70a,70b] C. Meroni,[69a] O. Meshkov,[113,111] J. K. R. Meshreki,[151] A. Messina,[73a,73b] J. Metcalfe,[6] A. S. Mete,[171] C. Meyer,[66] J. Meyer,[160] J-P. Meyer,[145] H. Meyer Zu Theenhausen,[61a] F. Miano,[156] M. Michetti,[19] R. P. Middleton,[144] L. Mijović,[50] G. Mikenberg,[180] M. Mikestikova,[141] M. Mikuž,[92] H. Mildner,[149] M. Milesi,[105] A. Milic,[167] D. A. Millar,[93] D. W. Miller,[37] A. Milov,[180] D. A. Milstead,[45a,45b] R. A. Mina,[153,gg] A. A. Minaenko,[123] M. Miñano Moya,[174] I. A. Minashvili,[159b] A. I. Mincer,[125] B. Mindur,[84a] M. Mineev,[80] Y. Minegishi,[163] L. M. Mir,[14] A. Mirto,[68a,68b] K. P. Mistry,[137] T. Mitani,[179] J. Mitrevski,[114] V. A. Mitsou,[174] M. Mittal,[60c] O. Miu,[167] A. Miucci,[20] P. S. Miyagawa,[149] A. Mizukami,[82] J. U. Mjörnmark,[97] T. Mkrtchyan,[184] M. Mlynarikova,[143] T. Moa,[45a,45b] K. Mochizuki,[110] P. Mogg,[52] S. Mohapatra,[39] R. Moles-Valls,[24] M. C. Mondragon,[107] K. Mönig,[46] J. Monk,[40] E. Monnier,[102] A. Montalbano,[152] J. Montejo Berlingen,[36] M. Montella,[95] F. Monticelli,[89] S. Monzani,[69a] N. Morange,[65] D. Moreno,[22] M. Moreno Llácer,[36] C. Moreno Martinez,[14] P. Morettini,[55b] M. Morgenstern,[120] S. Morgenstern,[48] D. Mori,[152] M. Morii,[59] M. Morinaga,[179] V. Morisbak,[134] A. K. Morley,[36] G. Mornacchi,[36] A. P. Morris,[95] L. Morvaj,[155] P. Moschovakos,[36] B. Moser,[120] M. Mosidze,[159b] T. Moskalets,[145] H. J. Moss,[149] J. Moss,[31,ll] E. J. W. Moyse,[103] S. Muanza,[102] J. Mueller,[139] R. S. P. Mueller,[114] D. Muenstermann,[90] G. A. Mullier,[97] J. L. Munoz Martinez,[14] F. J. Munoz Sanchez,[101] P. Murin,[28b] W. J. Murray,[178,144] A. Murrone,[69a,69b] M. Muškinja,[18] C. Mwewa,[33a] A. G. Myagkov,[123,mm] J. Myers,[132] M. Myska,[142] B. P. Nachman,[18] O. Nackenhorst,[47] A. Nag Nag,[48] K. Nagai,[135] K. Nagano,[82] Y. Nagasaka,[62] M. Nagel,[52] J. L. Nagle,[29] E. Nagy,[102] A. M. Nairz,[36] Y. Nakahama,[117] K. Nakamura,[82] T. Nakamura,[163] I. Nakano,[128] H. Nanjo,[133] F. Napolitano,[61a] R. F. Naranjo Garcia,[46] R. Narayan,[42] I. Naryshkin,[138] T. Naumann,[46] G. Navarro,[22] H. A. Neal,[106,a] P. Y. Nechaeva,[111] F. Nechansky,[46] T. J. Neep,[21] A. Negri,[71a,71b] M. Negrini,[23b] C. Nellist,[53] M. E. Nelson,[135] S. Nemecek,[141] P. Nemethy,[125] M. Nessi,[36,nn] M. S. Neubauer,[173] M. Neumann,[182] P. R. Newman,[21] Y. S. Ng,[19] Y. W. Y. Ng,[171] B. Ngair,[35e] H. D. N. Nguyen,[102] T. Nguyen Manh,[110] E. Nibigira,[38] R. B. Nickerson,[135] R. Nicolaidou,[145] D. S. Nielsen,[40] J. Nielsen,[146] N. Nikiforou,[11] V. Nikolaenko,[123,mm] I. Nikolic-Audit,[136] K. Nikolopoulos,[21] P. Nilsson,[29] H. R. Nindhito,[54] Y. Ninomiya,[82] A. Nisati,[73a] N. Nishu,[60c] R. Nisius,[115] I. Nitsche,[47] T. Nitta,[179] T. Nobe,[163] Y. Noguchi,[86] I. Nomidis,[136] M. A. Nomura,[29] M. Nordberg,[36] N. Norjoharuddeen,[135] T. Novak,[92] O. Novgorodova,[48] R. Novotny,[142] L. Nozka,[131] K. Ntekas,[171] E. Nurse,[95] F. G. Oakham,[34,e] H. Oberlack,[115] J. Ocariz,[136] A. Ochi,[83] I. Ochoa,[39] J. P. Ochoa-Ricoux,[147a] K. O'Connor,[26] S. Oda,[88] S. Odaka,[82] S. Oerdek,[53] A. Ogrodnik,[84a] A. Oh,[101] S. H. Oh,[49] C. C. Ohm,[154] H. Oide,[165] M. L. Ojeda,[167] H. Okawa,[169] Y. Okazaki,[86] Y. Okumura,[163] T. Okuyama,[82] A. Olariu,[27b] L. F. Oleiro Seabra,[140a] S. A. Olivares Pino,[147a]

D. Oliveira Damazio,[29] J. L. Oliver,[1] M. J. R. Olsson,[171] A. Olszewski,[85] J. Olszowska,[85] D. C. O'Neil,[152] A. P. O'neill,[135] A. Onofre,[140a,140e] P. U. E. Onyisi,[11] H. Oppen,[134] M. J. Oreglia,[37] G. E. Orellana,[89] D. Orestano,[75a,75b] N. Orlando,[14] R. S. Orr,[167] V. O'Shea,[57] R. Ospanov,[60a] G. Otero y Garzon,[30] H. Otono,[88] P. S. Ott,[61a] M. Ouchrif,[35d] J. Ouellette,[29] F. Ould-Saada,[134] A. Ouraou,[145] Q. Ouyang,[15a] M. Owen,[57] R. E. Owen,[21] V. E. Ozcan,[12c] N. Ozturk,[8] J. Pacalt,[131] H. A. Pacey,[32] K. Pachal,[49] A. Pacheco Pages,[14] C. Padilla Aranda,[14] S. Pagan Griso,[18] M. Paganini,[183] G. Palacino,[66] S. Palazzo,[50] S. Palestini,[36] M. Palka,[84b] D. Pallin,[38] I. Panagoulias,[10] C. E. Pandini,[36] J. G. Panduro Vazquez,[94] P. Pani,[46] G. Panizzo,[67a,67c] L. Paolozzi,[54] C. Papadatos,[110] K. Papageorgiou,[9,v] S. Parajuli,[43] A. Paramonov,[6] D. Paredes Hernandez,[63b] S. R. Paredes Saenz,[135] B. Parida,[166] T. H. Park,[167] A. J. Parker,[31] M. A. Parker,[32] F. Parodi,[55b,55a] E. W. Parrish,[121] J. A. Parsons,[39] U. Parzefall,[52] L. Pascual Dominguez,[136] V. R. Pascuzzi,[167] J. M. P. Pasner,[146] E. Pasqualucci,[73a] S. Passaggio,[55b] F. Pastore,[94] P. Pasuwan,[45a,45b] S. Pataraia,[100] J. R. Pater,[101] A. Pathak,[181,f] T. Pauly,[36] B. Pearson,[115] M. Pedersen,[134] L. Pedraza Diaz,[119] R. Pedro,[140a] T. Peiffer,[53] S. V. Peleganchuk,[122b,122a] O. Penc,[141] H. Peng,[60a] B. S. Peralva,[81a] M. M. Perego,[65] A. P. Pereira Peixoto,[140a] D. V. Perepelitsa,[29] F. Peri,[19] L. Perini,[69a,69b] H. Pernegger,[36] S. Perrella,[70a,70b] K. Peters,[46] R. F. Y. Peters,[101] B. A. Petersen,[36] T. C. Petersen,[40] E. Petit,[102] A. Petridis,[1] C. Petridou,[162] P. Petroff,[65] M. Petrov,[135] F. Petrucci,[75a,75b] M. Pettee,[183] N. E. Pettersson,[103] K. Petukhova,[143] A. Peyaud,[145] R. Pezoa,[147c] L. Pezzotti,[71a,71b] T. Pham,[105] F. H. Phillips,[107] P. W. Phillips,[144] M. W. Phipps,[173] G. Piacquadio,[155] E. Pianori,[18] A. Picazio,[103] R. H. Pickles,[101] R. Piegaia,[30] D. Pietreanu,[27b] J. E. Pilcher,[37] A. D. Pilkington,[101] M. Pinamonti,[74a,74b] J. L. Pinfold,[3] M. Pitt,[161] L. Pizzimento,[74a,74b] M.-A. Pleier,[29] V. Pleskot,[143] E. Plotnikova,[80] P. Podberezko,[122b,122a] R. Poettgen,[97] R. Poggi,[54] L. Poggioli,[65] I. Pogrebnyak,[107] D. Pohl,[24] I. Pokharel,[53] G. Polesello,[71a] A. Poley,[18] A. Policicchio,[73a,73b] R. Polifka,[143] A. Polini,[23b] C. S. Pollard,[46] V. Polychronakos,[29] D. Ponomarenko,[112] L. Pontecorvo,[36] S. Popa,[27a] G. A. Popeneciu,[27d] L. Portales,[5] D. M. Portillo Quintero,[58] S. Pospisil,[142] K. Potamianos,[46] I. N. Potrap,[80] C. J. Potter,[32] H. Potti,[11] T. Poulsen,[97] J. Poveda,[36] T. D. Powell,[149] G. Pownall,[46] M. E. Pozo Astigarraga,[36] P. Pralavorio,[102] S. Prell,[79] D. Price,[101] M. Primavera,[68a] S. Prince,[104] M. L. Proffitt,[148] N. Proklova,[112] K. Prokofiev,[63c] F. Prokoshin,[80] S. Protopopescu,[29] J. Proudfoot,[6] M. Przybycien,[84a] D. Pudzha,[138] A. Puri,[173] P. Puzo,[65] J. Qian,[106] Y. Qin,[101] A. Quadt,[53] M. Queitsch-Maitland,[46] A. Qureshi,[1] M. Racko,[28a] P. Rados,[105] F. Ragusa,[69a,69b] G. Rahal,[98] J. A. Raine,[54] S. Rajagopalan,[29] A. Ramirez Morales,[93] K. Ran,[15a,15d] T. Rashid,[65] S. Raspopov,[5] D. M. Rauch,[46] F. Rauscher,[114] S. Rave,[100] B. Ravina,[149] I. Ravinovich,[180] J. H. Rawling,[101] M. Raymond,[36] A. L. Read,[134] N. P. Readioff,[58] M. Reale,[68a,68b] D. M. Rebuzzi,[71a,71b] A. Redelbach,[177] G. Redlinger,[29] K. Reeves,[43] L. Rehnisch,[19] J. Reichert,[137] D. Reikher,[161] A. Reiss,[100] A. Rej,[151] C. Rembser,[36] M. Renda,[27b] M. Rescigno,[73a] S. Resconi,[69a] E. D. Resseguie,[137] S. Rettie,[175] E. Reynolds,[21] O. L. Rezanova,[122b,122a] P. Reznicek,[143] E. Ricci,[76a,76b] R. Richter,[115] S. Richter,[46] E. Richter-Was,[84b] O. Ricken,[24] M. Ridel,[136] P. Rieck,[115] C. J. Riegel,[182] O. Rifki,[46] M. Rijssenbeek,[155] A. Rimoldi,[71a,71b] M. Rimoldi,[46] L. Rinaldi,[23b] G. Ripellino,[154] I. Riu,[14] J. C. Rivera Vergara,[176] F. Rizatdinova,[130] E. Rizvi,[93] C. Rizzi,[36] R. T. Roberts,[101] S. H. Robertson,[104,q] M. Robin,[46] D. Robinson,[32] J. E. M. Robinson,[46] C. M. Robles Gajardo,[147c] A. Robson,[57] A. Rocchi,[74a,74b] E. Rocco,[100] C. Roda,[72a,72b] S. Rodriguez Bosca,[174] A. Rodriguez Perez,[14] D. Rodriguez Rodriguez,[174] A. M. Rodríguez Vera,[168b] S. Roe,[36] O. Røhne,[134] R. Röhrig,[115] C. P. A. Roland,[66] J. Roloff,[59] A. Romaniouk,[112] M. Romano,[23b,23a] N. Rompotis,[91] M. Ronzani,[125] L. Roos,[136] S. Rosati,[73a] K. Rosbach,[52] G. Rosin,[103] B. J. Rosser,[137] E. Rossi,[46] E. Rossi,[75a,75b] E. Rossi,[70a,70b] L. P. Rossi,[55b] L. Rossini,[69a,69b] R. Rosten,[14] M. Rotaru,[27b] J. Rothberg,[148] D. Rousseau,[65] G. Rovelli,[71a,71b] A. Roy,[11] D. Roy,[33e] A. Rozanov,[102] Y. Rozen,[160] X. Ruan,[33e] F. Rubbo,[153] F. Rühr,[52] A. Ruiz-Martinez,[174] A. Rummler,[36] Z. Rurikova,[52] N. A. Rusakovich,[80] H. L. Russell,[104] L. Rustige,[38,47] J. P. Rutherfoord,[7] E. M. Rüttinger,[149] M. Rybar,[39] G. Rybkin,[65] E. B. Rye,[134] A. Ryzhov,[123] P. Sabatini,[53] G. Sabato,[120] S. Sacerdoti,[65] H. F-W. Sadrozinski,[146] R. Sadykov,[80] F. Safai Tehrani,[73a] B. Safarzadeh Samani,[156] P. Saha,[121] S. Saha,[104] M. Sahinsoy,[61a] A. Sahu,[182] M. Saimpert,[46] M. Saito,[163] T. Saito,[163] H. Sakamoto,[163] A. Sakharov,[125,hh] D. Salamani,[54] G. Salamanna,[75a,75b] J. E. Salazar Loyola,[147c] P. H. Sales De Bruin,[172] A. Salnikov,[153] J. Salt,[174] D. Salvatore,[41b,41a] F. Salvatore,[156] A. Salvucci,[63a,63b,63c] A. Salzburger,[36] J. Samarati,[36] D. Sammel,[52] D. Sampsonidis,[162] D. Sampsonidou,[162] J. Sánchez,[174] A. Sanchez Pineda,[67a,67c] H. Sandaker,[134] C. O. Sander,[46] I. G. Sanderswood,[90] M. Sandhoff,[182] C. Sandoval,[22] D. P. C. Sankey,[144] M. Sannino,[55b,55a] Y. Sano,[117] A. Sansoni,[51] C. Santoni,[38] H. Santos,[140a,140b] S. N. Santpur,[18] A. Santra,[174] A. Sapronov,[80] J. G. Saraiva,[140a,140d] O. Sasaki,[82] K. Sato,[169] F. Sauerburger,[52] E. Sauvan,[5] P. Savard,[167,e] N. Savic,[115] R. Sawada,[163] C. Sawyer,[144] L. Sawyer,[96,oo] C. Sbarra,[23b] A. Sbrizzi,[23a] T. Scanlon,[95] J. Schaarschmidt,[148] P. Schacht,[115] B. M. Schachtner,[114] D. Schaefer,[37] L. Schaefer,[137] J. Schaeffer,[100] S. Schaepe,[36] U. Schäfer,[100] A. C. Schaffer,[65] D. Schaile,[114] R. D. Schamberger,[155] N. Scharmberg,[101] V. A. Schegelsky,[138] D. Scheirich,[143] F. Schenck,[19] M. Schernau,[171]

C. Schiavi,[55b,55a] S. Schier,[146] L. K. Schildgen,[24] Z. M. Schillaci,[26] E. J. Schioppa,[36] M. Schioppa,[41b,41a] K. E. Schleicher,[52] S. Schlenker,[36] K. R. Schmidt-Sommerfeld,[115] K. Schmieden,[36] C. Schmitt,[100] S. Schmitt,[46] S. Schmitz,[100] J. C. Schmoeckel,[46] U. Schnoor,[52] L. Schoeffel,[145] A. Schoening,[61b] P. G. Scholer,[52] E. Schopf,[135] M. Schott,[100] J. F. P. Schouwenberg,[119] J. Schovancova,[36] S. Schramm,[54] F. Schroeder,[182] A. Schulte,[100] H-C. Schultz-Coulon,[61a] M. Schumacher,[52] B. A. Schumm,[146] Ph. Schune,[145] A. Schwartzman,[153] T. A. Schwarz,[106] Ph. Schwemling,[145] R. Schwienhorst,[107] A. Sciandra,[146] G. Sciolla,[26] M. Scodeggio,[46] M. Scornajenghi,[41b,41a] F. Scuri,[72a] F. Scutti,[105] L. M. Scyboz,[115] C. D. Sebastiani,[73a,73b] P. Seema,[19] S. C. Seidel,[118] A. Seiden,[146] B. D. Seidlitz,[29] T. Seiss,[37] J. M. Seixas,[81b] G. Sekhniaidze,[70a] K. Sekhon,[106] S. J. Sekula,[42] N. Semprini-Cesari,[23b,23a] S. Sen,[49] S. Senkin,[38] C. Serfon,[77] L. Serin,[65] L. Serkin,[67a,67b] M. Sessa,[60a] H. Severini,[129] T. Šfiligoj,[92] F. Sforza,[55b,55a] A. Sfyrla,[54] E. Shabalina,[53] J. D. Shahinian,[146] N. W. Shaikh,[45a,45b] D. Shaked Renous,[180] L. Y. Shan,[15a] R. Shang,[173] J. T. Shank,[25] M. Shapiro,[18] A. Sharma,[135] A. S. Sharma,[1] P. B. Shatalov,[124] K. Shaw,[156] S. M. Shaw,[101] A. Shcherbakova,[138] M. Shehade,[180] Y. Shen,[129] N. Sherafati,[34] A. D. Sherman,[25] P. Sherwood,[95] L. Shi,[158,pp] S. Shimizu,[82] C. O. Shimmin,[183] Y. Shimogama,[179] M. Shimojima,[116] I. P. J. Shipsey,[135] S. Shirabe,[88] M. Shiyakova,[80,qq] J. Shlomi,[180] A. Shmeleva,[111] M. J. Shochet,[37] J. Shojaii,[105] D. R. Shope,[129] S. Shrestha,[127] E. M. Shrif,[33e] E. Shulga,[180] P. Sicho,[141] A. M. Sickles,[173] P. E. Sidebo,[154] E. Sideras Haddad,[33e] O. Sidiropoulou,[36] A. Sidoti,[23b,23a] F. Siegert,[48] Dj. Sijacki,[16] M. Silva Jr.,[181] M. V. Silva Oliveira,[81a] S. B. Silverstein,[45a] S. Simion,[65] E. Simioni,[100] R. Simoniello,[100] S. Simsek,[12b] P. Sinervo,[167] V. Sinetckii,[113,111] N. B. Sinev,[132] M. Sioli,[23b,23a] I. Siral,[106] S. Yu. Sivoklokov,[113] J. Sjölin,[45a,45b] E. Skorda,[97] P. Skubic,[129] M. Slawinska,[85] K. Sliwa,[170] R. Slovak,[143] V. Smakhtin,[180] B. H. Smart,[144] J. Smiesko,[28a] N. Smirnov,[112] S. Yu. Smirnov,[112] Y. Smirnov,[112] L. N. Smirnova,[113,rr] O. Smirnova,[97] J. W. Smith,[53] M. Smizanska,[90] K. Smolek,[142] A. Smykiewicz,[85] A. A. Snesarev,[111] H. L. Snoek,[120] I. M. Snyder,[132] S. Snyder,[29] R. Sobie,[176,q] A. Soffer,[161] A. Søgaard,[50] F. Sohns,[53] C. A. Solans Sanchez,[36] E. Yu. Soldatov,[112] U. Soldevila,[174] A. A. Solodkov,[123] A. Soloshenko,[80] O. V. Solovyanov,[123] V. Solovyev,[138] P. Sommer,[149] H. Son,[170] W. Song,[144] W. Y. Song,[168b] A. Sopczak,[142] F. Sopkova,[28b] C. L. Sotiropoulou,[72a,72b] S. Sottocornola,[71a,71b] R. Soualah,[67a,67c,ss] A. M. Soukharev,[122b,122a] D. South,[46] S. Spagnolo,[68a,68b] M. Spalla,[115] M. Spangenberg,[178] F. Spanò,[94] D. Sperlich,[52] T. M. Spieker,[61a] R. Spighi,[23b] G. Spigo,[36] M. Spina,[156] D. P. Spiteri,[57] M. Spousta,[143] A. Stabile,[69a,69b] B. L. Stamas,[121] R. Stamen,[61a] M. Stamenkovic,[120] E. Stanecka,[85] B. Stanislaus,[135] M. M. Stanitzki,[46] M. Stankaityte,[135] B. Stapf,[120] E. A. Starchenko,[123] G. H. Stark,[146] J. Stark,[58] S. H. Stark,[40] P. Staroba,[141] P. Starovoitov,[61a] S. Stärz,[104] R. Staszewski,[85] G. Stavropoulos,[44] M. Stegler,[46] P. Steinberg,[29] A. L. Steinhebel,[132] B. Stelzer,[152] H. J. Stelzer,[139] O. Stelzer-Chilton,[168a] H. Stenzel,[56] T. J. Stevenson,[156] G. A. Stewart,[36] M. C. Stockton,[36] G. Stoicea,[27b] M. Stolarski,[140a] S. Stonjek,[115] A. Straessner,[48] J. Strandberg,[154] S. Strandberg,[45a,45b] M. Strauss,[129] P. Strizenec,[28b] R. Ströhmer,[177] D. M. Strom,[132] R. Stroynowski,[42] A. Strubig,[50] S. A. Stucci,[29] B. Stugu,[17] J. Stupak,[129] N. A. Styles,[46] D. Su,[153] S. Suchek,[61a] V. V. Sulin,[111] M. J. Sullivan,[91] D. M. S. Sultan,[54] S. Sultansoy,[4c] T. Sumida,[86] S. Sun,[106] X. Sun,[3] K. Suruliz,[156] C. J. E. Suster,[157] M. R. Sutton,[156] S. Suzuki,[82] M. Svatos,[141] M. Swiatlowski,[37] S. P. Swift,[2] T. Swirski,[177] A. Sydorenko,[100] I. Sykora,[28a] M. Sykora,[143] T. Sykora,[143] D. Ta,[100] K. Tackmann,[46,tt] J. Taenzer,[161] A. Taffard,[171] R. Tafirout,[168a] H. Takai,[29] R. Takashima,[87] K. Takeda,[83] T. Takeshita,[150] E. P. Takeva,[50] Y. Takubo,[82] M. Talby,[102] A. A. Talyshev,[122b,122a] N. M. Tamir,[161] J. Tanaka,[163] M. Tanaka,[165] R. Tanaka,[65] S. Tapia Araya,[173] S. Tapprogge,[100] A. Tarek Abouelfadl Mohamed,[136] S. Tarem,[160] K. Tariq,[60b] G. Tarna,[27b,uu] G. F. Tartarelli,[69a] P. Tas,[143] M. Tasevsky,[141] T. Tashiro,[86] E. Tassi,[41b,41a] A. Tavares Delgado,[140a,140b] Y. Tayalati,[35e] A. J. Taylor,[50] G. N. Taylor,[105] W. Taylor,[168b] A. S. Tee,[90] R. Teixeira De Lima,[153] P. Teixeira-Dias,[94] H. Ten Kate,[36] J. J. Teoh,[120] S. Terada,[82] K. Terashi,[163] J. Terron,[99] S. Terzo,[14] M. Testa,[51] R. J. Teuscher,[167,q] S. J. Thais,[183] T. Theveneaux-Pelzer,[46] F. Thiele,[40] D. W. Thomas,[94] J. O. Thomas,[42] J. P. Thomas,[21] A. S. Thompson,[57] P. D. Thompson,[21] L. A. Thomsen,[183] E. Thomson,[137] E. J. Thorpe,[93] Y. Tian,[39] R. E. Ticse Torres,[53] V. O. Tikhomirov,[111,vv] Yu. A. Tikhonov,[122b,122a] S. Timoshenko,[112] P. Tipton,[183] S. Tisserant,[102] K. Todome,[23b,23a] S. Todorova-Nova,[5] S. Todt,[48] J. Tojo,[88] S. Tokár,[28a] K. Tokushuku,[82] E. Tolley,[127] K. G. Tomiwa,[33e] M. Tomoto,[117] L. Tompkins,[153,gg] B. Tong,[59] P. Tornambe,[103] E. Torrence,[132] H. Torres,[48] E. Torró Pastor,[148] C. Tosciri,[135] J. Toth,[102,ww] D. R. Tovey,[149] A. Traeet,[17] C. J. Treado,[125] T. Trefzger,[177] F. Tresoldi,[156] A. Tricoli,[29] I. M. Trigger,[168a] S. Trincaz-Duvoid,[136] W. Trischuk,[167] B. Trocmé,[58] A. Trofymov,[145] C. Troncon,[69a] M. Trovatelli,[176] F. Trovato,[156] L. Truong,[33c] M. Trzebinski,[85] A. Trzupek,[85] F. Tsai,[46] J. C-L. Tseng,[135] P. V. Tsiareshka,[108,ii] A. Tsirigotis,[162] N. Tsirintanis,[9] V. Tsiskaridze,[155] E. G. Tskhadadze,[159a] M. Tsopoulou,[162] I. I. Tsukerman,[124] V. Tsulaia,[18] S. Tsuno,[82] D. Tsybychev,[155] Y. Tu,[63b] A. Tudorache,[27b] V. Tudorache,[27b] T. T. Tulbure,[27a] A. N. Tuna,[59] S. Turchikhin,[80] D. Turgeman,[180] I. Turk Cakir,[4b,xx] R. J. Turner,[21] R. T. Turra,[69a] P. M. Tuts,[39] S. Tzamarias,[162] E. Tzovara,[100] G. Ucchielli,[47]

K. Uchida,[163] I. Ueda,[82] M. Ughetto,[45a,45b] F. Ukegawa,[169] G. Unal,[36] A. Undrus,[29] G. Unel,[171] F. C. Ungaro,[105] Y. Unno,[82] K. Uno,[163] J. Urban,[28b] P. Urquijo,[105] G. Usai,[8] Z. Uysal,[12d] L. Vacavant,[102] V. Vacek,[142] B. Vachon,[104] K. O. H. Vadla,[134] A. Vaidya,[95] C. Valderanis,[114] E. Valdes Santurio,[45a,45b] M. Valente,[54] S. Valentinetti,[23b,23a] A. Valero,[174] L. Valéry,[46] R. A. Vallance,[21] A. Vallier,[36] J. A. Valls Ferrer,[174] T. R. Van Daalen,[14] P. Van Gemmeren,[6] I. Van Vulpen,[120] M. Vanadia,[74a,74b] W. Vandelli,[36] A. Vaniachine,[166] D. Vannicola,[73a,73b] R. Vari,[73a] E. W. Varnes,[7] C. Varni,[55b,55a] T. Varol,[158] D. Varouchas,[65] K. E. Varvell,[157] M. E. Vasile,[27b] G. A. Vasquez,[176] J. G. Vasquez,[183] F. Vazeille,[38] D. Vazquez Furelos,[14] T. Vazquez Schroeder,[36] J. Veatch,[53] V. Vecchio,[75a,75b] M. J. Veen,[120] L. M. Veloce,[167] F. Veloso,[140a,140c] S. Veneziano,[73a] A. Ventura,[68a,68b] N. Venturi,[36] A. Verbytskyi,[115] V. Vercesi,[71a] M. Verducci,[72a,72b] C. M. Vergel Infante,[79] C. Vergis,[24] W. Verkerke,[120] A. T. Vermeulen,[120] J. C. Vermeulen,[120] M. C. Vetterli,[152,e] N. Viaux Maira,[147c] M. Vicente Barreto Pinto,[54] T. Vickey,[149] O. E. Vickey Boeriu,[149] G. H. A. Viehhauser,[135] L. Vigani,[61b] M. Villa,[23b,23a] M. Villaplana Perez,[69a,69b] E. Vilucchi,[51] M. G. Vincter,[34] G. S. Virdee,[21] A. Vishwakarma,[46] C. Vittori,[23b,23a] I. Vivarelli,[156] M. Vogel,[182] P. Vokac,[142] S. E. von Buddenbrock,[33e] E. Von Toerne,[24] V. Vorobel,[143] K. Vorobev,[112] M. Vos,[174] J. H. Vossebeld,[91] M. Vozak,[101] N. Vranjes,[16] M. Vranjes Milosavljevic,[16] V. Vrba,[142] M. Vreeswijk,[120] R. Vuillermet,[36] I. Vukotic,[37] P. Wagner,[24] W. Wagner,[182] J. Wagner-Kuhr,[114] S. Wahdan,[182] H. Wahlberg,[89] V. M. Walbrecht,[115] J. Walder,[90] R. Walker,[114] S. D. Walker,[94] W. Walkowiak,[151] V. Wallangen,[45a,45b] A. M. Wang,[59] C. Wang,[60c] C. Wang,[60b] F. Wang,[181] H. Wang,[18] H. Wang,[3] J. Wang,[157] J. Wang,[61b] P. Wang,[42] Q. Wang,[129] R.-J. Wang,[100] R. Wang,[60a] R. Wang,[6] S. M. Wang,[158] W. T. Wang,[60a] W. Wang,[15c,yy] W. X. Wang,[60a,yy] Y. Wang,[60a,zz] Z. Wang,[60c] C. Wanotayaroj,[46] A. Warburton,[104] C. P. Ward,[32] D. R. Wardrope,[95] N. Warrack,[57] A. Washbrook,[50] A. T. Watson,[21] M. F. Watson,[21] G. Watts,[148] B. M. Waugh,[95] A. F. Webb,[11] S. Webb,[100] C. Weber,[183] M. S. Weber,[20] S. A. Weber,[34] S. M. Weber,[61a] A. R. Weidberg,[135] J. Weingarten,[47] M. Weirich,[100] C. Weiser,[52] P. S. Wells,[36] T. Wenaus,[29] T. Wengler,[36] S. Wenig,[36] N. Wermes,[24] M. D. Werner,[79] M. Wessels,[61a] T. D. Weston,[20] K. Whalen,[132] N. L. Whallon,[148] A. M. Wharton,[90] A. S. White,[106] A. White,[8] M. J. White,[1] D. Whiteson,[171] B. W. Whitmore,[90] W. Wiedenmann,[181] M. Wielers,[144] N. Wieseotte,[100] C. Wiglesworth,[40] L. A. M. Wiik-Fuchs,[52] F. Wilk,[101] H. G. Wilkens,[36] L. J. Wilkins,[94] H. H. Williams,[137] S. Williams,[32] C. Willis,[107] S. Willocq,[103] J. A. Wilson,[21] I. Wingerter-Seez,[5] E. Winkels,[156] F. Winklmeier,[132] O. J. Winston,[156] B. T. Winter,[52] M. Wittgen,[153] M. Wobisch,[96] A. Wolf,[100] T. M. H. Wolf,[120] R. Wolff,[102] R. W. Wölker,[135] J. Wollrath,[52] M. W. Wolter,[85] H. Wolters,[140a,140c] V. W. S. Wong,[175] N. L. Woods,[146] S. D. Worm,[21] B. K. Wosiek,[85] K. W. Woźniak,[85] K. Wraight,[57] S. L. Wu,[181] X. Wu,[54] Y. Wu,[60a] T. R. Wyatt,[101] B. M. Wynne,[50] S. Xella,[40] Z. Xi,[106] L. Xia,[178] X. Xiao,[106] I. Xiotidis,[156] D. Xu,[15a] H. Xu,[60a,uu] L. Xu,[29] T. Xu,[145] W. Xu,[106] Z. Xu,[60b] Z. Xu,[153] B. Yabsley,[157] S. Yacoob,[33a] K. Yajima,[133] D. P. Yallup,[95] D. Yamaguchi,[165] Y. Yamaguchi,[165] A. Yamamoto,[82] M. Yamatani,[163] T. Yamazaki,[163] Y. Yamazaki,[83] Z. Yan,[25] H. J. Yang,[60c,60d] H. T. Yang,[18] S. Yang,[78] X. Yang,[60b,58] Y. Yang,[163] W-M. Yao,[18] Y. C. Yap,[46] Y. Yasu,[82] E. Yatsenko,[60c,60d] J. Ye,[42] S. Ye,[29] I. Yeletskikh,[80] M. R. Yexley,[90] E. Yigitbasi,[25] K. Yorita,[179] K. Yoshihara,[137] C. J. S. Young,[36] C. Young,[153] J. Yu,[79] R. Yuan,[60b,aaa] X. Yue,[61a] S. P. Y. Yuen,[24] M. Zaazoua,[35e] B. Zabinski,[85] G. Zacharis,[10] E. Zaffaroni,[54] J. Zahreddine,[136] A. M. Zaitsev,[123,mm] T. Zakareishvili,[159b] N. Zakharchuk,[34] S. Zambito,[59] D. Zanzi,[36] D. R. Zaripovas,[57] S. V. Zeißner,[47] C. Zeitnitz,[182] G. Zemaityte,[135] J. C. Zeng,[173] O. Zenin,[123] T. Ženiš,[28a] D. Zerwas,[65] M. Zgubič,[135] D. F. Zhang,[15b] G. Zhang,[15b] H. Zhang,[15c] J. Zhang,[6] L. Zhang,[15c] L. Zhang,[60a] M. Zhang,[173] R. Zhang,[24] X. Zhang,[60b] Y. Zhang,[15a,15d] Z. Zhang,[63a] Z. Zhang,[65] P. Zhao,[49] Y. Zhao,[60b] Z. Zhao,[60a] A. Zhemchugov,[80] Z. Zheng,[106] D. Zhong,[173] B. Zhou,[106] C. Zhou,[181] M. S. Zhou,[15a,15d] M. Zhou,[155] N. Zhou,[60c] Y. Zhou,[7] C. G. Zhu,[60b] H. L. Zhu,[60a] H. Zhu,[15a] J. Zhu,[106] Y. Zhu,[60a] X. Zhuang,[15a] K. Zhukov,[111] V. Zhulanov,[122b,122a] D. Zieminska,[66] N. I. Zimine,[80] S. Zimmermann,[52] Z. Zinonos,[115] M. Ziolkowski,[151] L. Živković,[16] G. Zobernig,[181] A. Zoccoli,[23b,23a] K. Zoch,[53] T. G. Zorbas,[149] R. Zou,[37] and L. Zwalinski[36]

(ATLAS Collaboration)

[1]*Department of Physics, University of Adelaide, Adelaide, Australia*
[2]*Physics Department, SUNY Albany, Albany New York, USA*
[3]*Department of Physics, University of Alberta, Edmonton AB, Canada*
[4a]*Department of Physics, Ankara University, Ankara, Turkey*
[4b]*Istanbul Aydin University, Istanbul, Turkey*
[4c]*Division of Physics, TOBB University of Economics and Technology, Ankara, Turkey*
[5]*LAPP, Université Grenoble Alpes, Université Savoie Mont Blanc, CNRS/IN2P3, Annecy, France*

[6]High Energy Physics Division, Argonne National Laboratory, Argonne Illinois, USA
[7]Department of Physics, University of Arizona, Tucson Arizona, USA
[8]Department of Physics, University of Texas at Arlington, Arlington Texas, USA
[9]Physics Department, National and Kapodistrian University of Athens, Athens, Greece
[10]Physics Department, National Technical University of Athens, Zografou, Greece
[11]Department of Physics, University of Texas at Austin, Austin Texas, USA
[12a]Bahcesehir University, Faculty of Engineering and Natural Sciences, Istanbul, Turkey
[12b]Istanbul Bilgi University, Faculty of Engineering and Natural Sciences, Istanbul, Turkey
[12c]Department of Physics, Bogazici University, Istanbul, Turkey
[12d]Department of Physics Engineering, Gaziantep University, Gaziantep, Turkey
[13]Institute of Physics, Azerbaijan Academy of Sciences, Baku, Azerbaijan
[14]Institut de Física d'Altes Energies (IFAE), Barcelona Institute of Science and Technology, Barcelona, Spain
[15a]Institute of High Energy Physics, Chinese Academy of Sciences, Beijing, China
[15b]Physics Department, Tsinghua University, Beijing, China
[15c]Department of Physics, Nanjing University, Nanjing, China
[15d]University of Chinese Academy of Science (UCAS), Beijing, China
[16]Institute of Physics, University of Belgrade, Belgrade, Serbia
[17]Department for Physics and Technology, University of Bergen, Bergen, Norway
[18]Physics Division, Lawrence Berkeley National Laboratory and University of California, Berkeley California, USA
[19]Institut für Physik, Humboldt Universität zu Berlin, Berlin, Germany
[20]Albert Einstein Center for Fundamental Physics and Laboratory for High Energy Physics, University of Bern, Bern, Switzerland
[21]School of Physics and Astronomy, University of Birmingham, Birmingham, United Kingdom
[22]Facultad de Ciencias y Centro de Investigaciónes, Universidad Antonio Nariño, Bogota, Colombia
[23a]INFN Bologna and Universita' di Bologna, Dipartimento di Fisica, Italy
[23b]INFN Sezione di Bologna, Italy
[24]Physikalisches Institut, Universität Bonn, Bonn, Germany
[25]Department of Physics, Boston University, Boston Massachusetts, USA
[26]Department of Physics, Brandeis University, Waltham Massachusetts, USA
[27a]Transilvania University of Brasov, Brasov, Romania
[27b]Horia Hulubei National Institute of Physics and Nuclear Engineering, Bucharest, Romania
[27c]Department of Physics, Alexandru Ioan Cuza University of Iasi, Iasi, Romania
[27d]National Institute for Research and Development of Isotopic and Molecular Technologies, Physics Department, Cluj-Napoca, Romania
[27e]University Politehnica Bucharest, Bucharest, Romania
[27f]West University in Timisoara, Timisoara, Romania
[28a]Faculty of Mathematics, Physics and Informatics, Comenius University, Bratislava, Slovak Republic
[28b]Department of Subnuclear Physics, Institute of Experimental Physics of the Slovak Academy of Sciences, Kosice, Slovak Republic
[29]Physics Department, Brookhaven National Laboratory, Upton New York, USA
[30]Departamento de Física, Universidad de Buenos Aires, Buenos Aires, Argentina
[31]California State University, California, USA
[32]Cavendish Laboratory, University of Cambridge, Cambridge, United Kingdom
[33a]Department of Physics, University of Cape Town, Cape Town, South Africa
[33b]iThemba Labs, Western Cape, South Africa
[33c]Department of Mechanical Engineering Science, University of Johannesburg, Johannesburg, South Africa
[33d]University of South Africa, Department of Physics, Pretoria, South Africa
[33e]School of Physics, University of the Witwatersrand, Johannesburg, South Africa
[34]Department of Physics, Carleton University, Ottawa ON, Canada
[35a]Faculté des Sciences Ain Chock, Réseau Universitaire de Physique des Hautes Energies—Université Hassan II, Casablanca, Morocco
[35b]Faculté des Sciences, Université Ibn-Tofail, Kénitra, Morocco
[35c]Faculté des Sciences Semlalia, Université Cadi Ayyad, LPHEA-Marrakech, Morocco
[35d]Faculté des Sciences, Université Mohamed Premier and LPTPM, Oujda, Morocco
[35e]Faculté des sciences, Université Mohammed V, Rabat, Morocco
[36]CERN, Geneva, Switzerland
[37]Enrico Fermi Institute, University of Chicago, Chicago Illinois, USA

[38]*LPC, Université Clermont Auvergne, CNRS/IN2P3, Clermont-Ferrand, France*
[39]*Nevis Laboratory, Columbia University, Irvington New York, USA*
[40]*Niels Bohr Institute, University of Copenhagen, Copenhagen, Denmark*
[41a]*Dipartimento di Fisica, Università della Calabria, Rende, Italy*
[41b]*INFN Gruppo Collegato di Cosenza, Laboratori Nazionali di Frascati, Italy*
[42]*Physics Department, Southern Methodist University, Dallas Texas, USA*
[43]*Physics Department, University of Texas at Dallas, Richardson Texas, USA*
[44]*National Centre for Scientific Research "Demokritos", Agia Paraskevi, Greece*
[45a]*Department of Physics, Stockholm University, Sweden*
[45b]*Oskar Klein Centre, Stockholm, Sweden*
[46]*Deutsches Elektronen-Synchrotron DESY, Hamburg and Zeuthen, Germany*
[47]*Lehrstuhl für Experimentelle Physik IV, Technische Universität Dortmund, Dortmund, Germany*
[48]*Institut für Kern- und Teilchenphysik, Technische Universität Dresden, Dresden, Germany*
[49]*Department of Physics, Duke University, Durham North Carolina, USA*
[50]*SUPA—School of Physics and Astronomy, University of Edinburgh, Edinburgh, United Kingdom*
[51]*INFN e Laboratori Nazionali di Frascati, Frascati, Italy*
[52]*Physikalisches Institut, Albert-Ludwigs-Universität Freiburg, Freiburg, Germany*
[53]*II. Physikalisches Institut, Georg-August-Universität Göttingen, Göttingen, Germany*
[54]*Département de Physique Nucléaire et Corpusculaire, Université de Genève, Genève, Switzerland*
[55a]*Dipartimento di Fisica, Università di Genova, Genova, Italy*
[55b]*INFN Sezione di Genova, Italy*
[56]*II. Physikalisches Institut, Justus-Liebig-Universität Giessen, Giessen, Germany*
[57]*SUPA—School of Physics and Astronomy, University of Glasgow, Glasgow, United Kingdom*
[58]*LPSC, Université Grenoble Alpes, CNRS/IN2P3, Grenoble INP, Grenoble, France*
[59]*Laboratory for Particle Physics and Cosmology, Harvard University, Cambridge Massachusetts, USA*
[60a]*Department of Modern Physics and State Key Laboratory of Particle Detection and Electronics, University of Science and Technology of China, Hefei, China*
[60b]*Institute of Frontier and Interdisciplinary Science and Key Laboratory of Particle Physics and Particle Irradiation (MOE), Shandong University, Qingdao, China*
[60c]*School of Physics and Astronomy, Shanghai Jiao Tong University, KLPPAC-MoE, SKLPPC, Shanghai, China*
[60d]*Tsung-Dao Lee Institute, Shanghai, China*
[61a]*Kirchhoff-Institut für Physik, Ruprecht-Karls-Universität Heidelberg, Heidelberg, Germany*
[61b]*Physikalisches Institut, Ruprecht-Karls-Universität Heidelberg, Heidelberg, Germany*
[62]*Faculty of Applied Information Science, Hiroshima Institute of Technology, Hiroshima, Japan*
[63a]*Department of Physics, Chinese University of Hong Kong, Shatin, N.T., Hong Kong, China*
[63b]*Department of Physics, University of Hong Kong, Hong Kong, China*
[63c]*Department of Physics and Institute for Advanced Study, Hong Kong University of Science and Technology, Clear Water Bay, Kowloon, Hong Kong, China*
[64]*Department of Physics, National Tsing Hua University, Hsinchu, Taiwan*
[65]*IJCLab, Université Paris-Saclay, CNRS/IN2P3, 91405, Orsay, France*
[66]*Department of Physics, Indiana University, Bloomington Indiana, USA*
[67a]*INFN Gruppo Collegato di Udine, Sezione di Trieste, Udine, Italy*
[67b]*ICTP, Trieste, Italy*
[67c]*Dipartimento Politecnico di Ingegneria e Architettura, Università di Udine, Udine, Italy*
[68a]*INFN Sezione di Lecce, Italy*
[68b]*Dipartimento di Matematica e Fisica, Università del Salento, Lecce, Italy*
[69a]*INFN Sezione di Milano, Italy*
[69b]*Dipartimento di Fisica, Università di Milano, Milano, Italy*
[70a]*INFN Sezione di Napoli, Italy*
[70b]*Dipartimento di Fisica, Università di Napoli, Napoli, Italy*
[71a]*INFN Sezione di Pavia, Italy*
[71b]*Dipartimento di Fisica, Università di Pavia, Pavia, Italy*
[72a]*INFN Sezione di Pisa, Italy*
[72b]*Dipartimento di Fisica E.Fermi, Università di Pisa, Pisa, Italy*
[73a]*INFN Sezione di Roma, Italy*
[73b]*Dipartimento di Fisica, Sapienza Università di Roma, Roma, Italy*
[74a]*INFN Sezione di Roma Tor Vergata, Italy*
[74b]*Dipartimento di Fisica, Università di Roma Tor Vergata, Roma, Italy*
[75a]*INFN Sezione di Roma Tre, Italy*

[75b]Dipartimento di Matematica e Fisica, Università Roma Tre, Roma, Italy
[76a]INFN-TIFPA, Italy
[76b]Università degli Studi di Trento, Trento, Italy
[77]Institut für Astro- und Teilchenphysik, Leopold-Franzens-Universität, Innsbruck, Austria
[78]University of Iowa, Iowa City Iowa, USA
[79]Department of Physics and Astronomy, Iowa State University, Ames Iowa, USA
[80]Joint Institute for Nuclear Research, Dubna, Russia
[81a]Departamento de Engenharia Elétrica, Universidade Federal de Juiz de Fora (UFJF), Juiz de Fora, Brazil
[81b]Universidade Federal do Rio De Janeiro COPPE/EE/IF, Rio de Janeiro, Brazil
[81c]Universidade Federal de São João del Rei (UFSJ), São João del Rei, Brazil
[81d]Instituto de Física, Universidade de São Paulo, São Paulo, Brazil
[82]KEK, High Energy Accelerator Research Organization, Tsukuba, Japan
[83]Graduate School of Science, Kobe University, Kobe, Japan
[84a]AGH University of Science and Technology, Faculty of Physics and Applied Computer Science, Krakow, Poland
[84b]Marian Smoluchowski Institute of Physics, Jagiellonian University, Krakow, Poland
[85]Institute of Nuclear Physics Polish Academy of Sciences, Krakow, Poland
[86]Faculty of Science, Kyoto University, Kyoto, Japan
[87]Kyoto University of Education, Kyoto, Japan
[88]Research Center for Advanced Particle Physics and Department of Physics, Kyushu University, Fukuoka, Japan
[89]Instituto de Física La Plata, Universidad Nacional de La Plata and CONICET, La Plata, Argentina
[90]Physics Department, Lancaster University, Lancaster, United Kingdom
[91]Oliver Lodge Laboratory, University of Liverpool, Liverpool, United Kingdom
[92]Department of Experimental Particle Physics, Jožef Stefan Institute and Department of Physics, University of Ljubljana, Ljubljana, Slovenia
[93]School of Physics and Astronomy, Queen Mary University of London, London, United Kingdom
[94]Department of Physics, Royal Holloway University of London, Egham, United Kingdom
[95]Department of Physics and Astronomy, University College London, London, United Kingdom
[96]Louisiana Tech University, Ruston Louisiana, USA
[97]Fysiska institutionen, Lunds universitet, Lund, Sweden
[98]Centre de Calcul de l'Institut National de Physique Nucléaire et de Physique des Particules (IN2P3), Villeurbanne, France
[99]Departamento de Física Teorica C-15 and CIAFF, Universidad Autónoma de Madrid, Madrid, Spain
[100]Institut für Physik, Universität Mainz, Mainz, Germany
[101]School of Physics and Astronomy, University of Manchester, Manchester, United Kingdom
[102]CPPM, Aix-Marseille Université, CNRS/IN2P3, Marseille, France
[103]Department of Physics, University of Massachusetts, Amherst Massachusetts, USA
[104]Department of Physics, McGill University, Montreal QC, Canada
[105]School of Physics, University of Melbourne, Victoria, Australia
[106]Department of Physics, University of Michigan, Ann Arbor Michigan, USA
[107]Department of Physics and Astronomy, Michigan State University, East Lansing Michigan, USA
[108]B.I. Stepanov Institute of Physics, National Academy of Sciences of Belarus, Minsk, Belarus
[109]Research Institute for Nuclear Problems of Byelorussian State University, Minsk, Belarus
[110]Group of Particle Physics, University of Montreal, Montreal QC, Canada
[111]P.N. Lebedev Physical Institute of the Russian Academy of Sciences, Moscow, Russia
[112]National Research Nuclear University MEPhI, Moscow, Russia
[113]D.V. Skobeltsyn Institute of Nuclear Physics, M.V. Lomonosov Moscow State University, Moscow, Russia
[114]Fakultät für Physik, Ludwig-Maximilians-Universität München, München, Germany
[115]Max-Planck-Institut für Physik (Werner-Heisenberg-Institut), München, Germany
[116]Nagasaki Institute of Applied Science, Nagasaki, Japan
[117]Graduate School of Science and Kobayashi-Maskawa Institute, Nagoya University, Nagoya, Japan
[118]Department of Physics and Astronomy, University of New Mexico, Albuquerque New Mexico, USA
[119]Institute for Mathematics, Astrophysics and Particle Physics, Radboud University Nijmegen/Nikhef, Nijmegen, Netherlands
[120]Nikhef National Institute for Subatomic Physics and University of Amsterdam, Amsterdam, Netherlands
[121]Department of Physics, Northern Illinois University, DeKalb Illinois, USA
[122a]Budker Institute of Nuclear Physics and NSU, SB RAS, Novosibirsk, Russia

[122b]*Novosibirsk State University Novosibirsk, Russia*
[123]*Institute for High Energy Physics of the National Research Centre Kurchatov Institute, Protvino, Russia*
[124]*Institute for Theoretical and Experimental Physics named by A.I. Alikhanov of National Research Centre "Kurchatov Institute", Moscow, Russia*
[125]*Department of Physics, New York University, New York New York, USA*
[126]*Ochanomizu University, Otsuka, Bunkyo-ku, Tokyo, Japan*
[127]*The Ohio State University, Columbus Ohio, USA*
[128]*Faculty of Science, Okayama University, Okayama, Japan*
[129]*Homer L. Dodge Department of Physics and Astronomy, University of Oklahoma, Norman Oklahoma, USA*
[130]*Department of Physics, Oklahoma State University, Stillwater Oklahoma, USA*
[131]*Palacký University, RCPTM, Joint Laboratory of Optics, Olomouc, Czech Republic*
[132]*Center for High Energy Physics, University of Oregon, Eugene Oregon, USA*
[133]*Graduate School of Science, Osaka University, Osaka, Japan*
[134]*Department of Physics, University of Oslo, Oslo, Norway*
[135]*Department of Physics, Oxford University, Oxford, United Kingdom*
[136]*LPNHE, Sorbonne Université, Université de Paris, CNRS/IN2P3, Paris, France*
[137]*Department of Physics, University of Pennsylvania, Philadelphia Pennsylvania, USA*
[138]*Konstantinov Nuclear Physics Institute of National Research Centre "Kurchatov Institute", PNPI, St. Petersburg, Russia*
[139]*Department of Physics and Astronomy, University of Pittsburgh, Pittsburgh Pennsylvania, USA*
[140a]*Laboratório de Instrumentação e Física Experimental de Partículas—LIP, Lisboa, Portugal*
[140b]*Departamento de Física, Faculdade de Ciências, Universidade de Lisboa, Lisboa, Portugal*
[140c]*Departamento de Física, Universidade de Coimbra, Coimbra, Portugal*
[140d]*Centro de Física Nuclear da Universidade de Lisboa, Lisboa, Portugal*
[140e]*Departamento de Física, Universidade do Minho, Braga, Portugal*
[140f]*Departamento de Física Teórica y del Cosmos, Universidad de Granada, Granada (Spain), Spain*
[140g]*Dep Física and CEFITEC of Faculdade de Ciências e Tecnologia, Universidade Nova de Lisboa, Caparica, Portugal*
[140h]*Instituto Superior Técnico, Universidade de Lisboa, Lisboa, Portugal*
[141]*Institute of Physics of the Czech Academy of Sciences, Prague, Czech Republic*
[142]*Czech Technical University in Prague, Prague, Czech Republic*
[143]*Charles University, Faculty of Mathematics and Physics, Prague, Czech Republic*
[144]*Particle Physics Department, Rutherford Appleton Laboratory, Didcot, United Kingdom*
[145]*IRFU, CEA, Université Paris-Saclay, Gif-sur-Yvette, France*
[146]*Santa Cruz Institute for Particle Physics, University of California Santa Cruz, Santa Cruz California, USA*
[147a]*Departamento de Física, Pontificia Universidad Católica de Chile, Santiago, Chile*
[147b]*Universidad Andres Bello, Department of Physics, Santiago, Chile*
[147c]*Departamento de Física, Universidad Técnica Federico Santa María, Valparaíso, Chile*
[148]*Department of Physics, University of Washington, Seattle Washington, USA*
[149]*Department of Physics and Astronomy, University of Sheffield, Sheffield, United Kingdom*
[150]*Department of Physics, Shinshu University, Nagano, Japan*
[151]*Department Physik, Universität Siegen, Siegen, Germany*
[152]*Department of Physics, Simon Fraser University, Burnaby BC, Canada*
[153]*SLAC National Accelerator Laboratory, Stanford California, USA*
[154]*Physics Department, Royal Institute of Technology, Stockholm, Sweden*
[155]*Departments of Physics and Astronomy, Stony Brook University, Stony Brook New York, USA*
[156]*Department of Physics and Astronomy, University of Sussex, Brighton, United Kingdom*
[157]*School of Physics, University of Sydney, Sydney, Australia*
[158]*Institute of Physics, Academia Sinica, Taipei, Taiwan*
[159a]*E. Andronikashvili Institute of Physics, Iv. Javakhishvili Tbilisi State University, Tbilisi, Georgia*
[159b]*High Energy Physics Institute, Tbilisi State University, Tbilisi, Georgia*
[160]*Department of Physics, Technion, Israel Institute of Technology, Haifa, Israel*
[161]*Raymond and Beverly Sackler School of Physics and Astronomy, Tel Aviv University, Tel Aviv, Israel*
[162]*Department of Physics, Aristotle University of Thessaloniki, Thessaloniki, Greece*
[163]*International Center for Elementary Particle Physics and Department of Physics, University of Tokyo, Tokyo, Japan*
[164]*Graduate School of Science and Technology, Tokyo Metropolitan University, Tokyo, Japan*
[165]*Department of Physics, Tokyo Institute of Technology, Tokyo, Japan*

[166]Tomsk State University, Tomsk, Russia
[167]Department of Physics, University of Toronto, Toronto ON, Canada
[168a]TRIUMF, Vancouver BC, Canada
[168b]Department of Physics and Astronomy, York University, Toronto ON, Canada
[169]Division of Physics and Tomonaga Center for the History of the Universe, Faculty of Pure and Applied Sciences, University of Tsukuba, Tsukuba, Japan
[170]Department of Physics and Astronomy, Tufts University, Medford Massachusetts, USA
[171]Department of Physics and Astronomy, University of California Irvine, Irvine California, USA
[172]Department of Physics and Astronomy, University of Uppsala, Uppsala, Sweden
[173]Department of Physics, University of Illinois, Urbana Illinois, USA
[174]Instituto de Física Corpuscular (IFIC), Centro Mixto Universidad de Valencia—CSIC, Valencia, Spain
[175]Department of Physics, University of British Columbia, Vancouver BC, Canada
[176]Department of Physics and Astronomy, University of Victoria, Victoria BC, Canada
[177]Fakultät für Physik und Astronomie, Julius-Maximilians-Universität Würzburg, Würzburg, Germany
[178]Department of Physics, University of Warwick, Coventry, United Kingdom
[179]Waseda University, Tokyo, Japan
[180]Department of Particle Physics, Weizmann Institute of Science, Rehovot, Israel
[181]Department of Physics, University of Wisconsin, Madison Wisconsin, USA
[182]Fakultät für Mathematik und Naturwissenschaften, Fachgruppe Physik, Bergische Universität Wuppertal, Wuppertal, Germany
[183]Department of Physics, Yale University, New Haven Connecticut, USA
[184]Yerevan Physics Institute, Yerevan, Armenia

[a]Deceased.
[b]Also at Department of Physics, King's College London, London, United Kingdom.
[c]Also at Istanbul University, Dept. of Physics, Istanbul, Turkey.
[d]Also at Instituto de Fisica Teorica, IFT-UAM/CSIC, Madrid, Spain.
[e]Also at TRIUMF, Vancouver BC, Canada.
[f]Also at Department of Physics and Astronomy, University of Louisville, Louisville, Kentucky, USA.
[g]Also at Physics Department, An-Najah National University, Nablus, Palestine.
[h]Also at Department of Physics, California State University, Fresno, USA.
[i]Also at Department of Physics, University of Fribourg, Fribourg, Switzerland.
[j]Also at Physics Dept, University of South Africa, Pretoria, South Africa.
[k]Also at Departament de Fisica de la Universitat Autonoma de Barcelona, Barcelona, Spain.
[l]Also at Tomsk State University, Tomsk, and Moscow Institute of Physics and Technology State University, Dolgoprudny, Russia.
[m]Also at The Collaborative Innovation Center of Quantum Matter (CICQM), Beijing, China.
[n]Also at Department of Physics, Ben Gurion University of the Negev, Beer Sheva, Israel.
[o]Also at Departamento de Física, Instituto Superior Técnico, Universidade de Lisboa, Lisboa, Portugal.
[p]Also at Universita di Napoli Parthenope, Napoli, Italy.
[q]Also at Institute of Particle Physics (IPP), Vancouver, Canada.
[r]Also at Department of Physics, University of Adelaide, Adelaide, Australia.
[s]Also at Dipartimento di Matematica, Informatica e Fisica, Università di Udine, Udine, Italy.
[t]Also at Department of Physics, St. Petersburg State Polytechnical University, St. Petersburg, Russia.
[u]Also at Borough of Manhattan Community College, City University of New York, New York New York, USA.
[v]Also at Department of Financial and Management Engineering, University of the Aegean, Chios, Greece.
[w]Also at Department of Physics, California State University, East Bay, USA.
[x]Also at Institucio Catalana de Recerca i Estudis Avancats, ICREA, Barcelona, Spain.
[y]Also at Department of Physics, University of Michigan, Ann Arbor Michigan, USA.
[z]Also at IJCLab, Université Paris-Saclay, CNRS/IN2P3, 91405, Orsay, France.
[aa]Also at Graduate School of Science, Osaka University, Osaka, Japan.
[bb]Also at Physikalisches Institut, Albert-Ludwigs-Universität Freiburg, Freiburg, Germany.
[cc]Also at Institute of Physics, Azerbaijan Academy of Sciences, Baku, Azerbaijan.
[dd]Also at Institute for Mathematics, Astrophysics and Particle Physics, Radboud University Nijmegen/Nikhef, Nijmegen, Netherlands.
[ee]Also at Institute of Theoretical Physics, Ilia State University, Tbilisi, Georgia.
[ff]Also at CERN, Geneva, Switzerland.
[gg]Also at Department of Physics, Stanford University, Stanford California, USA.
[hh]Also at Manhattan College, New York New York, USA.
[ii]Also at Joint Institute for Nuclear Research, Dubna, Russia.
[jj]Also at Hellenic Open University, Patras, Greece.

[kk]Also at The City College of New York, New York New York, USA.
[ll]Also at Department of Physics, California State University, Sacramento, USA.
[mm]Also at Moscow Institute of Physics and Technology State University, Dolgoprudny, Russia.
[nn]Also at Département de Physique Nucléaire et Corpusculaire, Université de Genève, Genève, Switzerland.
[oo]Also at Louisiana Tech University, Ruston Louisiana, USA.
[pp]Also at School of Physics, Sun Yat-sen University, Guangzhou, China.
[qq]Also at Institute for Nuclear Research and Nuclear Energy (INRNE) of the Bulgarian Academy of Sciences, Sofia, Bulgaria.
[rr]Also at Faculty of Physics, M.V. Lomonosov Moscow State University, Moscow, Russia.
[ss]Also at Department of Applied Physics and Astronomy, University of Sharjah, Sharjah, United Arab Emirates.
[tt]Also at Institut für Experimentalphysik, Universität Hamburg, Hamburg, Germany.
[uu]Also at CPPM, Aix-Marseille Université, CNRS/IN2P3, Marseille, France.
[vv]Also at National Research Nuclear University MEPhI, Moscow, Russia.
[ww]Also at Institute for Particle and Nuclear Physics, Wigner Research Centre for Physics, Budapest, Hungary.
[xx]Also at Giresun University, Faculty of Engineering, Giresun, Turkey.
[yy]Also at Institute of Physics, Academia Sinica, Taipei, Taiwan.
[zz]Also at LPNHE, Sorbonne Université, Université de Paris, CNRS/IN2P3, Paris, France.
[aaa]Also at Department of Physics and Astronomy, Michigan State University, East Lansing Michigan, USA.